Kinetics of biofilm detachment
by Brent Michael Peyton

A thesis submitted in partial fulfillment of the requirements for the degree of Doctor of Philosophy in Chemical Engineering
Montana State University

Abstract:
A biofilm is a matrix of cells and cellular products attached to a solid substratum. This biological matrix can increase operational costs and/or decrease product quality in a variety of industries, including oil and paper production, semiconductor manufacture, and drinking water distribution. Beneficial biofilms contribute to hazardous waste bioremediation and waste water treatment, and can offer significant improvements in bioprocessing technology. Understanding the processes which control the rate and extent of biofilm accumulation is critical to the control of both beneficial and detrimental biofilms.

One of the least understood processes affecting biofilm accumulation is detachment. Detachment is the removal of cells and cell products from an established biofilm and subsequent entrainment in the bulk liquid. The purpose of this research was to determine the effects of shear stress and substrate loading rate on the rate of biofilm detachment.

Mono-population Pseudomonas aeruginosa and undefined mixed population biofilms were grown on glucose in a RotoTorque biofilm reactor. Three levels of shear stress and substrate loading rate were used to determine their effects on the rate of detachment. Suspended cell concentrations were monitored to determine detachment rates, while other variables were measured to determine their influence on the detachment rate. Results indicate that detachment rate is directly related to biofilm growth rate, and that factors which limit growth rate will also limit detachment rate. No significant influence of shear stress on detachment rate was observed.

A new kinetic expression which incorporates substrate utilization rate, yield, and biofilm thickness was compared to published detachment expressions and gives a better correlation of data obtained both in this research and from previous research projects, for both mono- and mixed population biofilms.

KINETICS OF BIOFILM DETACHMENT

by

Brent Michael Peyton

A thesis submitted in partial fulfillment
of the requirements for the degree

of

Doctor of Philosophy

in

Chemical Engineering

MONTANA STATE UNIVERSITY
Bozeman, Montana

June 1992

APPROVAL

of a thesis submitted by

Brent Michael Peyton

This thesis has been read by each member of the thesis committee and has been found to be satisfactory regarding content, English usage, format, citations, bibliographic style, and consistency, and is ready for submission to the College of Graduate Studies.

6/8/92
Date

Chairperson, Graduate Committee

Approved for the Major Department

6/8/92
Date

Head, Major Department

Approved for the College of Graduate Studies

June 10, 1992
Date

Graduate Dean

STATEMENT OF PERMISSION TO USE

In presenting this thesis in partial fulfillment of the requirements for a doctoral degree at Montana State University, I agree that the Library shall make it available to borrowers under rules of the Library.

If I have indicated my intention to copyright this thesis by including a copyright notice page, copying is allowable only for scholarly purposes, consistent with "fair use" as prescribed in the U.S. Copyright Law. Requests for permission for extended quotation from or reproduction of this thesis in whole or in parts may be granted only by the copyright holder.

Signature Brent M. Peyton

Date June 9, 1992

ACKNOWLEDGEMENTS

This thesis is the culmination of years of work, which have been, for the most part, *fun*. This could not have been accomplished in a vacuum, so I would like to thank those who made my time in Bozeman both enjoyable and productive.

First and foremost, I thank Bill Characklis for being my research advisor, mentor, and friend, Bob Huddleston and Conoco, Inc. for continuous financial and moral support, and the other members of my thesis committee - Gordon McFeters, John Sears, Ron Larsen, and Jack Gilchrist - for their time and advice on this project.

Fellow graduate students Xiaoming Xu (who did a wonderful job on the mixed culture experiments), Bill Drury, Rick Veeh, Satoshi Okabe, Ross Lundman, Kirk Johnson, Wendy Swanson, Ewout van der Wende, and WhonChee Lee, made day-to-day life at the Center a pleasure. I am grateful to the people who were here with IPA and were always willing to help: Anne Camper, Warren Jones, Paul Stoodley, Zbigniew Lewandowski, Wendy Wesen, Jamie Hergistad, and especially Diane Williams, and to those at the Center whom I've known a shorter time, but who were also always helpful: Susan Cooper, Peg Dirckx, Lynda Anderson, Gil Geesey, Brian Goldstein, Marty Hamilton, Shawn Handran, Bill Harn, Cheryl Horning, Alma and Frank Roe, Mary Williams, and Nick Zelver. Special thanks to Al "Let's-Go-Fishing-Sometime" Cunningham for a little bit of everything, and Phil Stewart for editing, keeping me focused, and continuing detachment research at the Center.

Most of all I thank Kathy, my wife, who has done as much of the actual work on this thesis as I have, has put up with me these last few hectic months, and is typing away even as I finish writing this acknowledgement.

TABLE OF CONTENTS

	Page
INTRODUCTION	1
Relevance of Biofilms	1
Detachment	3
Research Goal and Objectives	4
BACKGROUND	6
Biofilm Processes	6
Adsorption	8
Adsorption of the Conditioning Film	8
Adsorption of Cells to Surface	9
Reversible / Irreversible Adsorption	11
Attachment	11
Detachment	12
Erosion	12
Sloughing	13
Human Intervention, Predator Grazing, and Abrasion	14
Biofilm Properties	15
Density	15
Film Morphology	17
Surface Film	17
Base Film	18
Material Balances	18
Bulk Liquid Compartment Glucose Carbon	19
Bulk Liquid Compartment Cell Number	19
Bulk Liquid Compartment Product Carbon	19
Biofilm Compartment Glucose Carbon	19
Biofilm Compartment Cell Number	19
Biofilm Compartment Product Carbon	19
Detachment Models	20
Derivation of Proposed Detachment Rate Expression	25
EXPERIMENTAL APPROACH	28
Microbial Species	28
Nutrient Medium	28
Rotating Annular Reactor (RotoTorque)	30
Cleaning and Preparation	30
Start-up Protocol	32
Operating Conditions	32
Analytical Methods	33
Glucose Analysis	33
Total Organic Carbon	33

TABLE OF CONTENTS - Continued

	Page
Soluble Organic Carbon	34
Biofilm Thickness	34
Biofilm Areal and Volumetric Density	34
Water Content	35
Effluent Particle Size Distribution	36
Cell Concentration	36
Carbohydrate Analysis	37
Electron Microscopy	37
Torque	37
Statistical Methods	38
RESULTS	40
Monopopulation Data	40
Biofilm Characterization	42
Biofilm Thickness	43
Biofilm Roughness	44
Biofilm Areal Mass Density	44
Biofilm Volumetric Density	47
Biofilm Areal Cell Density	47
Biofilm Volumetric Cell Density	49
Carbohydrate Analysis	49
Bulk Liquid Characterization	50
Glucose Concentration	50
Suspended Cell Concentration	50
Total and Soluble Organic Carbon	51
Biofilm Process Characterization	51
Glucose Utilization Rate	51
Observed Yield Coefficient	52
Cellular Production Rate	53
Cellular Detachment Rate	53
Particle Size Distribution	53
Photomicrographs	54
Step-Change Effects	58
Experiment R1	59
Experiment R6	59
Mixed Population Data	62
DISCUSSION	65
Biofilm Characteristics	65
Biofilm Thickness	65
Biofilm Roughness	66
Areal and Volumetric Mass Density	67
Carbohydrate Analysis	70

TABLE OF CONTENTS - Continued

	Page
Bulk Liquid Characteristics	71
Glucose Concentration	71
Biofilm Process Characteristics	71
Detachment Rate	71
Shear Stress	74
Substrate Utilization Rate	77
Particle Size Distribution	81
Hypothesized Detachment Mechanism	82
Detached Particle Size Distribution	82
Substrate Profiles	83
Inert Bead Tracer Studies	84
Photomicrographs	84
Detachment Mechanism	84
Industrial Relevance	86
CONCLUSIONS	88
RECOMMENDATIONS FOR FURTHER RESEARCH	89
NOMENCLATURE	90
BIBLIOGRAPHY	94
APPENDICES	111
APPENDIX A: RotoTorque Characteristics	112
APPENDIX B: Procedures and Methods	114
APPENDIX C: Raw Data 200 rpm	116
APPENDIX D: Raw Data 300 rpm	123
APPENDIX E: Raw Data 400 rpm	130
APPENDIX F: Torque Data and Shear Stress Calculation	137
APPENDIX G: ANOVA Results for Steady State Data Only	140
APPENDIX H: Mixed Population Results 200 rpm	152
APPENDIX I: Particle Size Distribution Data	159

LIST OF TABLES

Table		Page
1.	Biofilm density and thickness	16
2.	Variation of volumetric mass density with biofilm depth (Masuda et al. 1991)	16
3.	Summary of proposed detachment rate expressions	25
4.	Media composition entering RotoTorque reactor	29
5.	Statistical experiment design	38
6.	Summary of experimental conditions and steady state results	41
7.	Steady state substrate utilization and detachment rates	41
8.	Analysis of variance results	42
9.	Glycosyl residue compositions	49
10.	Squared correlation coefficients of reported detachment expressions	72
11.	Dependence of detachment rate on shear stress	75
12.	Bulk liquid measurements - R0	117
13.	Biofilm measurements - R0	117
14.	Bulk liquid measurements - R1	118
15.	Biofilm measurements - R1	119
16.	Bulk liquid measurements - R2	120
17.	Biofilm measurements - R2	120
18.	Optical thickness data 200 rpm	121

LIST OF TABLES - Continued

Table		Page
19.	Percent water data 200 rpm	122
20.	Bulk liquid measurements - R3	124
21.	Biofilm measurements - R3	124
22.	Bulk liquid measurements - R4	125
23.	Biofilm measurements - R4	125
24.	Bulk liquid measurements - S4	126
25.	Biofilm measurements - S4	126
26.	Bulk liquid measurements - T4	127
27.	Biofilm measurements - T4	127
28.	Bulk liquid measurements - R5	128
29.	Biofilm measurements - R5	128
30.	Optical thickness data 300 rpm	129
31.	Bulk liquid measurements - R6	131
32.	Biofilm measurements - R6	132
33.	Bulk liquid measurements - R7	133
34.	Biofilm measurements - R7	133
35.	Bulk liquid measurements - S7	134
36.	Biofilm measurements - S7	134
37.	Bulk liquid measurements - R8	135
38.	Biofilm measurements - R8	135
39.	Optical thickness data 400 rpm	136
40.	ANOVA results - Effluent glucose concentration	141
41.	ANOVA results - Glucose utilization rate	142

LIST OF TABLES - Continued

Table		Page
42.	ANOVA results - Suspended cell concentration	143
43.	ANOVA results - Cellular detachment rate	144
44.	ANOVA results - Average biofilm thickness	145
45.	ANOVA results - Biofilm roughness	146
46.	ANOVA results - Areal mass density	147
47.	ANOVA results - Volumetric mass density	148
48.	ANOVA results - Areal cell density	149
49.	ANOVA results - Volumetric cell density	150
50.	ANOVA results - Biofilm TOC	151
51.	Bulk liquid measurements - M1	153
52.	Biofilm measurements - M1	154
53.	Biofilm thickness distribution - M1	155
54.	Bulk liquid measurements - M2	156
55.	Biofilm measurements - M2	157
56.	Biofilm thickness distribution - M2	158
57.	Particle size distribution - R0	160
58.	Particle size distribution - S4	161
59.	Particle size distribution - T4	162

LIST OF FIGURES

Figure		Page
1.	Characteristic progression of biofilm accumulation with time	6
2.	Schematic illustration of processes contributing to biofilm accumulation	7
3.	Diagram of the processes fundamental to the initial microbial colonization of a substratum	9
4.	Schematic diagram of the processes contributing to biofilm detachment	12
5.	Schematic diagram of the base and surface film	17
6.	Comparison of detachment rates at two substrate loading rates (Trulear and Characklis 1982)	23
7.	Experimental apparatus including the RotoTorque	31
8.	Biofilm thickness measurement indicating biofilm roughness and average thickness	35
9.	Typical progression of biofilm thickness with time	43
10.	Steady state biofilm thickness with substrate loading rate	44
11.	Biofilm roughness as a function of measured average biofilm thickness	45
12.	Steady state areal mass density with substrate loading rate	45
13.	Regression of areal mass density with biofilm thickness	46
14.	Volumetric mass density with average biofilm thickness	47
15.	Areal cell density as a function of substrate loading rate	48

LIST OF FIGURES - Continued

Figure		Page
16.	Regression of areal cell density with biofilm thickness	48
17.	Steady state glucose concentration as a function of substrate loading rate	50
18.	Suspended cell concentration with substrate loading rate	51
19.	Observed cellular yield	52
20.	Steady state detachment rate as a function of substrate loading rate and shear stress	53
21.	Particle size distribution for experiment S4	54
22.	Effects of step change in pH from 6.8 to 5.8	60
23.	Effect of turning off the influent glucose	61
24.	Biomass detachment rate for experiments M1 and M2	62
25.	Distribution of biofilm thicknesses for experiment M1 after 288 hours	63
26.	Distribution of biofilm thicknesses for experiment M2 after 288 hours	64
27.	Dependence of steady state biofilm thickness on glucose utilization rate	66
28.	Fitted average and calculated local volumetric mass density with distance from substratum	69
29.	*Psuedomonas aeruginosa* detachment rates with proposed detachment rate expression	73
30.	Mixed population detachment rates with proposed detachment rate expression	73
31.	Trulear's (1980) mixed population detachment rates as a function of shear stress	75
32.	Specific growth rate as calculated by the Monod equation	81

LIST OF FIGURES - Continued

Figure		Page
33.	Glucose and specific growth rate profiles for zero-order kinetics	83
34.	Schematic of proposed detachment mechanism	85
35.	Diagram of travelling biofilm "dunes"	86
36.	Measured gap opening for shear stress monitoring	139
37.	Calculated shear stress from rotational speed	139

LIST OF PHOTOMICROGRAPHS

Photo		Page
1.	SEM photomicrograph (500 X) showing rippled biofilm surface	55
2.	Close-up (3,000 X) of Photo 1	56
3.	SEM photomicrograph (20,000 X) showing extent of polymer formation in biofilm	57
4.	TEM photomicrograph (5,000 X) showing cross-section of biofilm on substratum	58

ABSTRACT

A biofilm is a matrix of cells and cellular products attached to a solid substratum. This biological matrix can increase operational costs and/or decrease product quality in a variety of industries, including oil and paper production, semiconductor manufacture, and drinking water distribution. Beneficial biofilms contribute to hazardous waste bioremediation and waste water treatment, and can offer significant improvements in bioprocessing technology. Understanding the processes which control the rate and extent of biofilm accumulation is critical to the control of both beneficial and detrimental biofilms.

One of the least understood processes affecting biofilm accumulation is detachment. Detachment is the removal of cells and cell products from an established biofilm and subsequent entrainment in the bulk liquid. The purpose of this research was to determine the effects of shear stress and substrate loading rate on the rate of biofilm detachment.

Mono-population *Pseudomonas aeruginosa* and undefined mixed population biofilms were grown on glucose in a RotoTorque biofilm reactor. Three levels of shear stress and substrate loading rate were used to determine their effects on the rate of detachment. Suspended cell concentrations were monitored to determine detachment rates, while other variables were measured to determine their influence on the detachment rate. Results indicate that detachment rate is directly related to biofilm growth rate, and that factors which limit growth rate will also limit detachment rate. No significant influence of shear stress on detachment rate was observed.

A new kinetic expression which incorporates substrate utilization rate, yield, and biofilm thickness was compared to published detachment expressions and gives a better correlation of data obtained both in this research and from previous research projects, for both mono- and mixed population biofilms.

INTRODUCTION

A biofilm is a matrix of cells and cellular products attached to a solid surface or substratum. At the substratum, cells grow, reproduce, and produce extracellular polymers and other byproducts. Biofilms are found in most natural and industrial aquatic systems and account for much of the overall microbial activity in these systems. Biofilms reduce heat transfer in heat exchange equipment and reduce flow capacity in pipelines leading to increased energy consumption and increased costs. Biofilms also contribute significantly to corrosion, oil field reservoir plugging and petroleum souring, drinking water deterioration, and computer chip contamination. However, biofilms present positive opportunities in bioremediation of hazardous and toxic substances in ground and surface water and waste water treatment. Biofilm and other immobilized cell reactors offer significant advantages in bioprocessing, such as increased process flow rates without washing the organisms from the reactor. Engineers and scientists are just beginning to realize the significance of biofilms on process industries, natural aquatic systems, and medical technology. Integrated knowledge of microbiology, chemistry, and engineering is necessary to fully understand the processes affecting biofilm accumulation and activity.

Relevance of Biofilms

Biofilms are found in both natural and manmade aquatic systems. In streams and rivers, a large proportion of the microbial activity occurs in attached films.

Wuhrmann (1971) estimated that 90 to 99.99 percent of the bacterial activity in shallow streams is associated with biofilms. Biofilm organisms are responsible for the transformation and degradation of natural and manmade organic compounds in the water.

In industrial systems, biofilm research is usually aimed at the reduction of biofouling (unwanted biofilms). Many deleterious effects of biofilm formation have been reported. Heat transfer efficiency in heat exchangers and condensers is reduced by biofilm accumulation (Characklis et al., 1980 and 1984), and oilfield water injection systems plug with material detached from biofilm. Hydrogen sulfide "souring" of oil reserves may be partially attributable to attached sulfate-reducing bacteria which produce hydrogen sulfide in the oil-bearing formation. With secondary oil recovery becoming standard practice, souring of oil fields has become a major problem whereby the quality of vast oil reserves may be seriously compromised through microbial production of hydrogen sulfide. In a study of a gas storage and production facility (Dziewulski et al., 1990), indigenous microorganisms were implicated in the souring of natural gas when supplied with nutrients by the flow of water in and out of the field during injection and production. Biological plugging of oil sand reservoirs has been examined (Geesey et al., 1987) to determine the potential of the water source to induce biofilm-related plugging of the formation. The highest cell densities and EPS concentrations were found in the region where the water entered the sampled core. This may be the result of higher nutrient concentration at the core inlet or because of filtration of biomass which detached upstream in the process. In the oilfield, plugging around an injection well results in decreased injection rates and/or higher injection pressure. Despite the plugging phenomenon, some researchers (Crawford, 1966;

Lappin-Scott et al., 1988) have applied biofilm technology in an attempt to enhance oil recovery. By plugging the larger pores with biofilm, oil remaining in the smaller pores is presumably exposed to more flow and more oil is recovered. In the laboratory (Torbati et al., 1986), selective plugging of larger pores in sandstone was accomplished using a mixed population with a sucrose-mineral salts medium. The largest pore sizes were reduced from 59 to 69 microns (10^{-6}m) before plugging to 20 to 38 microns (10^{-6}m) after microbial plugging.

Detachment

Biofilm detachment is the process of removal and entrainment in the bulk liquid of biomass from an existing biofilm and is most likely the process which limits the extent of biofilm accumulation on a substratum. Detachment is also one of the least understood processes in terms of the variables which affect the process rates. Computer simulations indicate that the detachment rate coefficient is the most sensitive variable affecting the predicted rate and extent of biomass accumulation, but no expressions have yet been proposed which accurately predict the detachment rate for a wide range of environmental and operating conditions.

The prediction of detachment rates has been a priority in understanding biofouling in drinking water distribution systems, the computer chip industry, paper production, and oilfield injection water pipelines. In each of these industries, detached biomass reduces final product quality and/or increases operating costs. Biofilms in drinking water distribution systems may harbor pathogenic organisms (LeChevallier et al., 1987). Detachment of these organisms and entrainment in the bulk liquid can result in failure to meet drinking water quality standards. The computer chip industry

requires ultrapure water. Biofilm detachment (White et al., 1990) can lead to contamination of delicate components where a single bacterial cell is enough to cause a failure in a computer chip. In the paper industry, detachment of macroscopic biofilm particles results in defects in the paper that can lower product value and reduce the strength of the unfinished paper. This reduction in strength leads to expensive downtime when the paper sheets tear on the paper machine. In oilfield injection water pipelines, increased biomass detachment speeds fouling of pre-injection filters or plugging of the formation itself. This results in more frequent maintenance or replacement of the filters, while formation plugging around an injection well results in decreased injection rates or higher injection pressure. For all these industries, decreasing biofilm detachment rates would reduce operational costs and/or improve product quality.

The experimental program described herein was conducted to determine the influence of two important variables, shear stress and substrate loading rate, on the rate of biofilm detachment and to evaluate mathematical expressions for the prediction of detachment rates.

Research Goal and Objectives

The long term goal of this research is to determine the kinetics of biofilm detachment.

The objectives established for reaching this goal are as follows:

1) Determine the effects of shear stress and substrate loading rate on biofilm accumulation, biofilm density, and, specifically, biofilm detachment.

2) Differentiate between sloughing and erosion as separate detachment processes

based on detached biofilm particle size distributions.

3) Observe the influence of step changes, such as pH, on the biofilm and the detachment phenomenon.

BACKGROUND

Biofilm Processes

The progression of biofilm accumulation typically follows a sigmoidal-shaped curve in terms of biofilm mass, cell numbers or thickness (Figure 1).

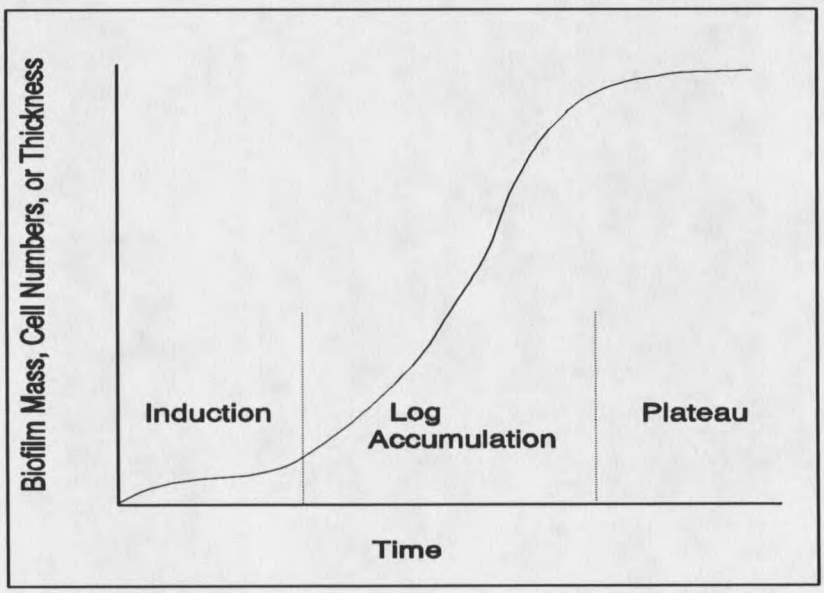

Figure 1. The characteristic progression of biofilm accumulation with time.

Biofilm accumulation is the net result of various processes which can be identified and quantified (Figure 2):

1) Adsorption - the initial colonization of a clean substratum by cells.

2) Desorption - the reentrainment into the bulk fluid of a cell adsorbed to the substratum.

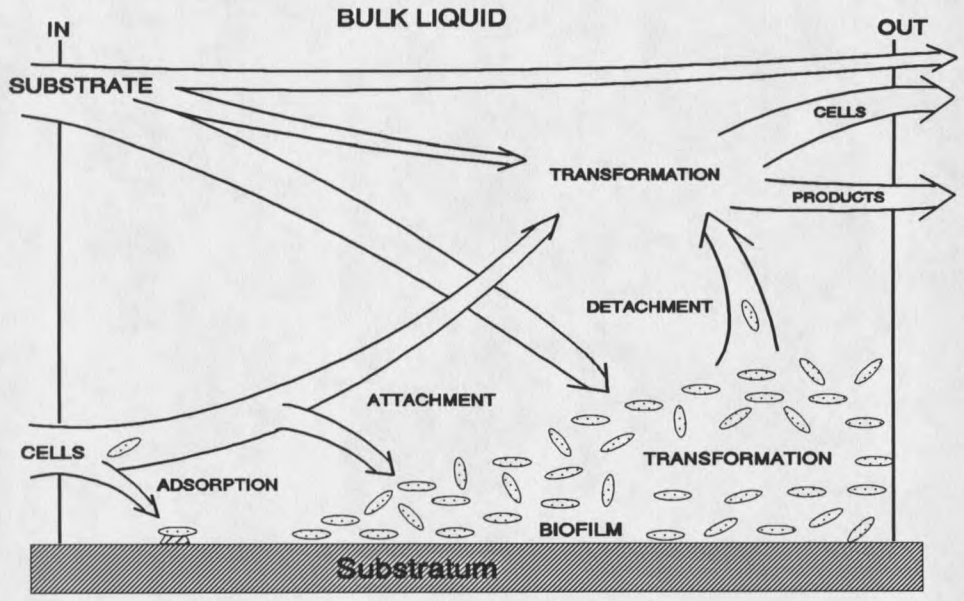

Figure 2. Schematic illustration of processes contributing to biofilm accumulation and activity, including substrate transport and transformation; cellular adsorption and attachment; and detachment of cells and products.

3) Attachment - the acquisition of cells from the bulk liquid by an existing biofilm.

4) Detachment - the entrainment into the bulk fluid of cells from an existing biofilm.

5) Growth - the increase in the number of biofilm cells as a result of replication.

6) Death - permanent loss of a cell's reproductive and metabolic activity.

7) Endogenous decay - biofilm cell metabolism of internal cellular materials.

8) Product formation - the production of polymers and metabolic byproducts in the biofilm.

To mathematically model the accumulation of a biofilm, a material balance is required. The general mass balance equation for biomass in a biofilm is:

$$Accumulation = Input - Output + Transformation \quad (1)$$

In the induction period, *before* a monolayer of biofilm has formed, biomass accumulation can be modelled as follows:

$$\underset{rate}{Accum.} = \underset{rate}{Adsorption} - \underset{rate}{Desorption} + \underset{rate}{Growth} \quad (2)$$

After a monolayer of biofilm has accumulated, the processes of adsorption and desorption become negligible as compared to growth and detachment (Escher and Characklis, 1990), so that the following equation applies:

$$\underset{rate}{Accum.} = \underset{rate}{Attachment} - \underset{rate}{Detachment} + \underset{rate}{Growth} \quad (3)$$

The processes in Eqs. 2 and 3 are described in the following sections.

Adsorption

Adsorption of the Conditioning Film. Immediately upon immersion of a clean surface, organic molecules adsorb to the clean surface. This organic layer is called the conditioning film. Conditioning films are mainly composed of polymers such as glycoproteins (Baier and Weiss, 1975; Baier, 1980) and are not static, but are subject to a high turnover rate (Brash and Samak, 1978). Bryers (1980) measured 1.5×10^{-2} g m^{-2} of chemical oxygen demand (COD) of organic compounds in a conditioning film on glass in a lab system. Little and Zsolnay (1985) have performed similar experiments with stainless steel in seawater and after 0.25 hours obtained up to 0.8×10^{-3} g m^{-2} of adsorbed organic matter. Deposition of proteins has been shown to affect adsorption of bacteria. Meadows (1971) found that albumin inhibited adsorption, while casein and gelatin enhanced microbial adsorption rates. Fletcher (1976) showed a precoating

of a mixture of albumin, gelatin, fibrinogen, and pepsin inhibited the adsorption of a pseudomonad on polystyrene. Although deposition of a conditioning film has been shown to occur before the adsorption of cells to the substratum (Marshall, 1979), it has not been shown to be a *prerequisite* for cell adsorption.

Adsorption of Cells to Surface. The first step in the development of a biofilm is the adsorption of a cell to a solid surface. Adsorption is defined as the interphase accumulation of cells from the bulk liquid directly on the substratum. Processes important to the adsorption phenomenon are shown in Figure 3.

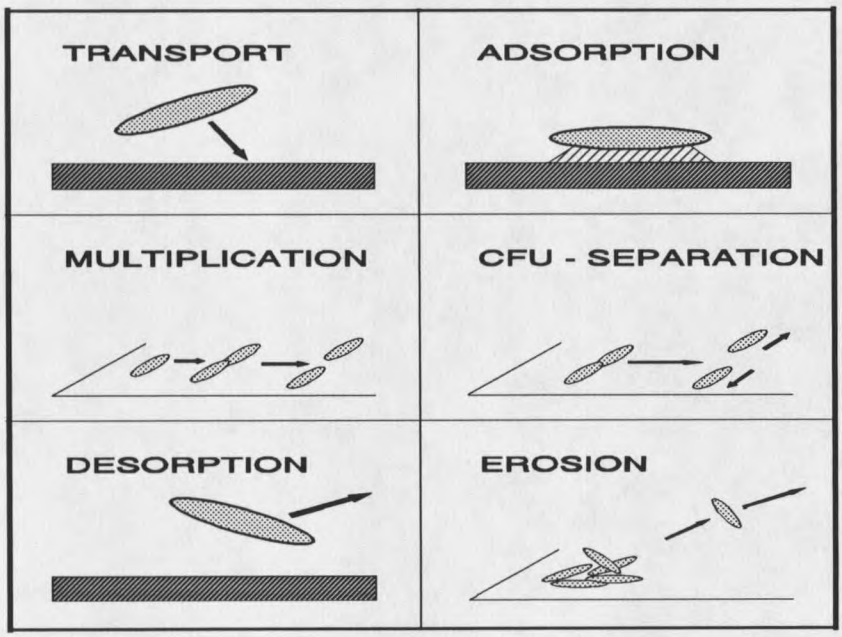

Figure 3. Diagram of the processes fundamental to the initial microbial colonization of a substratum.

CFU-separation, shown in Figure 3, is not important to the adsorption phenomenon itself, but in adsorption studies, cells which have separated on the substratum must be distinguished from cells adsorbing from the bulk liquid. Adsorption plays a major role in biofilm accumulation only in the initial stages of colonization. Subsequently,

growth of cells is the dominant process responsible for the accumulation of a biofilm. Much research has been done on the topic of adsorption; however, only recently have factors such as momentum transport been included in these studies. Shear stress has been shown to play an important role in the sticking efficiency of cells to a substratum (Hermanowicz et al., 1989; Powell and Slater, 1983; Escher and Characklis, 1990). The sticking efficiency is defined as

$$Sticking\ Efficiency = \frac{number\ of\ cells\ adsorbed\ to\ the\ substratum}{number\ of\ cells\ transported\ to\ the\ substratum} \qquad (4)$$

The sticking efficiency is the ratio of the rate of cell adsorption to the rate of transport of cells to the surface, and is, therefore, affected by the fluid flow regime under which the adsorption occurs. In turbulent flow, turbulent bursts from the bulk fluid penetrate to the wall (Cleaver and Yates, 1975 and 1976) and these bursts may contribute significantly to the transport of cells to the surface in turbulent flow (Escher and Characklis, 1990). Other processes which contribute to the transport of cells to the surface in both turbulent and laminar flow are cell motility (Jang and Yen, 1985), Brownian motion, and gravity.

Adsorption is affected by substratum properties (Mueller, 1990), with different materials experiencing varied rates of cellular adsorption under similar flow conditions. Roughness is also believed to strongly influence the adsorption properties of cells in flowing systems. For quiescent conditions, Van Haecke et al. (1990) concluded surface roughness had little effect on the adsorption kinetics of *Pseudomonas aeruginosa* on stainless steel. Under quiescent conditions, the cell surface hydrophobicity was the major parameter affecting adsorption, and measurable adsorption occurred within 30 seconds (8.33×10^{-3}h). The physiological state of the

cells can play an important role in the adsorption rate. Cell adsorption per unit area was found to be linear with specific growth rate history (Nelson et al., 1985) in a turbulent flow system. As the specific growth rate was increased, a linear decrease in adsorbed colony forming units was observed. Dawson (1981) has shown that starved *Vibrio* were more hydrophobic than normal cells, and formed polysaccharide-rich tubules which were believed to enhance adsorption. Extracellular polymeric substances (EPS) may assist in the binding of microbes to a substratum and, thus, influence adsorption. Electron microscopy (Fletcher and Floodgate, 1973; Marshall and Cruickshank, 1973) has shown the presence of EPS adsorbed to a substratum.

Reversible / Irreversible Adsorption. Most research has focused on irreversibly adsorbed cells, where only the cells which have "permanently" adsorbed to the substratum are included in the analysis. However, a few studies (Zobell, 1943; Marshall et al., 1971; Powell and Slater, 1983; Escher, 1986) show that some cells adsorb reversibly. Some cells are adsorbed to the substratum for a finite period of time, then desorb and are reentrained in the bulk liquid. Factors influencing irreversible adsorption are most likely those which also influence reversible adsorption.

Attachment

Attachment is defined as cells from the bulk liquid sticking to an *existing* biofilm. Attachment of cells could play an important role in the displacement of one cell species by another in an existing biofilm. Although methods have been developed and tested to determine the rate of attachment of suspended cells (Gunawan, 1991) and 1 micron ($1x10^{-6}$m) latex beads (Drury, 1992) to an existing biofilm, very little published quantitative information is available.

Detachment

Biofilm detachment is the process of removal and reentrainment of biomass in the bulk fluid. According to Bryers (1987) portions of a biofilm can be removed in any of the following ways: 1) erosion, 2) sloughing , 3) human intervention, 4) predator grazing, and 5) abrasion (Figure 4). Most research has been focused on the areas of erosion and sloughing. Detachment is one of the least understood processes affecting biofilm accumulation, and is probably the most important process limiting both the rate and extent of biofilm accumulation.

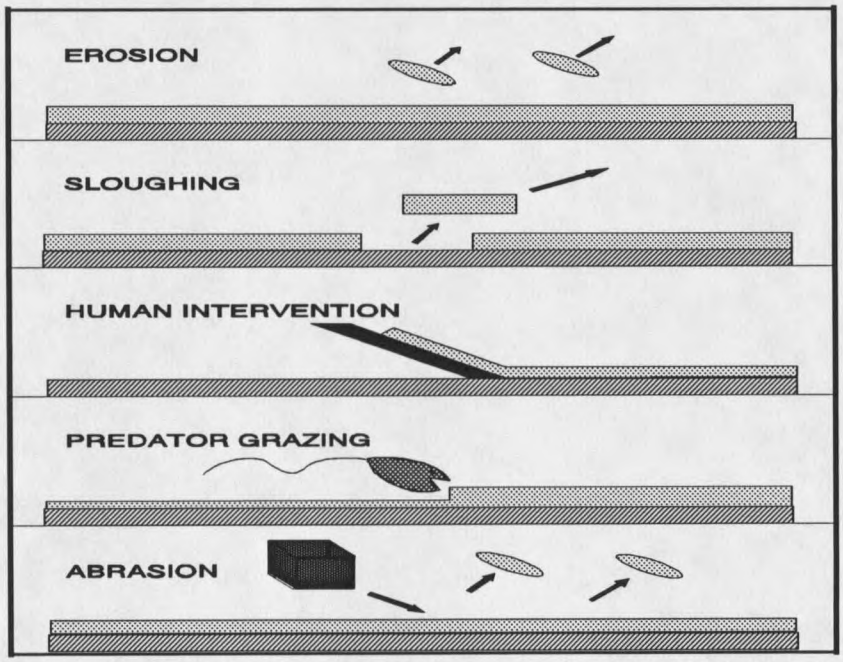

Figure 4. Schematic diagram of the processes contributing to biofilm detachment.

Erosion. Erosion is the removal of small portions of biofilm, thought to be a result of shear forces exerted by moving fluid in contact with the biofilm surface. Erosion is frequently treated as a continuous process, occurring evenly over the entire surface of the biofilm provided environmental conditions are constant. Erosion rate has

been shown to be proportional to the microbial growth rate in monopopulation *Pseudomonas aeruginosa* biofilms (Bakke et al., 1984).

Turakhia and Characklis (1989) observed decreases in the erosion rate of a *Pseudomonas aeruginosa* biofilm with increased free calcium concentration in the bulk liquid. In the initial stages of biofilm development, erosion was not observed with a rough substratum, whereas erosion was evident with a smooth substratum (Chang and Rittman, 1988). It is believed that the cells accumulated in the roughness crevices and were not carried away by bulk liquid flow.

Sloughing. In contrast to erosion, sloughing is the detachment of large portions of a biofilm, and is an apparently random, discrete process. Sloughing often occurs in older, thicker biofilms, or when environmental conditions change rapidly. Biofilms grown in high substrate, low shear stress conditions are particularly susceptible to massive detachment as a result of sloughing. Few researchers have focused on detachment as a result of sloughing, and most have treated it as an annoying phenomena which distorts and complicates biofilm research. Howell and Atkinson (1976) were the first to formally attempt to model sloughing events. In their model, oxygen depletion in the depth of the biofilm triggers a sloughing event. Sloughing has also been theorized to result from substrate depletion deep in a biofilm and subsequent decay of the cell and polymer matrix which holds the biofilm to the substratum (Heukelekian and Crosby, 1956a and 1956b). Sloughing has also been associated with the formation of nitrogen bubbles in denitrifying biofilms (Jansen and Kristensen, 1980). Spontaneous sloughing of biofilm has been observed after step increases in lactose and especially lactate concentrations, while step changes in glucose had no significant effect on biofilm sloughing (Bakke, 1983). In a related paper, a model of

bacterial flocs (Lee et al., 1975) predicts that an increase in substrate concentration causes a breakup of the floc. This is consistent with observations at activated sludge facilities.

Sloughing has been observed after a decrease in substrate concentration. Bott and Miller (1983) observed a 50% decrease in biofilm weight in aluminum tubes at a liquid velocity of 0.5 m s^{-1} (1800 m h^{-1}) within four days after stopping the nutrient supply of 4 g m^{-3} glucose. However at a liquid velocity of 2.0 m s^{-1} (7200 m h^{-1}), the decrease in biofilm weight was insignificant. This data indicate that the fluid conditions under which the biofilm was grown may have an effect on its susceptibility to sloughing. Sloughing has been induced (Turakhia et al., 1983) by the addition of EGTA, a calcium-specific chelant. The divalent calcium ions give tertiary structure to the polymer matrix and may play a major role in the determination of biofilm strength. Thus, calcium removal results in partial collapse of the biofilm structure.

Human Intervention, Predator Grazing, and Abrasion. Detachment via human intervention is the removal of biofilm as a result of chemical or physical means, such as the addition of biocides or scraping with brushes or other abrasive materials. Most of the research in this area is empirical and related to the control of biofouling and corrosion in industrial systems. More fundamental biocide research has been accomplished (Marshall et al., 1989) by searching for mechanisms and direct effects within the biofilm rather than percent kill for a given biocide.

Predator grazing is the consumption of biofilm mass by larger organisms, such as protozoa. This process of biofilm removal does not fit directly under the definition of biofilm detachment, since biomass is not reentrained in the bulk liquid, but the removal process is included here for completeness. Active protozoan predation of a

biofilm community was observed by Fenchel (1986) suggesting predation may benefit a waste water treatment biofilm community by maintaining the bacteria in a more active physiological state. Higher organisms such as snails, worms, and insects will also feed on biofilms (Tchobanoglous, 1979).

The detachment of biomass resulting from collisions of solid particles with the biofilm is termed abrasion. In fluidized bed bioreactors, abrasion is the dominant form of detachment (Chang, 1991), e.g. removal of biofilm in a sand filter during backwash.

Biofilm Properties

Density

Biofilm density is the amount of biomass existing in a given volume of biofilm and is generally reported on a basis of dry mass per unit wet volume (Table 1). Biofilm density is an important parameter in the mathematical modeling of biofilm processes, since biomass concentration is often related to the activity of a biofilm. Typically, biofilm density is measured by determining the average thickness of the biofilm and then scraping a known area of biofilm into a pre-weighed drying dish. The biofilm is dried and the dry weight determined. Density can then be directly calculated. Rittman and McCarty (1980 and 1981) calculated a biofilm density assuming biofilm dry weight is 50% carbon; however, the results are lower than those typically obtained with the more direct method of measurement. The only data available on the variation of biofilm density with biofilm depth is by Masuda et al. (1991) given in Table 2. A "microslicer" was used to section the biofilm. The density was then determined for each biofilm section.

Table 1. A comparison of biofilm volumetric mass density and thickness (dry mass per unit wet volume).

Biofilm Type[a]	Volumetric Density (10^3g m^{-3})	Thickness (10^{-6}m)	Reference
A	66 - 130	160 - 210	(Characklis 1980)
A	50[b]	100	(Rittman and McCarty 1978)
B	20 - 105	30 - 1300	(Hoehn and Ray 1973)
B	5[c]	119 - 126	(Herbert 1976)
B	5[c]	0 - 125	(Rittman and McCarty 1980)
B	10 - 65	10 - 124	(Trulear and Characklis 1982)
C	42 - 109	150 - 580	(Williamson and McCarty 1976)
D	27	0 - 60	(Bakke 1983)

[a] A: steady state, heterotrophic mixed population; B: heterotrophic mixed population; C: steady state, nitrifying mixed population; D: steady state, *Pseudomonas aeruginosa*.
[b] Calculated assuming biofilm is 80% volatile solids.
[c] Calculated assuming biofilm is 50% carbon.

Table 2. Volumetric mass density (ρ_f) with biofilm depth (Masuda et al., 1991).

Film Morphology	Volumetric Density (10^3 dry g m^{-3})	Depth from Bulk Liquid-Biofilm Interface (10^{-6}m)	Thickness of Biofilm Section (10^{-6}m)
Surface Film	37	0 - 400	400
Intermediate	98	400 - 600	200
Base Film	102	600 - 730	130

Biofilm density has been correlated with shear stress. Characklis (1980) reports biofilm density increased with increasing shear stress at low substrate loading rates. This is somewhat in contrast to Kornegay and Andrews (1967) who showed that at

high substrate loading rates no change in biofilm density occurred with changes in shear stress. The relationship between substrate loading rate and shear stress on biofilm density must be determined for more accurate computer simulation of biofilm system behavior.

Film Morphology

A biofilm may be subdivided into two compartments, 1) surface film and 2) base film, and may consist entirely of one compartment or a combination of both.

Surface Film. The surface film is defined as the heterogeneous biofilm region near the biofilm-bulk liquid interface (Figure 5).

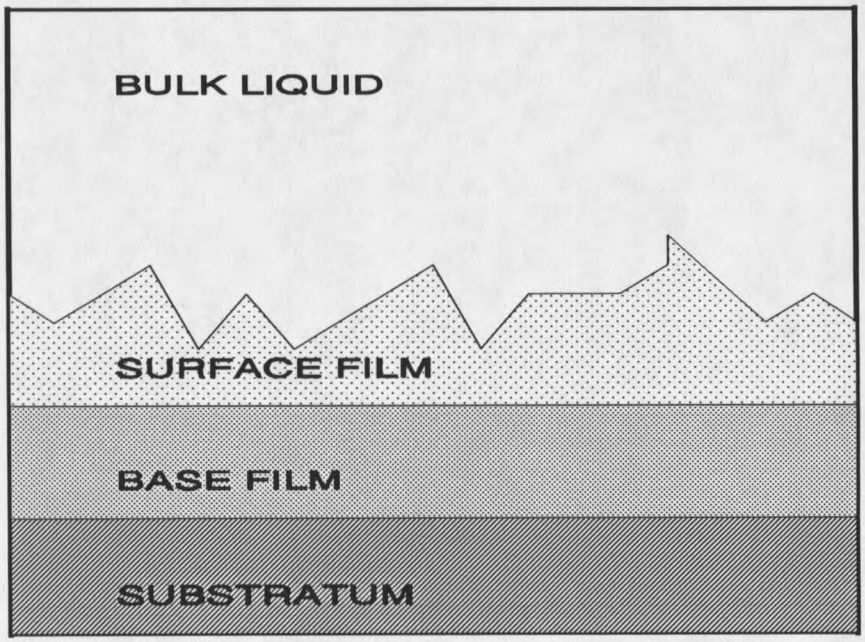

Figure 5. Schematic diagram of the base and surface film.

In turbulent flow, advective transport dominates the movement of nutrients in the surface film. The surface film is characterized by a rough, visco-elastic surface, and

may contribute significantly to fluid friction. The surface film is also believed to influence particle capture in biofilms. Suschka (1987) postulated the existence of a surface film with a different porosity than that of the base film. A three-fold difference in experimentally measured and theoretically calculated residence times in trickling filters led him to the conclusion there must be two liquid film layers; one layer of "free" liquid flowing over the top of the biofilm and another "captured" layer flowing within the biofilm. Detailed study of this rougher surface film has not been addressed except to acknowledge its existence.

Base Film. The base film is a relatively continuous accumulation of cells and polymer, and is more dense than the surface film. The density and continuity provide a structure which may limit the amount of advective transport within the base film. Mass transport of nutrients through the base film is, therefore, thought to be dominated by molecular diffusion.

Material Balances

Material balance equations are necessary for the description and characterization of biofilm process rates. A general material balance equation takes the form given in Eq. 1. This equation can be applied to any reactor geometry and any mass component. In the general case, the reaction rate is represented as one term in the equation. However in actual component material balances, the reaction term can be comprised of as many terms as there are reactions producing or consuming the component. In the following equations, a reaction which produces a component is positive and a reaction which consumes a component is negative. Therefore, all rate coefficients are positive.

Bulk Liquid Compartment Glucose Carbon

$$V\frac{dG_{l(C)}}{dt} = Q(G_{i(C)}-G_{l(C)}) - V\frac{\mu X_{lC(C)}}{Y_{\frac{x}{s}}} - A\, j_{fG(C)} - V\frac{R_{lP(C)}X_{lC(C)}}{Y_{\frac{p}{s}}} \quad (5)$$

Bulk Liquid Compartment Cell Number

$$V\frac{dX_{lC}}{dt} = Q(X_{iC}-X_{lC}) + V\mu X_{lC} - A\, R_a + A\, R_d \quad (6)$$

Bulk Liquid Compartment Product Carbon

$$V\frac{dP_{l(C)}}{dt} = Q(P_{i(C)}-P_{l(C)}) + VR_{lP(C)}X_{lC(C)} + A\, j_{lP(C)} \quad (7)$$

Biofilm Compartment Glucose Carbon

$$V\frac{dG_{f(C)}}{dt} = A\, j_{fG(C)} - A\frac{\mu X_{fC(C)}}{Y_{\frac{x}{s}}} - A\frac{R_{fP(C)}X_{fC(C)}}{Y_{\frac{p}{s}}} \quad (8)$$

Biofilm Compartment Cell Number

$$A\frac{dX_{fC}}{dt} = A\mu X_{fC} + A\, R_a - A\, R_d \quad (9)$$

Biofilm Compartment Product Carbon

$$A\frac{dP_{f(C)}}{dt} = A\, R_{fP(C)}X_{fC(C)} - A\, j_{lP(C)} \quad (10)$$

Detachment Models

The importance of biofilm detachment can be illustrated mathematically by considering an ideal biofilm. At steady state, the accumulation term of Eq. 9 is zero and can be rearranged to give Eq. 11, which shows that for steady state biofilms, the detachment rate equals the sum of the biomass attachment rate and the growth rate.

$$R_{dC} = R_{aC} + \mu X_{fC} \tag{11}$$

For systems with low suspended cell concentrations, typical of a vessel with a short residence time, the attachment rate is low (Gunawan, 1991) such that

$$R_{aC} << \mu X_{fC} \tag{12}$$

and Eq. 11 reduces to

$$R_{dC} = \mu X_{fC} \tag{13}$$

This is a simplified model of a biofilm because the specific growth rate may not be the same throughout the entire biofilm due to possible diffusional resistances. However, Eq. 13 indicates that, at steady state, the net rate of growth in the biofilm, μX_{fC}, must equal the net rate of biofilm detachment. The expression is a first order detachment rate in total biomass. The first order expression has been frequently used (Rittman, 1982; Kreikenbohm and Stephan, 1985; Chang and Rittman, 1987) in biofilm modelling.

For computer simulation of biofilm accumulation in both laboratory and industrial systems, a mathematical expression for each biofilm process is required.

Numerous expressions have been proposed for calculating the rate of biofilm detachment. While each has given reasonable results for the specific experimental conditions to which it was applied, none are general enough to extrapolate to other environmental conditions. The abundance of detachment rate equations partially reflects the failure of any one expression to model the detachment rate over a wide range of conditions. The variables previously incorporated into biofilm detachment expressions include the following: areal biomass density, X_f (M L^{-2}); volumetric biomass density, ρ_f (M L^{-3}); biofilm thickness, L_f (L); shear stress, τ (M L^{-1} t^{-2}); and specific growth rate, μ (t^{-1}).

An expression for detachment as a first order function of shear stress and biomass concentration is given by Bakke et al. (1990).

$$R_d = k_d \tau \rho_f \qquad (14)$$

In a turbulent flow pipeline system, Bakke solved the equation to explicitly include bulk fluid velocity, which resulted in Eq. 15.

$$R_d = k_d v^{1.75} X_f \qquad (15)$$

Bakke (1986) concluded that changes in shear stress had no lasting effect on the detachment rate. A step change in the shear stress did result in a brief increase in detachment rate, but after five residence times at the higher shear stress, detachment rate returned to the previous steady state rates. At this time, there is no data to support the detachment rate expressions proposed in Eqs. 14 and 15.

Other models employ a second order detachment rate with respect to biofilm mass (Bryers, 1984; Crawford, 1987; Trulear and Characklis, 1982):

$$R_d = k_d X_f^2 \quad (16)$$

In a multi-species biofilm model, a second order (in biofilm thickness) detachment rate expression was used (Wanner and Gujer, 1986):

$$R_d = k_d L_f^2 \rho_f \quad (17)$$

Eq. 17 incorporates two important biofilm properties (Characklis et al., 1990):

1) Hydrodynamic erosion may be related to biofilm thickness, L_f, and

2) Biofilm strength may be related to biofilm density, ρ_f.

Second and higher order detachment rate expressions permit steady state in simplified mathematical simulations where the substrate concentration is assumed to be constant throughout the biofilm. If a first order detachment expression is used, the model will *not* predict a steady state. The biofilm will either continue growing *ad infinitum* or disappear altogether.

Speitel and DiGiano (1987) propose an expression for the detachment rate which includes a first order function in biofilm mass with the addition of a growth-related detachment term to give the following detachment rate expression:

$$R_d = L_f (k'_d + k''_d \mu) \quad (18)$$

Eq. 18 fits the experimental data better than a simple first order detachment expression during periods of high biofilm accumulation rates. The growth-related detachment was incorporated to account for the high biofilm loss rates observed during periods of high substrate degradation rate. The experiments were performed in granular activated carbon columns using effluent suspended biomass to determine

biofilm detachment rates. The growth-associated erosion coefficient, k''_d, appears to be substrate specific.

In an experimental apparatus similar to Speitel and DiGiano, Chang and Rittman (1988) observed high detachment rates during periods of high growth. During periods of rapid biofilm growth, biofilm erosion rate increased, but not as described by a first order detachment function. Trulear and Characklis (1982) reported biofilm detachment rate as a function of biofilm mass, but the data from two separate experiments were graphically combined and interpreted with one function. In light of the data presented by Speitel and DiGiano (1987) concerning the relationship between growth rate and biofilm detachment, the data reported by Trulear and Characklis indicate growth-related detachment (Figure 6).

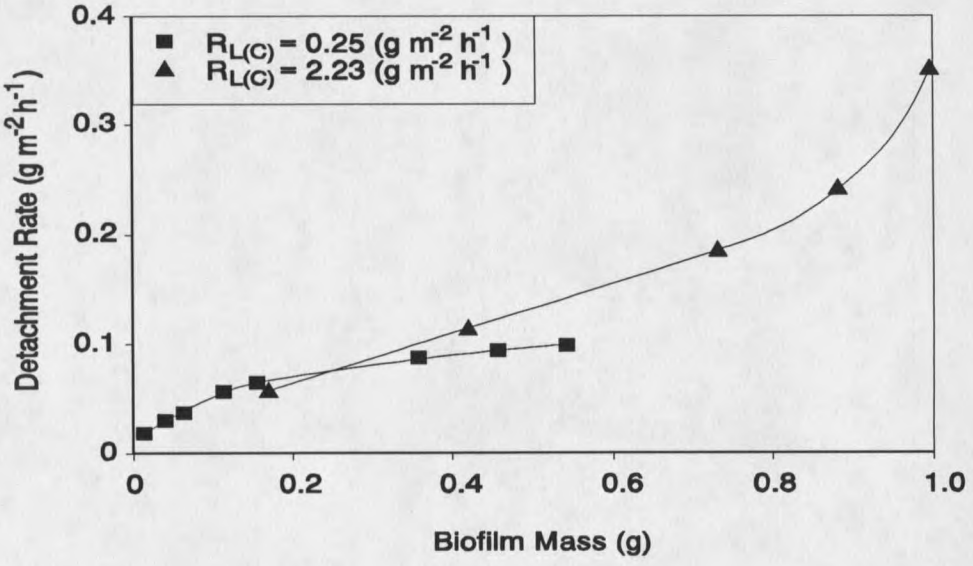

Figure 6. Detachment rate versus total biofilm mass in identical reactors at two substrate loading rates (Trulear and Characklis 1982). Detachment rate increased with increased substrate loading rate.

Qualitatively, at a higher substrate loading rate, the growth rate is higher and, therefore, the detachment rate should be higher for a given amount of biomass. It appears that for $R_{L(C)}$ = 0.25 g m^{-2} h^{-1} and biofilm mass = 0.4 g, the detachment rate remains nearly level at 0.1 g m^{-2} h^{-1}, while at $R_{L(C)}$ = 2.23 g m^{-2} h^{-1} and biofilm mass = 0.4 g, the detachment rate is just beginning to increase rapidly. Rittman (1982) also uses the data of Trulear and Characklis to calculate an "erosion loss coefficient". However, Rittman also ignores the fact that the data were obtained under two different substrate loading rates.

The research of Chang and Rittman (1988) compares the effects of surface irregularities on biofilm shear losses and accumulation in packed columns of granular activated carbon (GAC). By using spherical and irregularly shaped GAC, values for a first order erosion coefficient were estimated. During the induction period, the irregularly shaped GAC showed greater cellular attachment and no erosion. However, as biofilm accumulated, the erosion coefficient for both types of GAC began to increase. Finally, at steady state, the erosion coefficients for both the spherical and irregular GAC approached the same values. Thus, surface roughness and shear stress may play an important role in initial events, but becomes less important to detachment rates after the biofilm completely covers the surface irregularities. It has not been shown how the surface roughness affects the rate and amount of sloughing.

A summary of proposed detachment models is given in Table 3.

Table 3. Summary of proposed detachment rate expressions.

Eq. #	Reported Detachment Rate Expression R_d [=] M L^{-2} t^{-1}	Reference(s)
(16)	$k_d X_f^2$	(Trulear and Characklis, 1982) (Bryers, 1984) (Crawford, 1987)
(19)	$k_d \rho_f L_f \tau^{0.58}$	(Rittman, 1982)
(17)	$k_d \rho_f L_f^2$	(Wanner and Gujer, 1986)
(18)	$L_f(k'_d + k''_d \mu)$	(Speitel and DiGiano, 1987)
(20)	$k_d \rho_f L_f = k_d X_f$	(Chang and Rittman, 1987) (Rittman, 1989) (Kreikenbohm and Stephan, 1985)
(14)	$k_d \rho_f \tau$	(Bakke et al., 1990)

Derivation of Proposed Detachment Rate Expression

An expression for calculating the detachment rate was derived from an empirical modification of the suspended cell material balance on a biofilm reactor. The general material balance on cells in a biofilm reactor yields the following equation:

$$V\frac{dX_{lC(C)}}{dt} = Q(X_{iC(C)} - X_{lC(C)}) + \mu X_{lC(C)}V + R_{dC(C)}A - R_{aC(C)}A \qquad (21)$$

Appropriate to this thesis, Eq. 21 can be simplified by the following assumptions: 1) a sterile influent ($X_{iC(C)} << X_{lC(C)}$); 2) the attachment rate of cells is much lower than the detachment rate ($R_{aC(C)} << R_{dC(C)}$); 3) the short reactor cell residence time, 0.25

hours, renders growth in suspension negligible ($\mu X_{1C(C)} V << R_{dC(C)} A$); and 4) the reactor is at pseudo-steady state with regard to the effluent cell concentration ($V dX_{1C(C)}/dt << R_{dC(C)} A$). Thus, Eq. 21 reduces to Eq. 22, which indicates that the detachment rate is proportional to the effluent suspended cell concentration.

$$R_{dC(C)} = \frac{Q}{A} X_{1C(C)} \tag{22}$$

The dependence of detachment rate on substrate utilization rate can be established by using the definition of the cellular yield, at steady state in a biofilm reactor (Eq. 23).

$$(X_{1C(C)} - X_{iC(C)})_{ss} = (S_{i(C)} - S_{(C)})_{ss} Y_{\frac{x}{s}} \tag{23}$$

For a sterile influent, combining Eq. 23 and Eq. 22 gives Eq. 24 which indicates steady state detachment rate is proportional to substrate utilization rate with the proportionality coefficient equal to the cellular yield.

$$R_{dC(C)_{ss}} = \frac{Q}{A}(S_{i(C)} - S_{(C)})_{ss} Y_{\frac{x}{s}} = R_{fC(C)} \tag{24}$$

Eq. 24 is also the biomass production rate and determines the upper bound on the detachment rate for a given set of environmental conditions. However, Eq. 24 does not describe the detachment rate at unsteady state.

For the description of detachment rates at both steady and unsteady state, an empirical modification to Eq. 24 is proposed. Detachment rate has been expressed as a first order function of biofilm thickness by others (Table 3). Film thickness is a fundamental variable, is easy to monitor on a routine basis, and has been used in a

proposed mechanistic detachment model (Stewart, 1992). It is proposed that the detachment rate expression should be proportional to the product of the substrate utilization rate, cellular yield, and biofilm thickness:

$$R_{dC(C)} = k_d \frac{Q}{A}(S_{i(C)} - S_{(C)}) Y_{\frac{x}{s}} L_f \qquad (25)$$

EXPERIMENTAL APPROACH

The overall experimental approach was to allow a biofilm to accumulate under well defined environmental conditions. Shear stress and substrate loading rates were varied from one experiment to another in a manner which simplified statistical analysis of the results. The primary objective of this investigation was to determine the influence of shear stress and substrate loading rate on biofilm detachment rate.

Microbial Species

A pure culture of *Pseudomonas aeruginosa* was used in this experimental program. The species is a Gram negative, motile, facultative aerobe capable of denitrification. Separate vials of the stock culture were maintained in glycerol at -40°C to insure a reproducible inoculum. The *Ps. aeruginosa* strain is a known biofilm former (Bakke et al., 1984) for which growth kinetic and stoichiometric coefficients have been determined previously (Robinson et al., 1984).

Two undefined mixed population experiments were inoculated with effluent water from the Center's reverse osmosis system. The mixed population and monopopulation *Ps. aeruginosa* experiments were identical in all other respects.

Nutrient Medium

The nutrient medium utilized in this research is identical to that used by Siebel (1987), with the exception of the calcium concentration, which was lower in order to

prevent calcium phosphate precipitation. Bacteria were grown on a minimal salts medium with glucose as the sole carbon and energy source. The composition of the various media, as delivered to the reactor, are given in Table 4.

Table 4. Media composition entering RotoTorque reactor. All units in g m^{-3}.

Inlet glucose concentration =	2	10	18
Glucose carbon	0.8	4.0	7.2
NH_4Cl	0.72	3.6	6.5
$MgSO_4 \cdot 7H_2O$	0.2	1.0	1.8
$(NH_4)_6Mo_7O_{24} \cdot 4H_2O$	0.0001	0.0005	0.0009
$ZnSO_4 \cdot 7H_2O$	0.01	0.05	0.09
$MnSO_4 \cdot H_2O$	0.0008	0.004	0.0072
$CuSO_4 \cdot 5H_2O$	0.0002	0.001	0.0018
$Na_2B_4O_7 \cdot 10H_2O$	0.0001	0.0005	0.0009
$FeSO_4 \cdot 7H_2O$	0.0112	0.056	0.1008
$(HOCOCH_2)_3N$	0.04	0.2	0.36
$CaCl_2$	0.003	0.015	0.027
Na_2HPO_4	95.5	95.5	95.5
KH_2PO_4	102.0	102.0	102.0

Concentrated micronutrient solutions were prepared in 11 liter ($1.1 \times 10^{-2} m^3$) Nalgene bottles and autoclaved for 4 hours at 121°C. After autoclaving, 20 ml ($2 \times 10^{-5} m^3$) of sterile concentrated glucose solution was added to each micronutrient bottle to give a final glucose concentration of 500 g m^{-3}. Concentrated phosphate buffer solution was prepared in 3.5 liter ($3.5 \times 10^{-3} m^3$) glass containers and autoclaved for 1 hour. Dilution water consisted of distilled water filtered through two 0.2 micron ($2 \times 10^{-7} m$) Gelman cartridge filters. Concentrated micronutrient solution and concentrated buffer solution were mixed with dilution water immediately prior to entering the biofilm reactor. Micronutrient flow rates were adjusted to give the desired influent concentration of either 0.8, 4.0 or 7.2 g glucose carbon m^{-3}. This resulted in substrate

loading rates of 0.0102, 0.0512, and 0.0922 g glucose carbon m^{-2} h^{-1}, respectively. The pH was buffered at 6.7 ± 0.02 throughout the experimental series.

Rotating Annular Reactor (RotoTorque)

The RotoTorque reactor design (Figure 7) has proved to be very versatile for biofilm research and has several characteristics which make it superior to other biofilm reactors. The first of these characteristics is independent control of shear stress. The inner cylinder can be rotated at any speed and the torque can be measured (Characklis and Roe, 1984) to determine average shear stress on the biofilm. This permits quantitative monitoring and control of shear stress independent of the flow rate through the reactor. The RotoTorque also has a large surface area to volume ratio, which means a large amount of biomass can be produced with relatively low volumetric flow rates, while still maintaining a short residence time to minimize growth of suspended organisms. Twelve removable coupons allow direct sampling of biofilm without taking the reactor off line. Draft tubes inside the inner cylinder completely mix the reactor contents, giving it the mixing characteristics of a CFSTR (Trulear, 1983). A more detailed description of the RotoTorque is given in Appendix A.

Cleaning and Preparation

The RotoTorque reactor was disassembled and cleaned before each experiment. The cleaning procedure consisted of scrubbing the reactor and removable coupons with a brush and hot water containing "Micro" lab soap. Harsh chemicals were not utilized because of possible residual effects. After the reactor had been thoroughly cleaned, it was reassembled and autoclaved empty for 0.5 hours at 121°C.

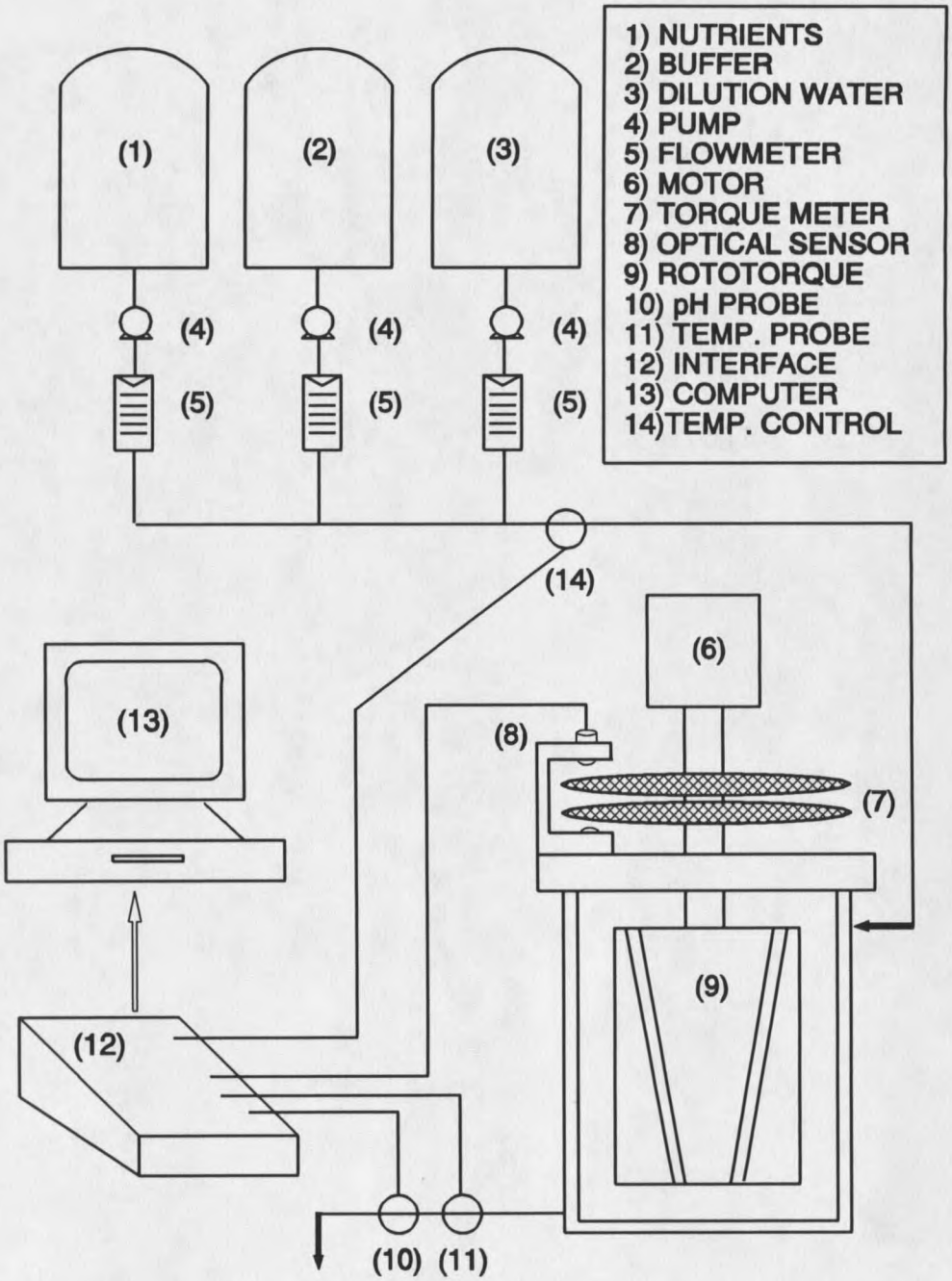

Figure 7. Experimental apparatus including the RotoTorque.

Start-up Protocol

The RotoTorque and tubing were autoclaved for 0.5 hours at 121°C and allowed to cool. After attaching the glucose/micronutrient, phosphate buffer, and dilution water tubes, the reactor was filled by pumping in a 1:1:10 mixture of the three solutions, respectively. Once the reactor was full, the flow was stopped and 0.5 ml ($5.0 \times 10^{-7} m^3$) of the *Ps. aeruginosa* stock culture (10^{19}cells m^{-3}) was introduced into the reactor. The RotoTorque was operated in batch mode at 200 rpm for 24 hours, at which point liquid flow was initiated and the rpm was set to the desired value. This time was defined as experimental time zero. The phosphate buffer volumetric flow rate was constant at 24 ml h^{-1} ($2.4 \times 10^{-5} m^3$ h^{-1}) throughout all experiments. The glucose/micronutrient solution volumetric flow rate was adjusted to give the desired influent glucose concentration. The flow rate of the dilution water was adjusted to give a total volumetric flow rate of 2382 ml h^{-1} ($2.382 \times 10^{-3} m^3$ h^{-1}). This resulted in the value of $QA^{-1} = 1.281 \times 10^{-2} m$ h^{-1}.

Operating Conditions

The temperature, pH, rotational speed, and torque were monitored with a laboratory interface (SCI Technologies, Bozeman, MT). Readings were continuously logged by computer. The reactor temperature was maintained at 20 ± 0.1°C with a water bath (Neslab, Portsmouth, NH). Rotational speed was maintained at 200 ± 0.3, 302 ± 0.5, or 400 ± 0.6 rpm. A torque transducer mounted on the drive shaft between the reactor and the motor was continuously monitored to record changes in frictional resistance. The reactor was operated with a residence time of 0.25 hours ($D = 4$ h^{-1}), minimizing the effects of cellular growth in suspension.

Analytical Methods

Glucose Analysis

Glucose was analyzed utilizing the Sigma Diagnostics® enzymatic glucose determination kit (Sigma procedure 510). Reactor effluent samples were filtered with a 0.2 micron ($2x10^{-7}m$) syringe cellulose nitrate filter into 20 ml ($2x10^{-5}m^3$) polyethylene scintillation vials. All glucose samples were frozen immediately after sampling, and were analyzed after the experiment was completed. The Sigma procedure is designed to measure up to 3000 g m^{-3} and had to be modified to reflect the lower concentrations used in this work. By not diluting the sample 1:20, concentrations up to 150 g m^{-3} can be measured. The following reagent volumes were used for two glucose concentration ranges:

1) 0 - 10 g m^{-3} glucose: 2.5 ml ($2.5x10^{-6}m^3$) sample and 5 ml ($5.0x10^{-6}m^3$) combined color reagent.

2) 10 - 150 g m^{-3} glucose: 0.5 ml ($5.0x10^{-7}m^3$) sample and 5 ml ($5.0x10^{-6}m^3$) combined color reagent.

Total Organic Carbon

Liquid effluent samples (20 ml [$2.0x10^{-5}m^3$]) were placed in glass scintillation vials which had been cleaned in a 450° C furnace for a minimum of 3 hours. Samples were immediately frozen for later organic carbon analysis.

Thawed samples were acidified to pH 2 with concentrated phosphoric acid and then externally purged with oxygen to remove inorganic carbon as CO_2. Organic carbon determination was made with an ultraviolet-promoted persulfate oxidation followed by infrared detection (Dohrmann DC-80 total organic carbon analyzer).

Soluble Organic Carbon

Two liquid effluent samples (40 ml [$4.0 \times 10^{-5} m^3$]) were placed in stainless steel centrifuge tubes and centrifuged at 20,000 rpm, 4°C for 0.25 hours. The top 5 ml ($5 \times 10^{-6} m^3$) of liquid from each centrifuge tube was then carefully decanted into glass scintillation vials which had been ignited at 450°C for a minimum of 3 hours. The decanted 10 ml ($1.0 \times 10^{-5} m^3$) samples were frozen until organic carbon analysis (see TOC above). This method was developed in an effort to reduce experimental error in SOC measurements.

Biofilm Thickness

Biofilm thickness was measured with an optical microscope using the method of Bakke and Olsson (1986). The optical thickness is not the same as the actual mechanical thickness because of differences in the refractive index of air and water. Therefore, a correction factor must be applied, according to Bakke and Olsson:

$$MechanicalBiofilmThickness = OpticalBiofilmThickness \times \frac{4}{3} \qquad (26)$$

Eight thickness measurements were taken for each biofilm coupon removed. The standard deviation of the thickness is an indirect measure of biofilm roughness (Figure 8). In this thesis the terms "film thickness" and "biofilm thickness" refer to the average mechanical thickness.

Biofilm Areal and Volumetric Density

Biofilm was scraped from a known area of the RotoTorque coupon into a preweighed aluminum dish, which had been dried at 104°C overnight. The dish

containing biofilm was permitted to dry overnight and was weighed again to determine dry mass. The biofilm areal density was calculated as follows:

$$Biofilm\ Areal\ Density = \frac{Scraped\ Biofilm\ Weight}{Scraped\ Biofilm\ Area} \quad (27)$$

The volumetric density was calculated by dividing the areal density by the average biofilm thickness.

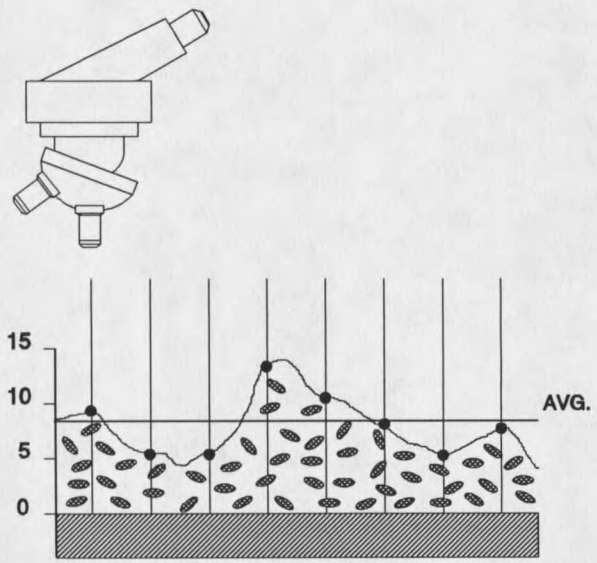

Figure 8. Schematic of biofilm thickness measurement indicating biofilm roughness and average thickness.

Water Content

For experiments R0 and R1 the biofilm water content was measured. A removed coupon was allowed to drain in a vertical position for 2 minutes (0.0333 h). Biofilm was scraped into a preweighed pan and weighed immediately. It was then permitted to dry overnight and weighed again to determine the dry mass. Percent water was determined by subtracting the dry weight to wet weight ratio from one. Water content results for experiments R0 and R1 are given in Appendix C.

Effluent Particle Size Distribution

RotoTorque effluent (10 ml [$1x10^{-5}m^3$]) was placed in a plastic scintillation vial which contained 10 ml ($1x10^{-5}m^3$) of phosphate buffered formalin. This was refrigerated, but not frozen, until analysis. A volume of 1 ml ($1.0x10^{-6}m^3$) of Hoechst stain (#33342 at 56 g m^{-3} or 100 μM) was added to 1 ml ($1.0x10^{-6}m^3$) of the sample. The sample was vortex mixed, covered, and allowed to sit for 0.75 hours. After 0.75 hours, 1 to 4 ml ($1.0x10^{-6}$ to $4.0x10^{-6}$ m^3) of cell-free water was added to the vial and mixed. Of this mixture, between 1 and 5 ml ($1.0x10^{-6}$ and $5.0x10^{-6}$ m^3) were then filtered through a 25 mm, 0.2 micron (0.025 m, $2.0x10^{-7}$m) pore size Ergalan black stained filter. The filter was then examined with an image analyzer (American Innovisions, San Diego, CA) to determine the size and number of the effluent particles. Thirty frames were analyzed to increase the accuracy, compared to 10 frames used for a standard cell count. Particle sizes were divided into 10 logarithmic size divisions which range from 0.122 to 122 square microns ($1.22x10^{-13}m^2$ to $1.22x10^{-10}m^2$) for histogram generation.

Cell Concentration

Effluent suspended cell concentrations were determined in the same manner as effluent particle size distributions were determined with two exceptions: 1) samples were homogenized with a tissue homogenizer and 2) ten frames were counted.

To convert cell numbers to cell carbon, the factor $1.462x10^{13}$ cells [g cell Carbon]$^{-1}$ was used. This factor is the product of average cell volume ($5.81x10^{-19}m^3$ $cell^{-1}$) (this research), wet cell specific gravity ($1.07x10^{-6}$g wet cell m^{-3}) (Doetsch and Cook, 1973), dry cell mass to wet cell mass ratio (0.22 g dry cell [g wet cell]$^{-1}$) (Luria,

1960), and cellular carbon content (0.5 g cell Carbon [g dry cell]$^{-1}$) (Doetsch and Cook, 1973; Luria, 1960).

Carbohydrate Analysis

At the end of experiments S4, T4, and R8, intact biofilm samples (~0.01 g) were scraped into microcentrifuge vials, lyophilized, and sent to Dr. Russell Carlson (University of Georgia Complex Carbohydrate Research Center, 220 Riverbend Road, Athens, GA, 30602). The samples were analyzed for glycosyl composition by the TMS methylglycosides and alditol acetate derivatives methods described by York et al. (1985).

Electron Microscopy

Polycarbonate filters were cut into 1 cm X 1 cm ($1.0x10^{-2}$m X $1.0x10^{-2}$m) squares and then taped to the RotoTorque coupons with waterproof tape. The filter was then removed and preserved according to the method given in Appendix B until transmission or scanning electron microscopy could be done.

Torque

The torque was monitored continuously and recorded every eight hours throughout the experiment. The monitoring apparatus consisted of two aluminum disks in the RotoTorque drive train. These disks would have been free to rotate independently except for a calibrated spring which connected the two. The disks were designed so that a change in torque resulted in a change in the opening created by a gap in each disk (Characklis and Roe, 1984). The gap distance was monitored optically (SCI Laboratory Interface). Detailed information on the measurement and calculation of torque are given in Appendix F.

Statistical Methods

A 3^2 factorial experimental design (Petersen, 1985) was used to determine the effects on biofilm cellular detachment rate of substrate loading rate and shear stress, each at three levels. The three rotational speeds were 200, 300, or 400 rpm, resulting in shear stresses of 1.44, 2.20 and 2.97 N m^{-2}, respectively. The influent glucose carbon concentration was adjusted to either 0.8, 4.0, or 7.2 g glucose carbon m^{-3}, giving substrate loading rates, $R_{L(C)}$, of 1.02×10^{-2}, 5.12×10^{-2}, and 9.22×10^{-2} g glucose carbon m^{-2} h^{-1}, respectively. Table 5 gives the number of experiment replications at each condition.

Table 5. Statistical experiment design.

		Influent Glucose Conc.		
		0.8 g m^{-3}	4.0 g m^{-3}	7.2 g m^{-3}
Rotational Speed	200 rpm	1	1	1
	300 rpm	1	3	1
	400 rpm	1	2	1

Each replication is a separate, independent experiment, with twelve monopopulation *Ps. aeruginosa* experiments performed altogether. An advantage of this design is the ability to distinguish the main effects of each factor (shear stress or substrate loading rate) and any possible interactive effects between the two. Data was analyzed with the statistical software package "MSUSTAT", which was used for the analysis of

variance and multiple regression (MSUSTAT, 1986). Significance was determined at the 95% level ($p=0.05$).

Throughout the thesis, data are reported as the mean ± standard error. In some cases, which are clearly noted, the standard *deviation* of the biofilm thickness is used. This is because the biofilm roughness is defined as the standard deviation of the biofilm thickness, whereas the standard error does not directly reflect the film roughness.

RESULTS

Biofilm experiments were conducted at three different rotational speeds and three substrate loading rates. During these experiments the following variables were measured:

1) Biofilm
- Thickness (L_f)
- Roughness (std. dev. of L_f)
- Areal and volumetric mass density (X_f and ρ_f)
- Areal and volumetric cell density (X_{fC} and ρ_{fC})
- Areal and volumetric TOC density ($X_{f(C)}$ and $\rho_{f(C)}$)

2) Bulk liquid
- Glucose concentration ($G_{l(C)}$)
- Suspended cell concentration (X_{lC})
- Total organic carbon concentration (TOC)
- Soluble organic carbon concentration (SOC)

Monopopulation Data

A comprehensive listing of the raw experimental data is given in Appendix C, D, and E for rotational speeds 200, 300, and 400 rpm, respectively. A summary of experimental conditions and steady state results is given in Table 6, with steady state process rates given in Table 7. A statistical analysis of variance (ANOVA) was performed on the steady state values of many of the variables measured. A summary of the results of this analysis are given in Table 8, with the full ANOVA results given

Table 6. Summary of experimental conditions and steady state results.

Exp. Code	rpm	τ	$S_{i(C)}$	$\overline{S}_{(C)}$	$\overline{X}_{lC}$	$\overline{L}_f$	$\overline{X}_f$	$\overline{\rho}_f$
R0	200	1.44	7.2	0.55	19.70	31.9	0.64	18.4
R1	200	1.44	4.0	0.61	11.43	15.8	0.79	48.9
R2	200	1.44	0.8	0.45	01.68	06.2	0.39	61.6
R3	300	2.20	7.2	0.43	18.85	31.0	1.21	45.2
R4	300	2.20	4.0	0.36	08.90	19.5	1.00	48.8
S4	300	2.20	4.0	0.56	07.46	18.6	0.84	42.7
T4	300	2.20	4.0	0.56	06.69	17.3	0.64	42.3
R5	300	2.20	0.8	0.32	00.77	07.4	0.74	97.2
R6	400	2.97	7.2	1.47	17.43	31.6	1.60	54.5
R7	400	2.97	4.0	0.72	06.04	20.6	1.04	50.7
S7	400	2.97	4.0	0.56	07.29	19.2	0.92	44.1
R8	400	2.97	0.8	0.25	02.30	04.1	0.20	37.2

Units:
$S_{i(C)}$, $S_{(C)}$ [=] g GC m^{-3}
X_{lC} [=] 10^{12} cells m^{-3}
τ [=] N m^{-2}
L_f [=] 10^{-6} m
X_f [=] dry g wet m^{-2}
ρ_f [=] 10^3 dry g wet m^{-3}

Table 7. Steady state values for the substrate carbon utilization rate and the cell carbon detachment rate.

Exp. Code	τ	$R_{L(C)}$	$R_{U(C)ss} \pm SE(R_{U(C)ss})$	$R_{dC(C)ss} \pm SE(R_{dC(C)ss})$
R0	1.44	92.2	84.80 ± 0.86	17.25 ± -
R1	1.44	51.2	43.84 ± 0.28	06.97 ± 0.70
R2	1.44	10.2	04.19 ± 0.23	01.64 ± 0.18
R3	2.20	92.2	86.72 -	16.99 ± 0.46
R4	2.20	51.2	46.68 ± 1.00	07.81 ± 0.48
S4	2.20	51.2	43.86 ± 0.27	06.54 ± 0.65
T4	2.20	51.2	44.24 ± 0.15	05.86 ± 0.46
R5	2.20	10.2	06.64 ± 1.02	00.68 ± 0.07
R6	2.97	92.2	73.43 ± 1.06	15.27 ± 0.78
R7	2.97	51.2	41.67 ± 0.42	05.29 ± 1.51
S7	2.97	51.2	44.31 ± 0.44	06.38 ± 0.58
R8	2.97	10.2	07.64 ± 0.70	02.02 ± 0.24

Units: $R_{L(C)}$, $R_{U(C)ss}$ [=] 10^{-3} g GC m^{-2} h^{-1}
$R_{dC(C)ss}$ [=] 10^{-3} g CC m^{-2} h^{-1}
τ [=] N m^{-2}

Table 8. Summary of results from ANOVA of measured dependent variables at steady state against independent variables of shear stress and substrate loading rate.

Variable	p-value*	
	$R_{L(C)}$	τ
Biofilm Characteristics		
Biofilm Thickness	<0.0001	0.7945
Biofilm Roughness	<0.0001	0.0690
Biofilm Areal Mass Density	<0.0001	0.0132
Biofilm Volumetric Mass Density	0.1268	0.1293
Biofilm Areal Cell Density	<0.0001	0.1798
Biofilm Volumetric Cell Density	0.0260	0.1797
Biofilm Areal TOC	0.1491	0.0072
Bulk Liquid Characteristics		
Glucose Concentration	<0.0001	<0.0001
Suspended Cell Concentration	<0.0001	0.5202
Biofilm Process Rates		
Glucose Utilization Rate	<0.0001	<0.0001
Cellular Detachment Rate	<0.0001	0.5202

* The p-value is the probability that the true value of the dependent variable is the same at all three values of the independent variable.

in Appendix G. Throughout this thesis, substrate concentrations and fluxes are reported as carbon equivalents. Cell concentrations are reported as cell numbers, with the conversion from cell numbers to cell carbon given in the Experimental Approach section under "Cell Concentration".

Biofilm Characterization

The biofilm physical properties were characterized by measuring thickness and areal density. The standard deviation of eight optical thickness measurements was

used to quantify the biofilm roughness. Areal density was measured as cell number, total biomass, and total organic carbon (TOC) per unit biofilm area. Volumetric densities of each component were calculated by dividing the areal density by the average biofilm thickness. At the end of experiments S4, T4, and R8, intact, lyophilized biofilm samples were analyzed to determine carbohydrate composition.

Biofilm Thickness. A typical time progression of the average biofilm thickness is given in Figure 9 for the three levels of substrate loading rate.

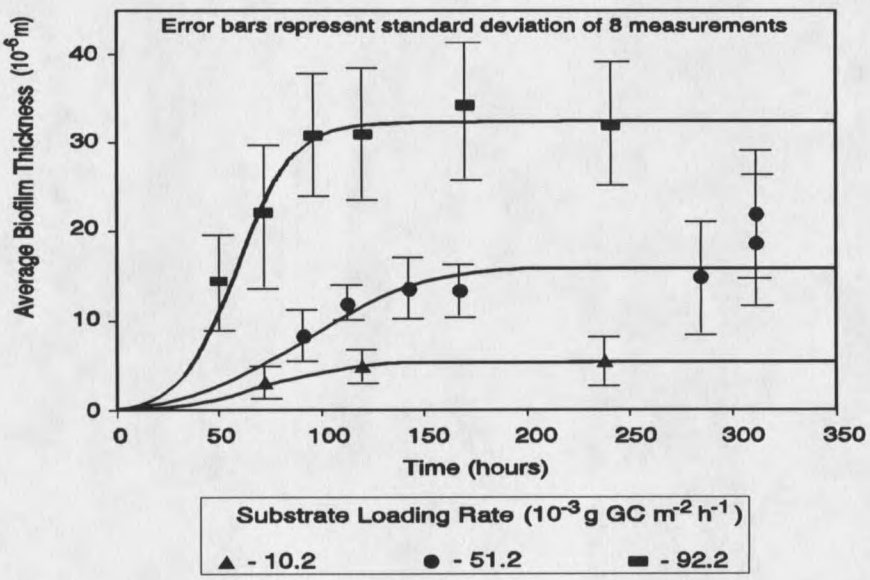

Figure 9. Typical progression of biofilm thickness with time for the three substrate loading rates used.

The biofilm thickness increased rapidly in the log phase of accumulation and then leveled off at the steady state value. The steady state biofilm thicknesses with substrate loading rate and shear stress are given in Figure 10. It can be seen that thickness increased linearly with increases in substrate loading rate and no consistent trend with shear stress was observed.

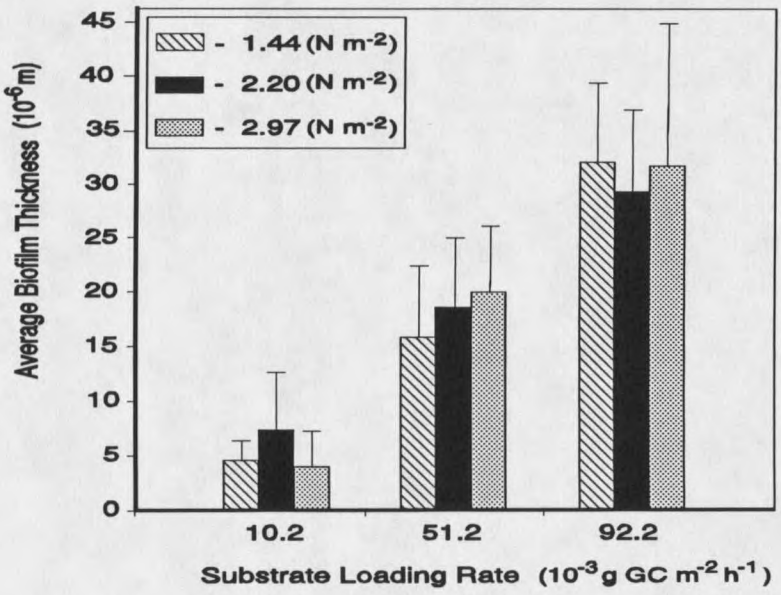

Figure 10. Steady state biofilm thickness increased with substrate loading rate. Shear stress had no significant effect. Error bars are standard deviation of 8 to 40 measurements and are indicative of the roughness of the biofilm.

Biofilm Roughness. Defined as the standard deviation of 8 optical thickness measurements, the biofilm roughness increased with increasing biofilm thickness (Figure 11). The slope of 0.22 (unitless) indicates that the standard deviation of the biofilm thickness was approximately 1/5 of the measured average value. Statistical analysis indicates that substrate loading rate significantly influenced biofilm roughness. No significant or consistent dependence on shear stress was observed.

Biofilm Areal Mass Density. The areal mass density was found to increase with substrate loading rate (Figure 12) and increasing biofilm thickness (Figure 13).

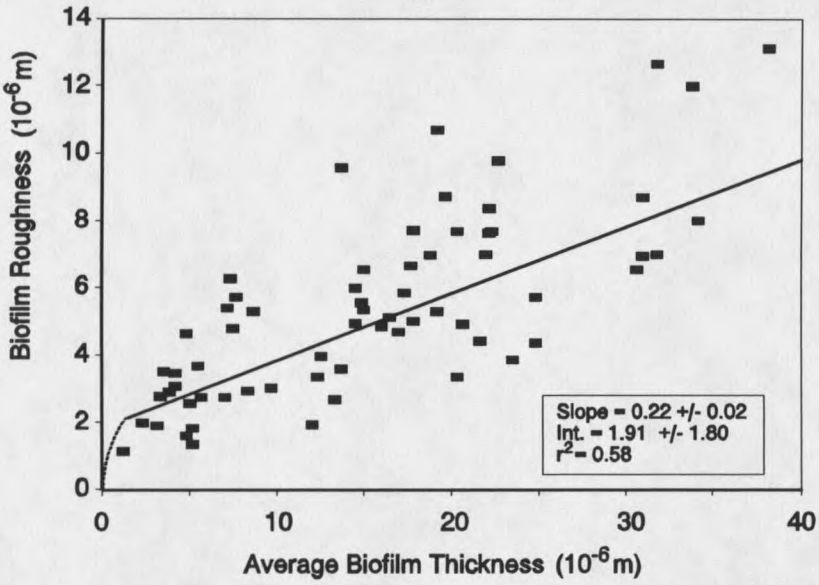

Figure 11. Biofilm roughness, the standard deviation of eight optical thickness measurements, was approximately one-fifth of the measured average biofilm thickness.

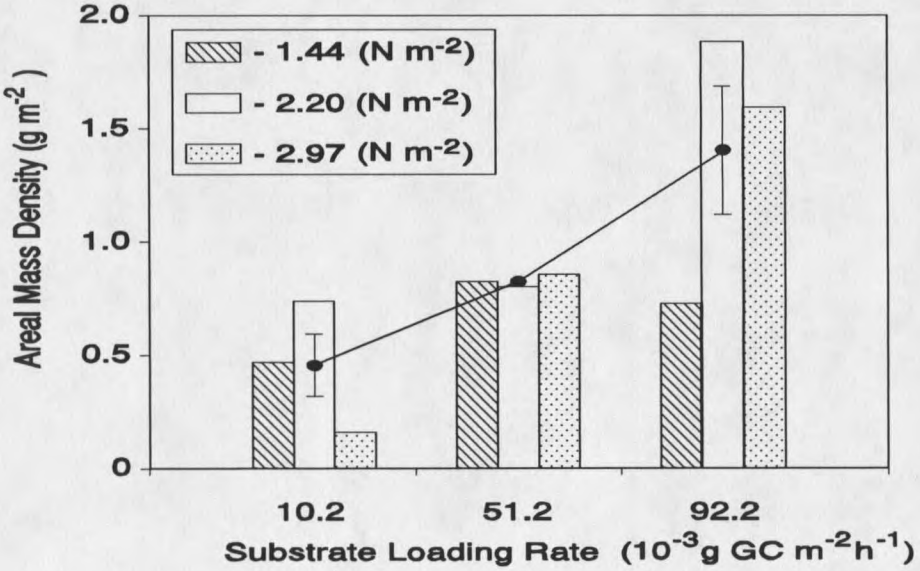

Figure 12. Steady state areal mass density increased with increasing substrate loading rate, but showed no consistent pattern with varied shear stress.

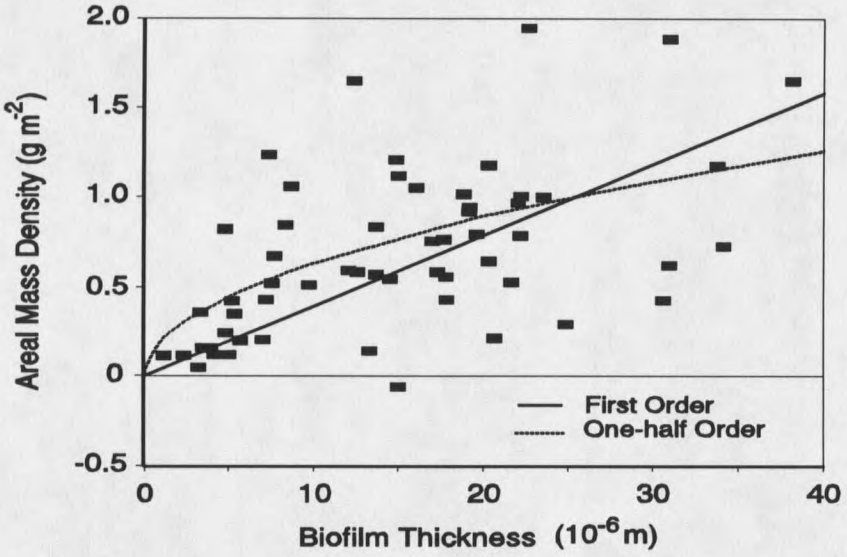

Figure 13. Biofilm areal mass density increased with increasing biofilm thickness. First order and one-half order regression lines are plotted. These regressions give squared correlation coefficients of 0.17 and 0.29, respectively.

Regression of this data with a first order model (Eq. 28) and a one-half order model (Eq. 29) in biofilm thickness gave squared correlation coefficients of 0.17 and 0.29, respectively.

$$X_f = k_{\rho 1} L_f \tag{28}$$

$$X_f = k_{\rho 1/2} \sqrt{L_f} \tag{29}$$

The coefficients determined were 39.5 ± 3.11 (10^3g m^{-3}) for the first order model (Eq. 28), and 0.199 ± 0.041 (10^3g m$^{-5/2}$) for the one-half order model (Eq. 29). Areal mass density was found to increase with increasing substrate loading rate, but no consistent trend was found with changes in shear stress.

Biofilm Volumetric Density. Defined as the dry mass per unit wet biofilm volume, the volumetric mass density decreased with increasing biofilm thickness (Figure 14). The lines on Figure 14 are calculated from the regressions of the areal mass density (Eqs. 28 and 29) and thickness. The volumetric mass density decreased with increasing substrate loading rate. However, the decrease was statistically insignificant at the 95% level. No consistent or statistically significant influence of shear stress was observed.

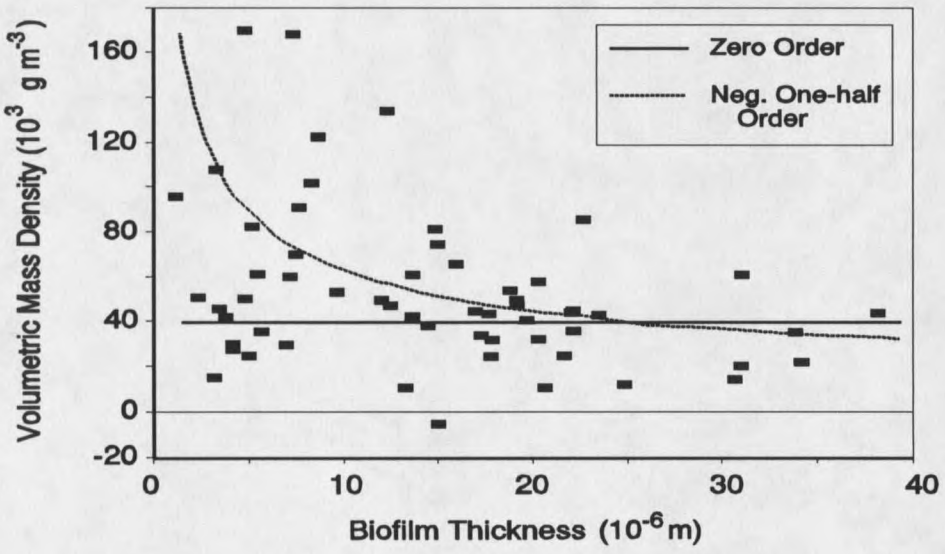

Figure 14. Volumetric mass density decreased with increasing biofilm thickness. Lines are calculated from Eqs. 28 and 29, giving zero and negative one-half order expressions in biofilm thickness.

Biofilm Areal Cell Density. Biofilm areal cell density was found to increase with increasing substrate loading rate (Figure 15) and with biofilm thickness. In Figure 16, a linear regression with biofilm thickness gave a squared correlation coefficient of 0.76. Areal cell density was not significantly affected by shear stress.

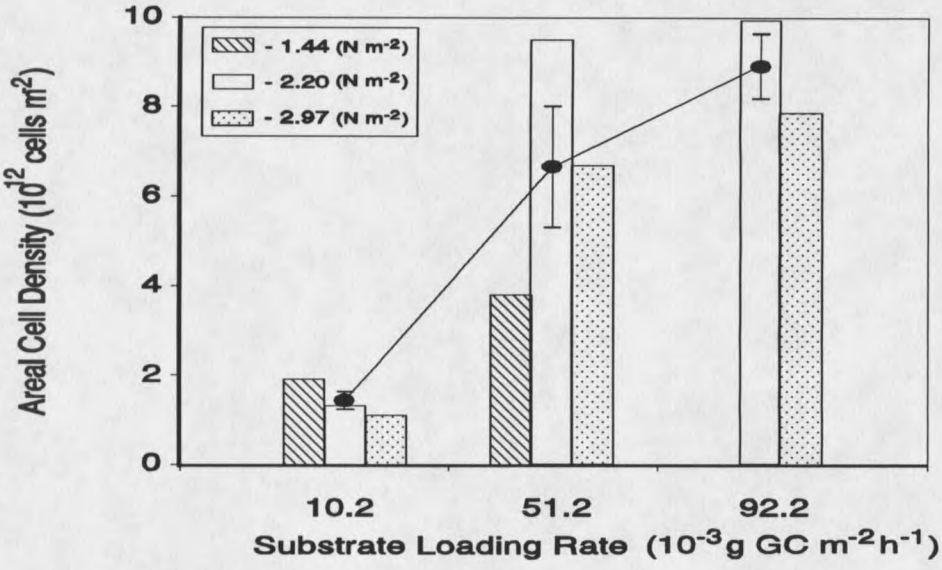

Figure 15. Areal cell density increased with increasing substrate loading rate, but was not significantly affected by shear stress.

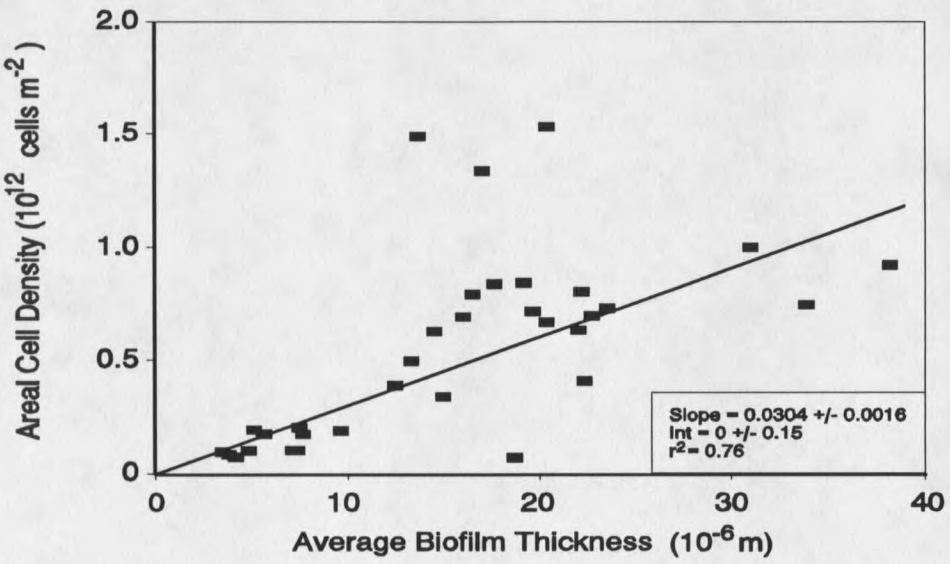

Figure 16. The areal cell density increased linearly with biofilm thickness.

Biofilm Volumetric Cell Density. The volumetric cell density is calculated by dividing the areal cell density by the average biofilm thickness. The slope of the line obtained by linear regression of the areal cell density against the average biofilm thickness, $3.04 \times 10^{16} \pm 0.16 \times 10^{16}$ cells m^{-3}, is the average biofilm volumetric cell density. The ANOVA results showed that the substrate loading rate had some significant influence on the volumetric cell density in the biofilm. However, there was no consistent trend. Shear stress had no significant effect.

Carbohydrate Analysis. Glycosyl residue compositions were determined for biofilms at the end of experiments S4, T4, and R8, with the results given in Table 9. Sample T4 was determined with a Gram stain to be contaminated with Gram positive rods. The concentration of rhamnose, glucose, and galactose in this sample differs significantly from the other two samples.

Table 9. Glycosyl residue compositions (g residue [g biofilm]$^{-1}$) for biofilms in experiments S4, T4, and R8.

Glycosyl Residue	Exp S4	Exp R8	Exp T4 (contaminated)
rhamnose	0.014	0.016	0.0079
ribose	0.017	0.021	0.023
mannose	0.0093	0.0066	0.0060
glucose	0.024	0.021	0.071
galactose	0	0	0.0054
glucosamine	0.0007	0.0016	0.0008

Bulk Liquid Characterization

In addition to data on the biofilm itself, important characteristics of the bulk liquid must be known. The bulk liquid was described by the following measurements: glucose concentration, suspended cell concentration, and the organic carbon fractions. Organic carbon was measured as total and soluble organic carbon (TOC and SOC).

Glucose Concentration. The steady state effluent glucose concentration increased slightly with increasing substrate loading rate, but showed no consistent trend with varying shear stress (Figure 17). ANOVA results indicate that both independent variables had a significant effect on the effluent glucose concentration, although no consistent trend was observed with shear stress.

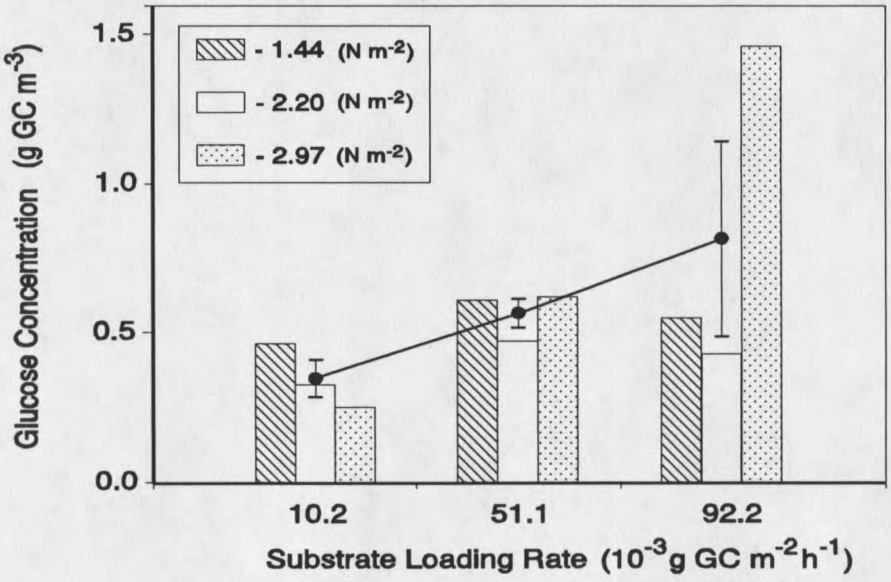

Figure 17. The steady state glucose concentration increased with increasing substrate loading rate.

Suspended Cell Concentration. The steady state suspended cell concentration increased significantly with increasing substrate loading rates, but was not significantly

affected by shear stress (Figure 18).

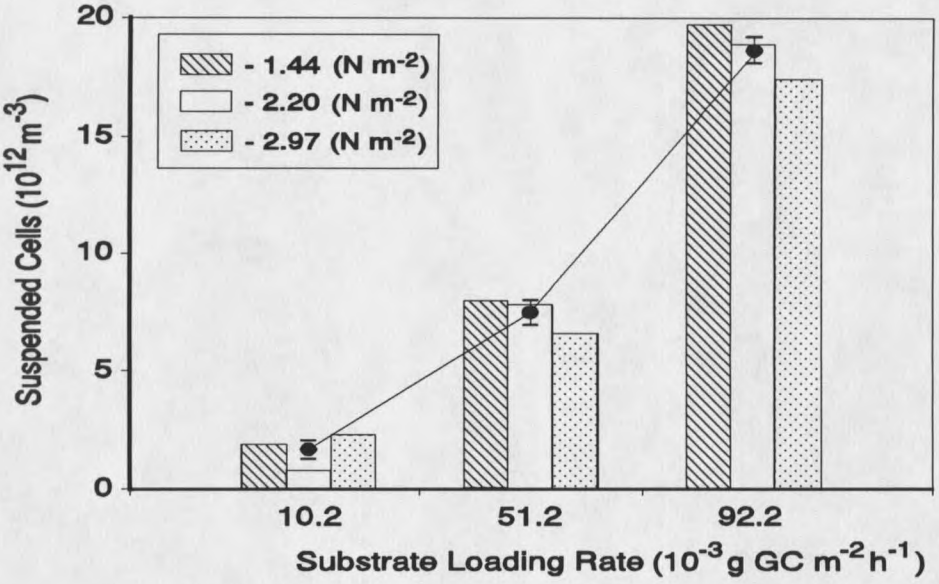

Figure 18. Suspended cell concentration increased with increasing substrate loading rates, but was not significantly influenced by shear stress.

Total and Soluble Organic Carbon. The steady state TOC and SOC concentrations increased with increasing substrate loading rate, but were not significantly affected by shear stress.

Biofilm Process Characterization

Biofilm process rates determine the net accumulation rate of a biofilm. With the variables given in the previous sections on biofilm and bulk liquid characterization, the glucose utilization rate, the cellular detachment rate, the cellular production rate, and the observed yield can be calculated.

Glucose Utilization Rate. The glucose utilization rate is calculated by Eq. 30, and gives the average substrate flux into the biofilm.

(30)

ANOVA results indicate that the glucose utilization rate was significantly influenced by both glucose loading rate and shear stress, although no consistent trend was observed as a function of shear stress. Because of the relative constancy of the effluent glucose concentration, the glucose utilization rate was highly dependent on the influent glucose concentration.

Observed Yield Coefficient. Measurements of the steady state glucose utilization rate and the steady state cellular detachment rates allow the calculation of an observed yield coefficient from Eq. 24. The observed yield, from Figure 19, is 0.182 with a standard error of 0.020, in units of g cell carbon [g glucose carbon]$^{-1}$.

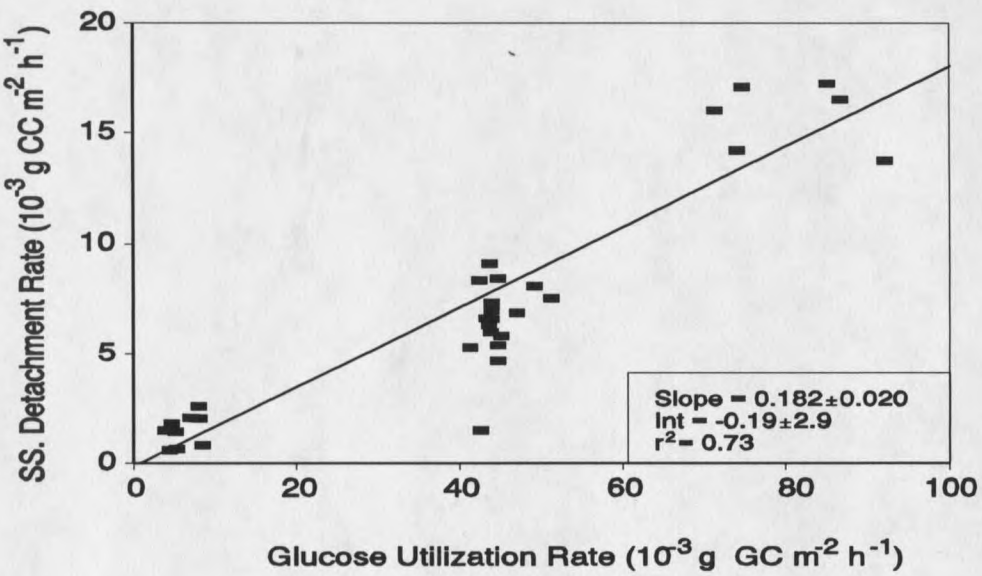

Figure 19. The slope of steady state detachment rate versus steady state substrate utilization rate is observed cellular yield (0.182 g CC [g GC]$^{-1}$) of *Ps. aeruginosa* biofilm.

Cellular Production Rate. From the observed yield and the glucose utilization rate, the cellular production rate can be calculated (Eq. 24). Steady state cell production rate determines the maximum level of continuous sustainable detachment.

Cellular Detachment Rate. The cellular detachment rate is calculated by Eq. 22, and gives the average cellular flux away from the biofilm. The steady state detachment rate increased with increasing substrate loading rate, but was not significantly affected by shear stress (Figure 20).

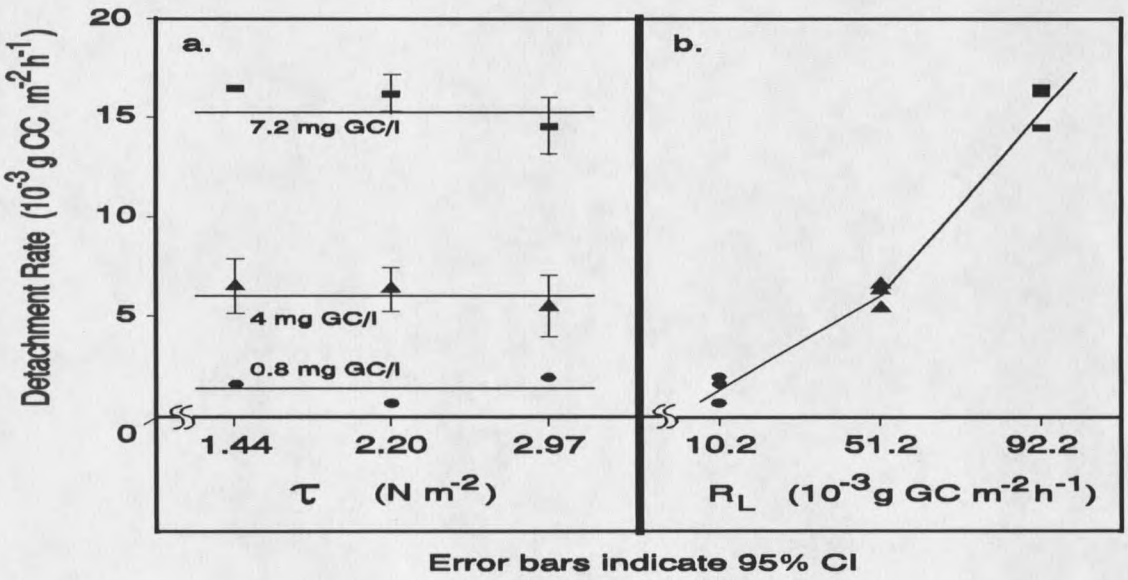

Figure 20. Steady state detachment rate increased with increasing substrate loading rate, but was not significantly affected by shear stress.

Particle Size Distribution. Particle size distributions from experiments R0, S4, and T4 show that the average detached particle size was 0.886 ± 0.072, 1.160 ± 0.163, and 0.838 ± 0.152 10^{-12} m^2, respectively, indicating that the majority of detached particles were single cells (Figure 21). Particles up to 40×10^{-12} m^2 were observed (Appendix I). Based on estimated particle volumes, however, the overall

detachment of biomass is nearly evenly distributed from single cells up to large particles (Figure 21). Assuming a cubic shape, the average particle volume was 16.6×10^{-18} m^3, which corresponds to an observed area of 6.5×10^{-12} m^2. This indicates that biofilm detachment is the result of a wide distribution of particle volumes.

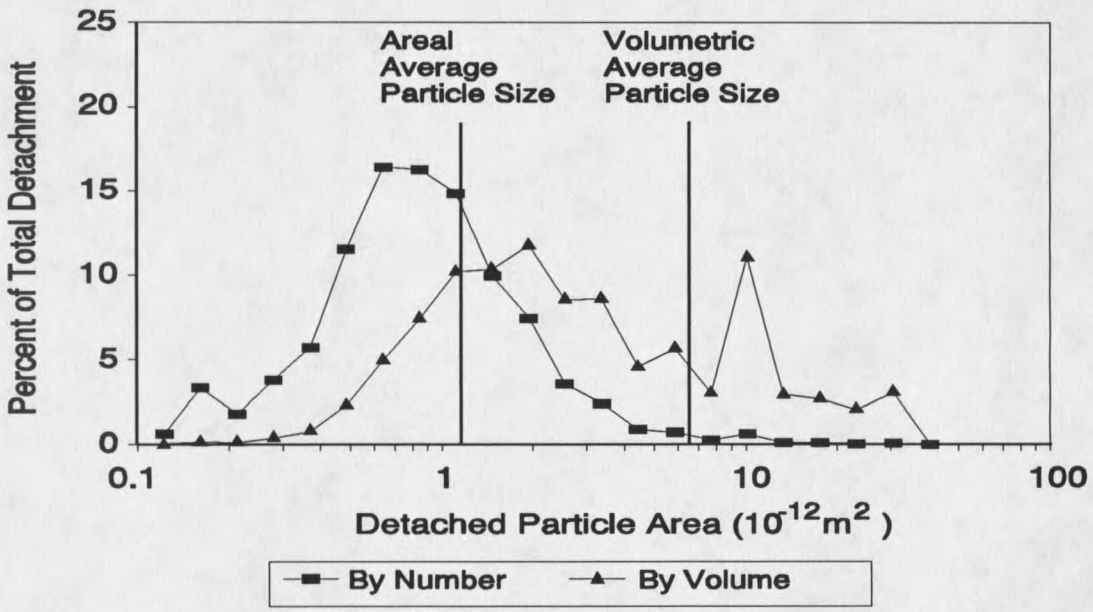

Figure 21. Particle size distribution as a percent of the total observed number and total calculated volume of detached particles from a *Ps. aeruginosa* biofilm, experiment S4.

Photomicrographs. The photomicrographs given in Photos 1 and 2 show a "rippled" biofilm surface. Biofilm ripples similar to these were observed with phase microscopy. Photo 3 is an SEM photomicrograph showing extracellular polymer formation in the biofilm. A TEM photomicrograph (Photo 4) displays a uniform distribution of cells in a biofilm cross-section.

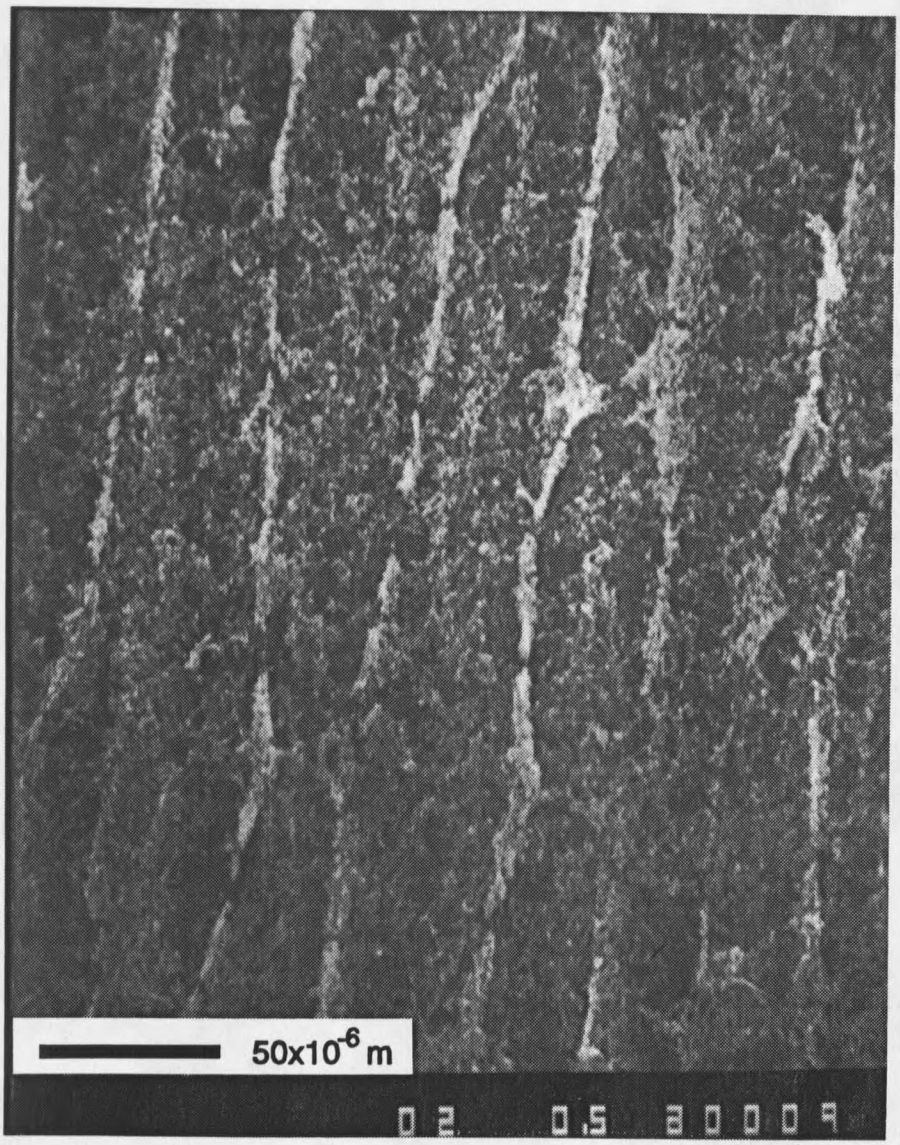

Photo 1. SEM photomicrograph (500 X) shows a rippled biofilm surface perpendicular to the direction of bulk liquid flow.

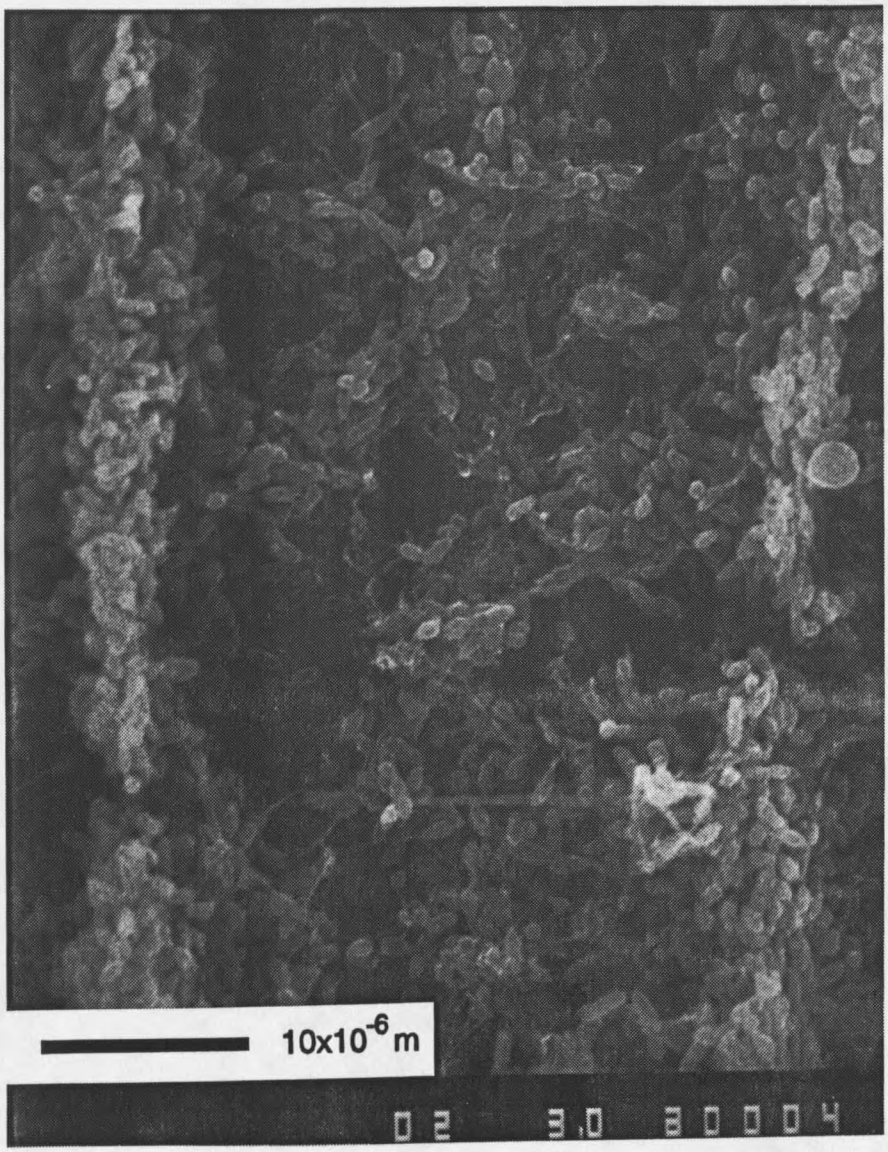

Photo 2. Close-up (3,000 X) of Photo 1.

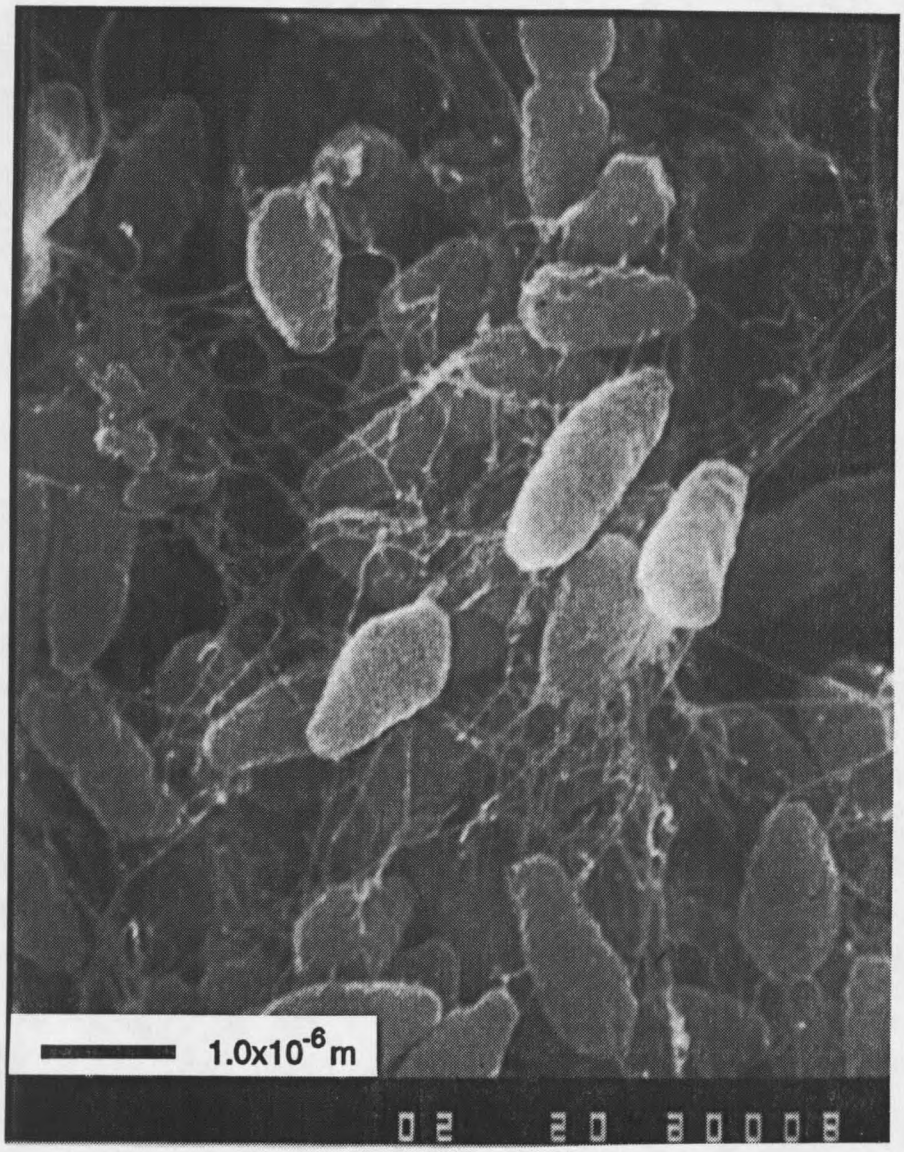

Photo 3. SEM photomicrograph (20,000 X) showing extent of polymer formation in *Ps. aeruginosa* biofilm.

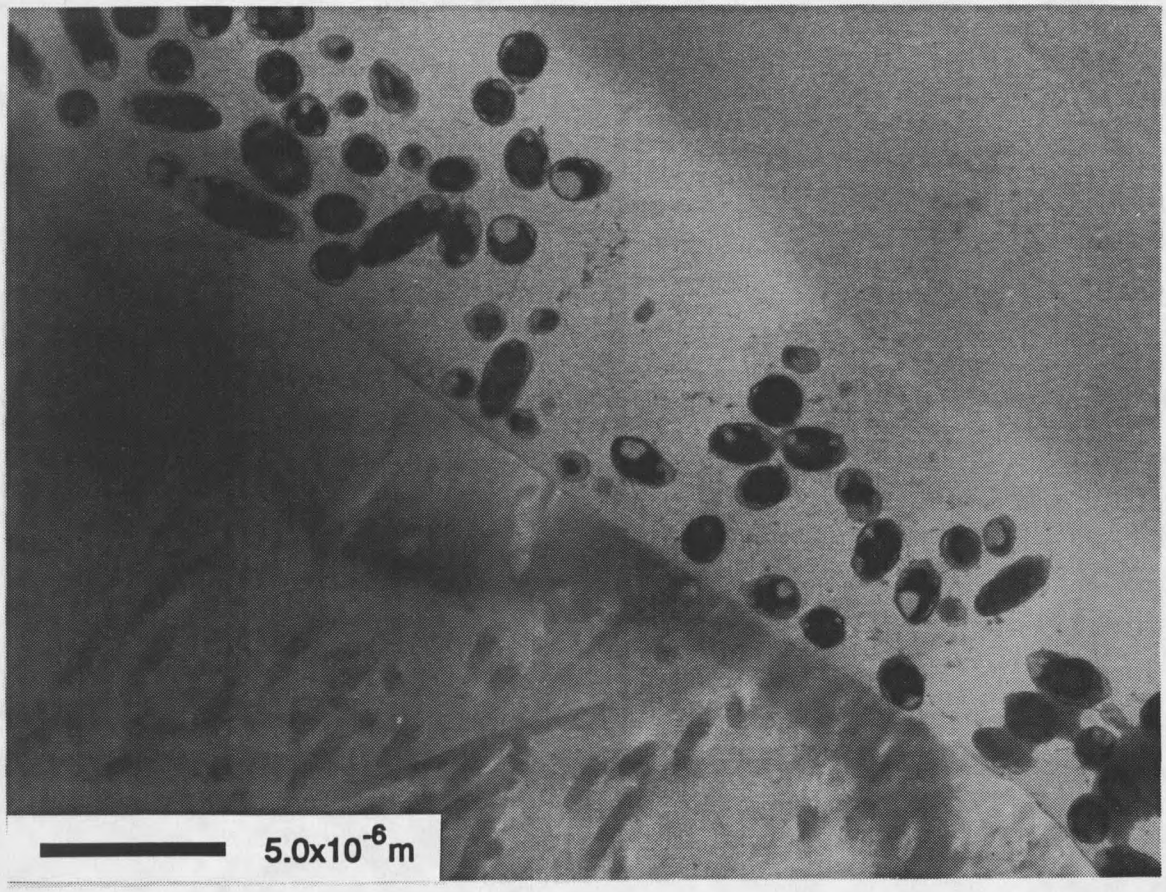

Photo 4. TEM photomicrograph (5,000 X) showing cross-section of biofilm on polycarbonate substratum.

Step-Change Effects

At the end of experiments R1 and R6 a step change in the influent liquid stream was made. A pH change from 6.8 to 5.8 was made in experiment R1, while in experiment R6 the influent glucose concentration was turned off.

Experiment R1. A pH step-change from 6.8 to 5.8 was effected at 313 hours into the experiment (Figure 22). This resulted in a possible, though insignificant, increase in the film thickness followed by a possible decline in thickness. The suspended cell concentration was elevated for 2.5 hours but returned to just below normal after 7 hours. A small but significant sloughing event occurred just prior to the pH step change. This resulted in distorted suspended cell data. The effluent glucose concentration increased very slightly from 0.61 g GC m^{-3} to 1 g GC m^{-3} and remained stable. While the change in effluent substrate concentration is notable, it only represents in a 6% change in the substrate utilization rate over the reactor.

Experiment R6. The influent glucose concentration was set to zero at 190 hours. This resulted in an immediate decrease in biofilm thickness and increase in detachment rate (Figure 23). Biofilm thickness decreased to 26% of the original level in 2.5 hours. Calculations indicate that detachment rate had increased rapidly and was already decreasing before any measurements were taken. Glucose concentrations at t = 190.5 h and t = 191 h were slightly higher than expected. This indicates that the glucose concentrations reported are probably higher than the actual glucose concentration in the RotoTorque. This may be due to analytical errors during glucose analysis.

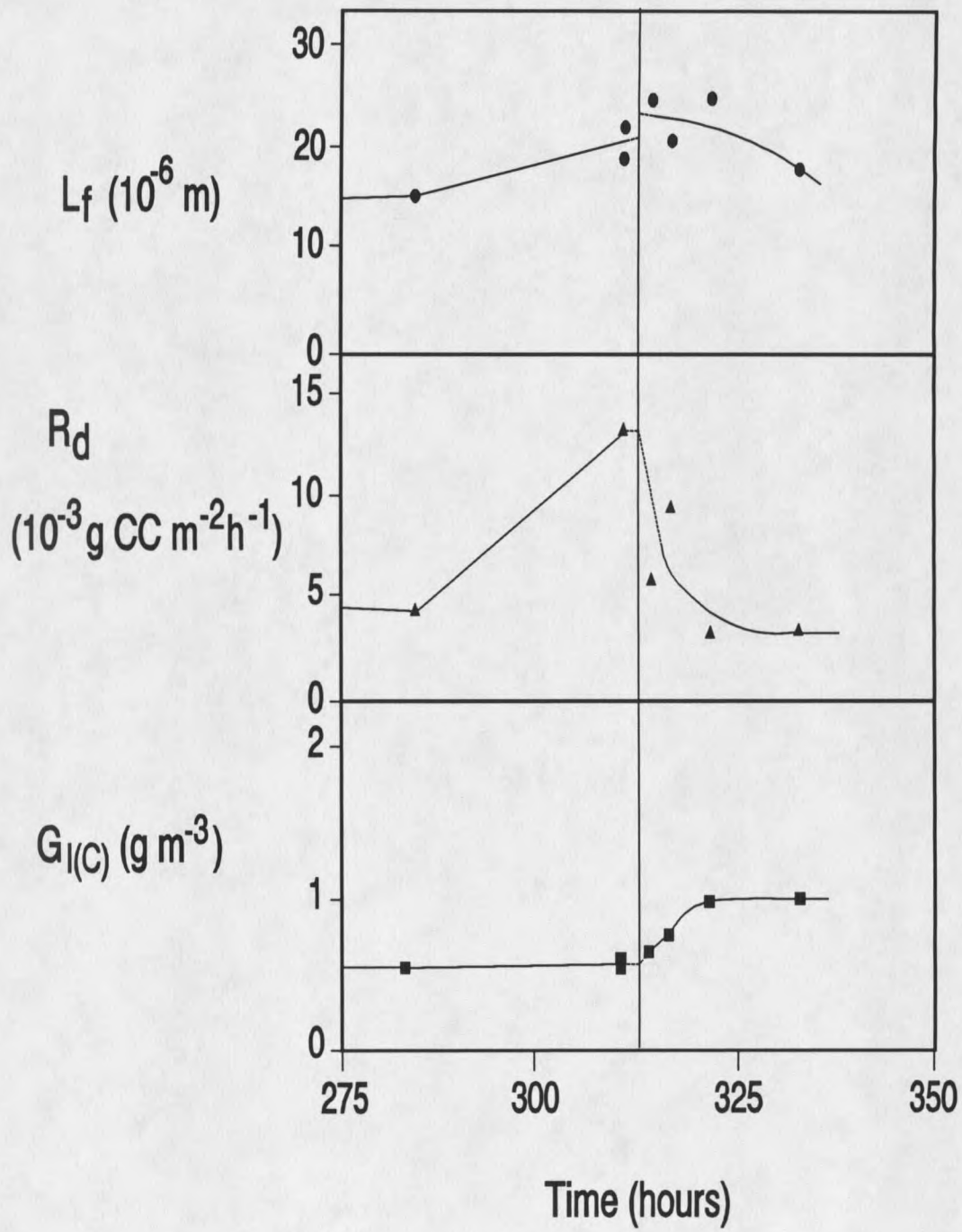

Figure 22. A step change in buffered pH from 6.8 to 5.8 resulted in slight changes in thickness, detachment rate, and effluent glucose concentration, although the substrate utilization rate only decreased by 6%.

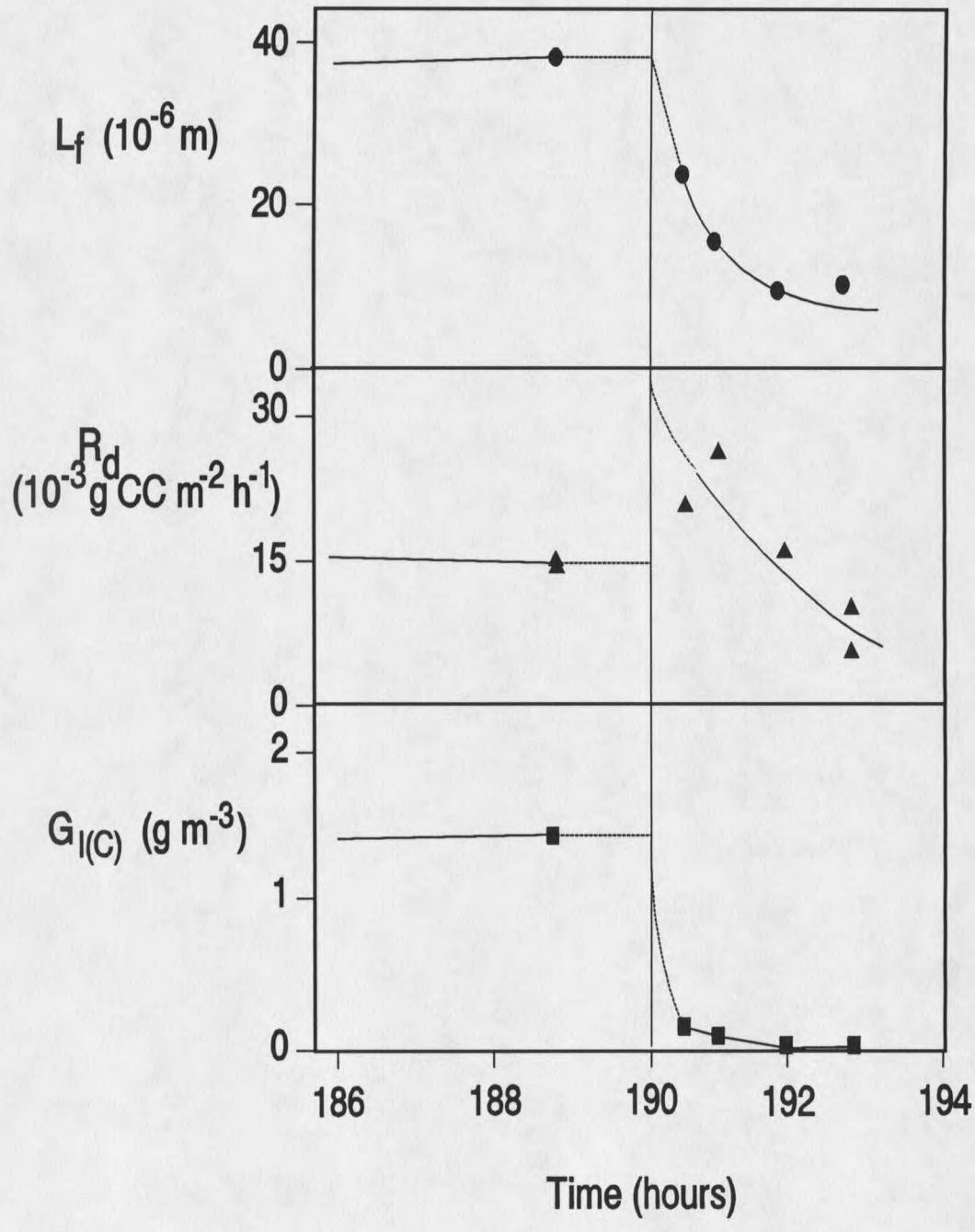

Figure 23. Turning off the influent glucose resulted in an immediate decrease in film thickness as a result of detachment.

Mixed Population Data

Two mixed culture experiments (M1 & M2) were conducted at 200 rpm. Experiments M1 and M2 were run at influent glucose concentrations of 7.2 and 0.8 g GC m^{-3}, respectively, and were identical to the monopopulation *Ps. aeruginosa* experiments with the exception of the initial inoculum. Detachment rate was monitored by total suspended solids in the effluent. Figure 24 shows the biomass detachment rate for both mixed population experiments with the proposed detachment rate expression (Eq. 25).

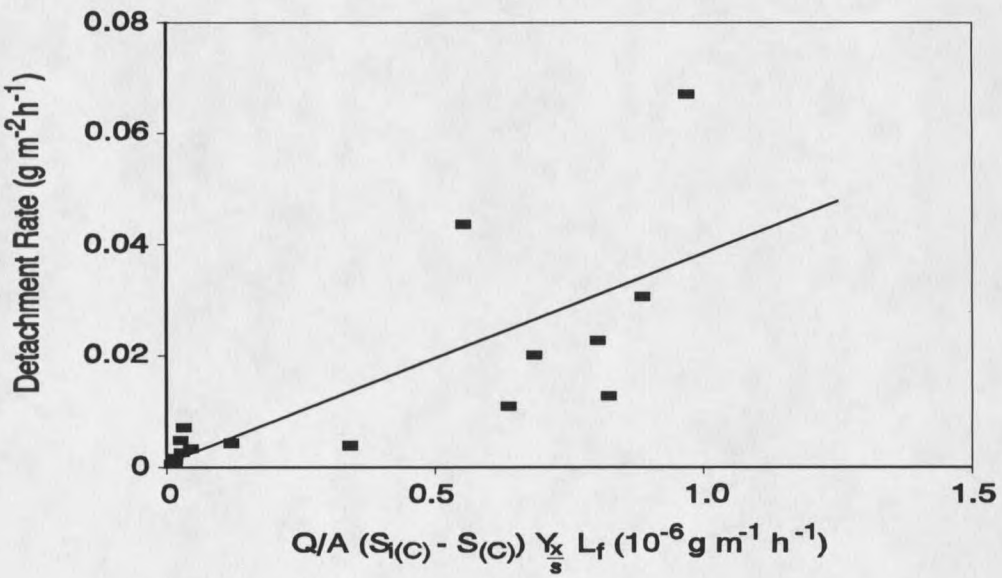

Figure 24. Biomass detachment rate for both M1 and M2 with the proposed detachment rate expression (Eq. 25).

Figures 25 and 26 show the distribution of biofilm thickness on the RotoTorque coupons (0.017 m wide X 0.22 m long). Each bar represents the thickness of an area of 0.0057 m wide X 0.0138 m long. "Upstream" or "downstream" indicates the

direction of bulk liquid flow across the coupon. Measurements were taken at 288 hours in each of the two experiments. Thickness distributions for experiment M1 (Figure 25) show distinct changes in thickness as a function of location. Biofilm thickness at upstream locations were nearly an order of magnitude higher than corresponding downstream locations which were only 0.011 m away. At the lower substrate loading rate of experiment M2 biofilm thickness was thinner and much more evenly distributed on the coupon (Figure 26).

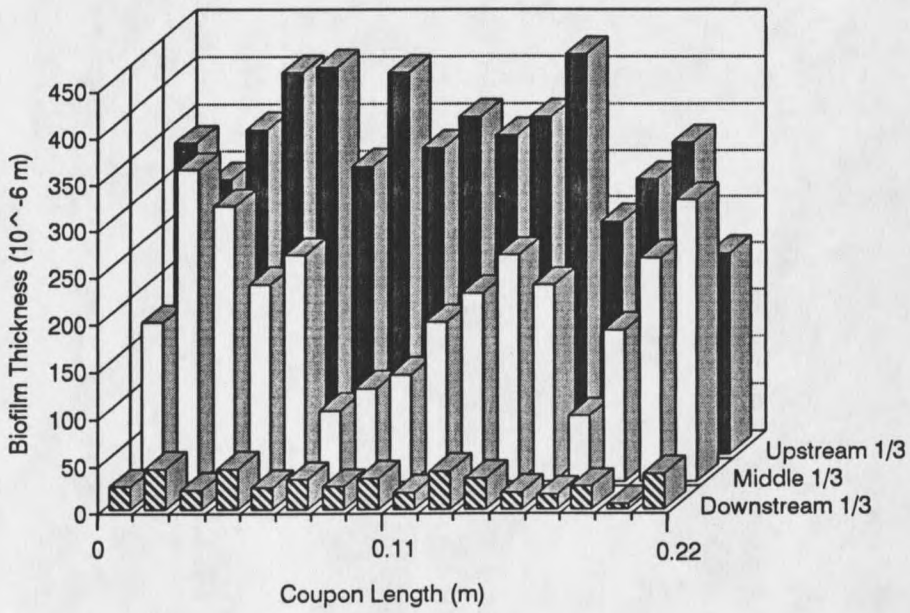

Figure 25. Distribution of biofilm thicknesses for experiment M1 after 288 hours.

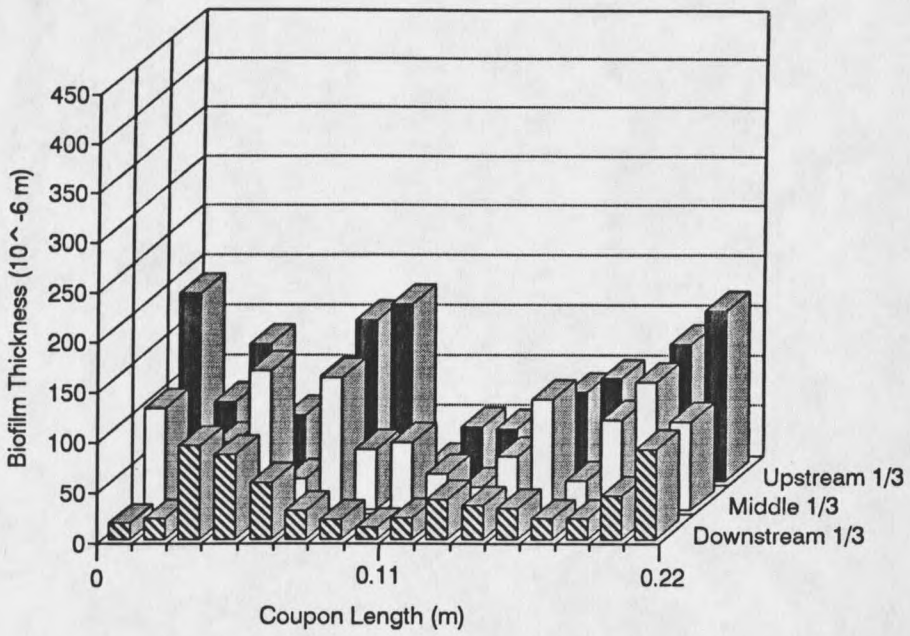

Figure 26. Distribution of biofilm thicknesses for experiment M2 after 288 hours.

DISCUSSION

Biofilm Characteristics

Biofilm Thickness

Steady state biofilm thickness is dependent on the substrate loading rate. Average steady state values for the thicknesses were 31.85, 17.61 and 6.20 microns (10^{-6}m) for substrate loading rates of 0.0102, 0.0512 and 0.0922 g GC m^{-2} h^{-1}, respectively. Data on *Ps. aeruginosa* biofilm thickness at such low substrate loading rates (0.0102 g GC m^{-2} h^{-1}) were not available prior to this research. Previous research (Trulear, 1983; Siebel, 1987) with *Ps. aeruginosa* in RotoTorques indicated that the average steady state biofilm thickness was always approximately 30 microns (10^{-6}m), although the lowest reported substrate loading rate was 0.0653 g GC m^{-2} h^{-1} (Trulear, 1983). This research indicates that the film thickness is dependent upon substrate loading rate between 0.0102 and 0.0922 g GC m^{-2} h^{-1}. Figure 27 shows that the steady state film thickness increases with substrate loading rate up to approximately 0.120 g GC m^{-2} h^{-1} and then asymptotically approaches 33 microns (10^{-6}m). At this point, it is unclear why the plateau thickness for *Ps. aeruginosa* is 33 microns (10^{-6}m), but it may be related to the thickness of the laminar sublayer and the strength of EPS bonds between cells. Mixed population film thicknesses for identical substrate loading rates and rotational speeds are typically an order of magnitude higher (Figures 25 and 26 and Appendix H) indicating that strength and structure of the biofilm may be the key variable which determines biofilm thickness at higher substrate loading rates.

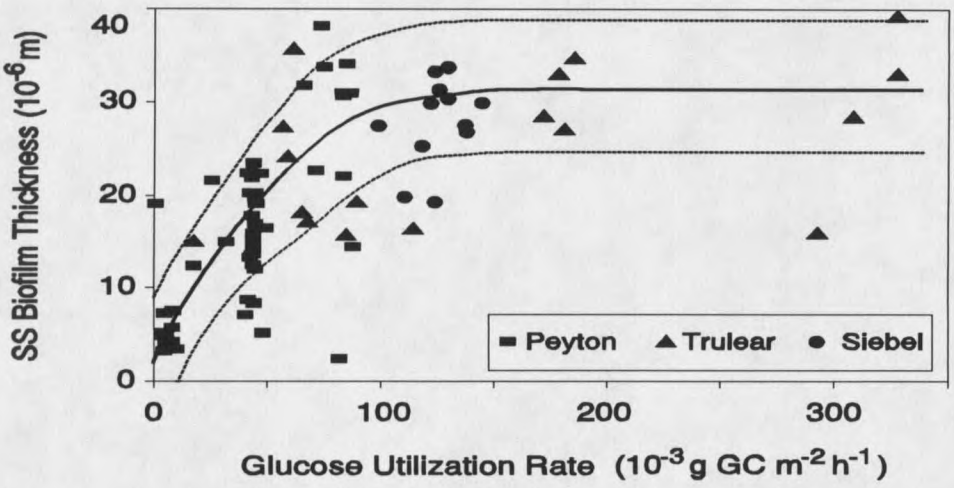

Figure 27. The dependence of steady state biofilm thickness for *Ps. aeruginosa* in a rototorque on the glucose utilization rate (--- 95% confidence interval).

Biofilm Roughness

Data on biofilm roughness may provide insight for microscale computer modelling efforts. The results obtained indicate that the standard deviation of the *Ps. aeruginosa* biofilm thickness is approximately one-fifth (0.22) of the average (Figure 11). Typical values of film thickness would fall within 2 standard deviations on either side of the mean. As an example, for a 30 micron (10^{-6}m) average film thickness, individual thickness measurements may range from 18 to 42 microns (10^{-6}m). At this time, no models account for film roughness and the differences in fluid dynamics and mass transfer that may result. Rougher films would most likely have higher mass transfer coefficients than smoother films, which would result in a higher growth rate for a given bulk liquid substrate concentration.

Mixed population biofilm roughness was sometimes higher than the average

measured value. This indicates that not only are mixed culture biofilms thicker, but that the morphology is more heterogeneous.

Areal and Volumetric Mass Density

For modelling purposes, it would be useful to obtain correlations which account for the changes in biofilm structure as the biofilm ages and matures. The areal mass density was fit with both a one-half order (Eq. 29) and first order (Eq. 28) expression in average biofilm thickness (Figure 13). The regression analysis gave squared correlation coefficients (r^2) of 0.29 and 0.17, respectively, indicating that, although the data is very noisy, the one-half order expression better describes the data. From these regressions, the volumetric mass density can be calculated by dividing by the thickness and can be plotted against the observed values. Fitting the areal mass density with a first order regression in film thickness (Figure 14) results in a zero order, or constant volumetric mass density (Eq. 31).

$$\rho_f = k_{\rho_1} \tag{31}$$

$$\rho_f = \frac{k_{\rho_{1/2}}}{\sqrt{L_f}} \tag{32}$$

Also, fitting the areal mass density with a one-half order expression in biofilm thickness gives a negative one-half order expression in film thickness for the volumetric mass density (Eq. 32).

Most biofilm models assume constant biofilm volumetric mass density (Howell and Atkinson, 1976; Rittman and McCarty, 1978, 1980, and 1981; Wanner and Gujer, 1986; Chang and Rittman, 1987 and 1988; Namkung and Rittman, 1987; Suidan et

al., 1987; Skowlund and Kirmse, 1989) (Eq. 31). Although not conclusive, the data obtained from this research suggests that volumetric mass density may be better modelled with a negative one-half order expression in biofilm thickness. This expression predicts high volumetric density values for very thin films. As calculated from Eq. 32, the predicted volumetric mass density for a one micron ($1x10^{-6}$m) biofilm is $199x10^{3}$g m^{-3}. Eq. 32 predicts that thinner films are more dense and thicker films are less dense.

A speculative extension of this regression analysis can be made in order to calculate the *local* volumetric mass density with biofilm depth. This is based on two critical, untested assumptions: 1) biofilm density at a given depth remains constant over time, and 2) the density of a monolayer of cells (L_f=$5x10^{-7}$m) can be accurately predicted by Eq. 32. The measured mass density values are the observed average density over the entire biofilm thickness. Using the calculus definition of an average:

$$\overline{\rho_f} \equiv \frac{\int_0^{L_f} \rho_{f_z} dz}{\int_0^{L_f} dz} \tag{33}$$

Integrating the denominator, and separating the numerator gives:

$$\overline{\rho_f} L_f = \int_0^{5x10^{-7}} \rho_{f_m} dz + \int_{5x10^{-7}}^{L_f} \rho_{f_z} dz \tag{34}$$

Using assumption 2 that the density of a monolayer is constant and known, and using a series approximation to the integral gives the final form which can be solved stepwise to determine the local density profile with depth in the biofilm.

$$\overline{\rho_f} L_f - 5x10^{-7} \rho_{f_m} = \sum_{5x10^{-7}}^{L_f} \rho_{f_z} \Delta z \qquad (35)$$

Stepwise solution of Eq. 35 gives the results shown in Figure 28. This density model predicts that the influence of deeper biofilm layers on average density is significant. For example, if, by Eq. 32, a 10 micron ($1.0x10^{-5}$m) biofilm has an average density of $62.9x10^3$ dry g m^{-3} and a 20 micron ($2.0x10^{-5}$m) biofilm has an average density of $44.5x10^3$ dry g m^{-3}, then, assuming the density of the lower 10 micron ($1.0x10^{-5}$m) film remains constant, the upper 10 microns ($1.0x10^{-5}$m) of biofilm must have a density of $26.1x10^3$ dry g m^{-3} to give the observed average of $44.5x10^3$ dry g m^{-3}.

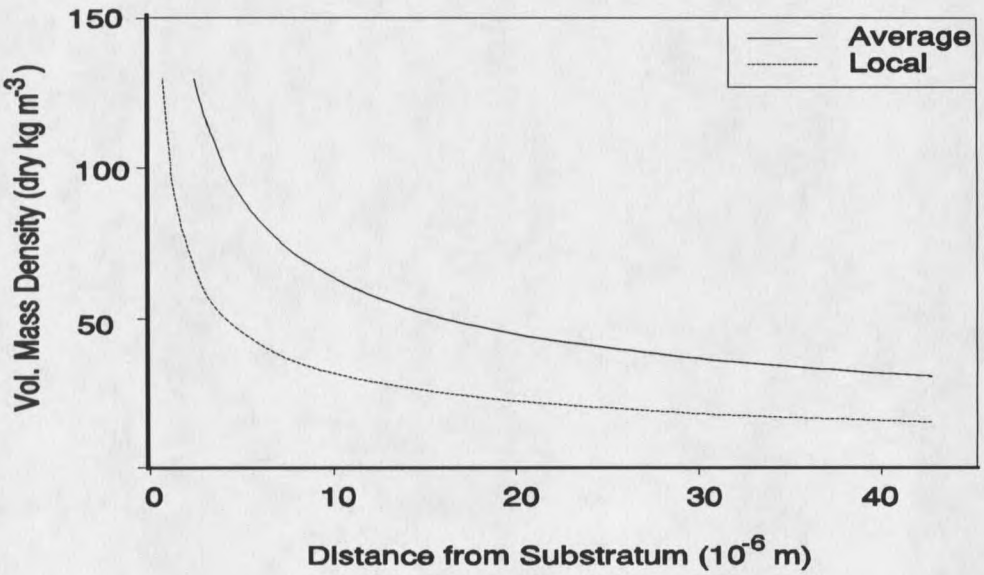

Figure 28. Fitted average and calculated local volumetric mass density with distance from the substratum.

This analysis is intended to be a conceptual approach to modelling biofilm volumetric density and is based on very noisy measurements of volumetric mass

density. Analytical errors are more likely to occur when measuring the density of thinner films. A small error in the average biofilm thickness may result in a larger error in the calculated volumetric density, which in turn will scatter the data more for thinner films. Further volumetric mass density data is required to verify this approach, which may put too much emphasis on density of a monolayer biofilm. Even so, this model is qualitatively consistent with the measurements of biofilm density with depth by Masuda et al. (1991) (Table 2). The data of Masuda et al. indicated that the average density of the total biofilm was 65.3×10^3dry g wet m^{-3}.

Carbohydrate Analysis

There were no significant differences in the results of the glycosyl composition between the samples from experiments S4 and R8 indicating that substrate loading rate and shear stress had little effect on the overall carbohydrate composition of the *Ps. aeruginosa* biofilm. However, it is interesting to note that the methods used for carbohydrate determination would have detected the presence of acidic sugars such as manuronic and glucuronic acid, which are the two monomers that form alginate. It is clear that no alginate was detected in any of the three samples. The composition of the contaminated biofilm (Gram positive rods) from experiment T4 differed significantly in the rhamnose, glucose, and galactose concentrations. The composition reported for the uncontaminated samples is typical of the lipopolysaccharide layer, commonly known as the outer wall, of Gram negative organisms. Brock and Madigan (1988) report that the lipopolysaccharide of another Gram negative organism, *Salmonella*, has been studied extensively and has been found to contain rhamnose, mannose, glucose, galactose, and N-acetylglucosamine. With the exception of galactose, these components were found in the uncontaminated *Ps. aeruginosa*

samples, while galactose was present in the contaminated sample, T4. The contaminated sample also had a much higher concentration of glucose present than the other two samples.

The carbohydrate analysis indicates that different organisms in biofilm influence the EPS composition. It may be possible to use this analysis to determine the presence of contamination, even when the contaminating organism is difficult to culture on auger plates.

Bulk Liquid Characteristics

Glucose Concentration

Steady state glucose concentrations showed significant increases with increasing substrate loading rate. Although the differences were statistically significant, no consistent trend was observed with varying rotational speeds. Influent glucose concentrations varied by a factor of nine, ranging from 7.2 to 0.8 g GC m^{-3}, but average effluent concentrations only varied by a factor of two, ranging from 0.8 to 0.32 g GC m^{-3}. It appears that effluent substrate concentration is relatively independent of input substrate concentration. It is interesting to note that the computer simulation "BIOSIM" qualitatively predicts this result.

Biofilm Process Characteristics

Detachment Rate

Published detachment expressions were compared by ranking the squared correlation coefficient (r^2) between each detachment expression and the data found in this investigation, the combined data set, and the mixed population data set. In Table

10, it can be seen that the proposed equation (Eq. 25) gives the best correlation in all three detachment data sets. The observed data, as a function of the proposed detachment expression for the combined data set and the mixed population data set, are shown graphically in Figures 29 and 30, respectively.

Table 10. Squared correlation coefficients (r^2) of reported detachment expressions. Equations are ranked from top to bottom by average r^2 for the three columns.

Eq. #	Detachment Rate Expression R_d [=] M L^{-2} t^{-1}	Data from this Investigation r^2	Data from this Investigation Combined with Trulear (1983), Turakhia (1986), Siebel (1987) r^2	Mixed Population Data from Trulear (1980) r^2
(25)	$k_d Q/A(S_{i(C)}-S_{(C)})Y_{x/s}L_f$	0.56	0.59	0.73
(18)	$L_f (k'_d + k''_d \mu)$	0.37	0.20	0.42
(17)	$k_d \rho_f L_f^2$	0.43	0.42	0.13
(16)	$k_d X_f^2$	0.22	0.26	0.27
(20)	$k_d \rho_f L_f$	0.25	0.24	0.24
(19)	$k_d \rho_f L_f \tau^{0.58}$	0.025	0.23	0.060
(14)	$k_d \rho_f \tau$	0.028	0.026	0.021

The data indicate that shear stress had no significant influence on the detachment rate over a wide range of environmental conditions. In addition, the product of substrate utilization rate, yield, and biofilm thickness gave the best description of detachment rate.

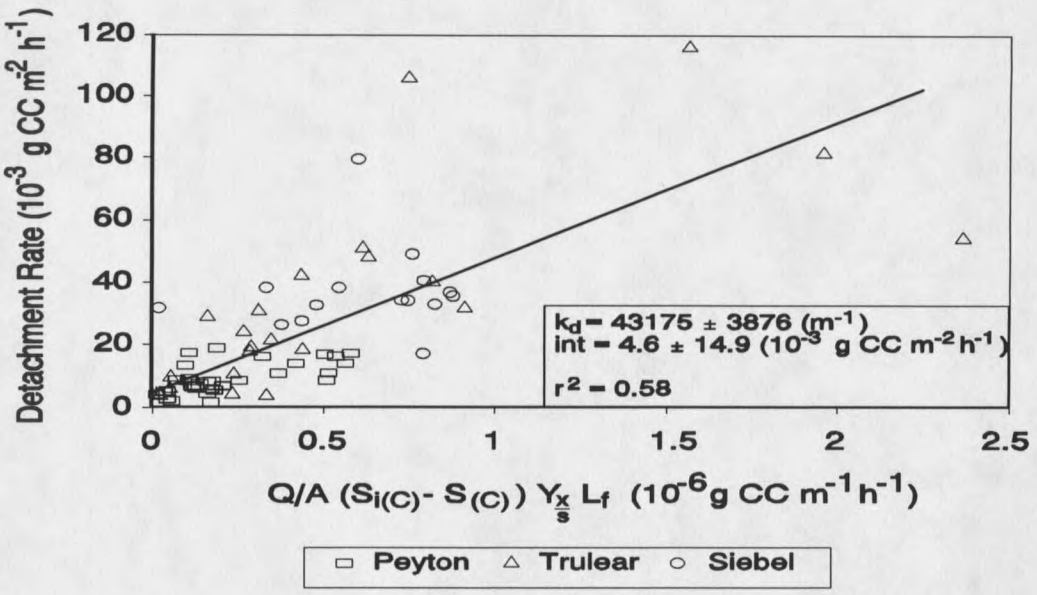

Figure 29. Monopopulation *Ps. aeruginosa* detachment rates from this research combined with other experimental investigations are linearly related to the proposed detachment rate expression (r^2 = 0.59).

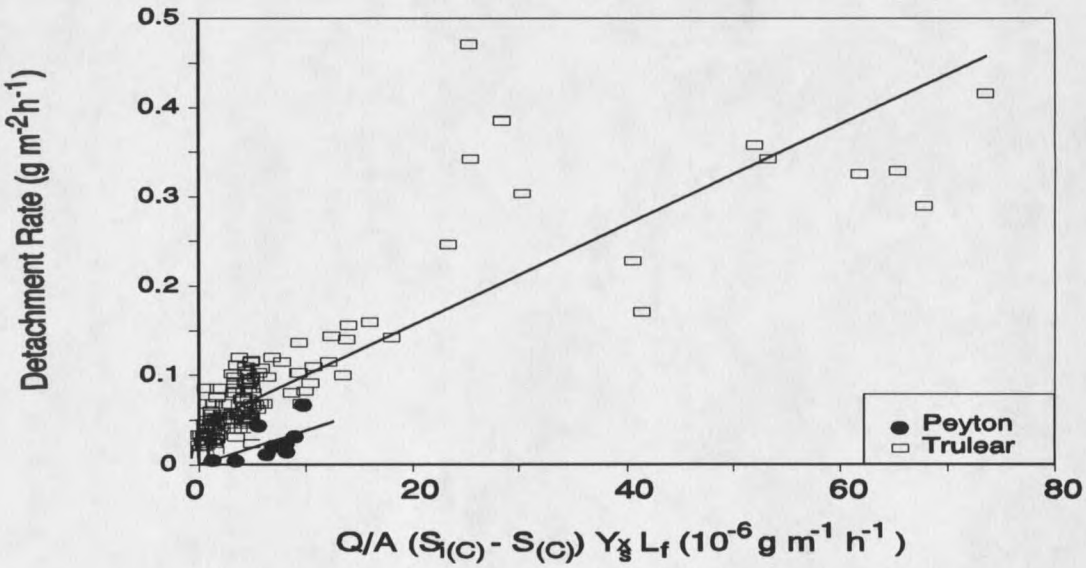

Figure 30. Mixed population detachment rates from this research and Trulear (1980) yield squared correlation coefficients of 0.58 and 0.73, respectively, for the proposed detachment rate expression (Eq. 25).

Shear Stress

To further define the role of shear stress, Eqs. 14 and 19 were rewritten in the more general form given in Eqs. 36 and 37, and were linearized to determine the value of n required to best fit the data.

$$R_d = k_d \rho_f \tau^n \tag{36}$$

$$R_d = k_d \rho_f L_f \tau^n \tag{37}$$

Exponent values from the data of this thesis alone and in combination with several other investigations with *Ps. aeruginosa* biofilms (Trulear, 1983; Siebel, 1987; Turakhia, 1986) were analyzed (Table 11). The mixed population data of Trulear, previously evaluated by Rittman (1982) to determine Eq. 19 (Table 3), was analyzed in an identical manner. From the data obtained in this research, the exponent on shear stress was negative and statistically indistinguishable from zero. However, the values were not significantly different, at the 95% level, from $n = 0.58$ (Eq. 19) or $n = 1.0$ (Eq. 14) proposed by other authors. Only the value of $n = 0.55$ from Eq. 37 for the combined data set was similar to the proposed value of $n = 0.58$ (Eq. 19).

Trulear's (1980) original mixed culture detachment data with shear stress are replotted in Figure 31. A squared correlation coefficient (r^2) of 0.00038 between detachment rate and shear stress indicates no correlation.

Table 11. Dependence of detachment rate on shear stress. The influence of shear stress was determined as an exponent on shear stress from Eqs. 36 and 37.

	n (Eq. 37)	SE(n) (Eq. 37)	n (Eq. 36)	SE(n) (Eq. 36)
Proposed Value (Reference)	0.58 (Rittman 1982)	-	1.0 (Bakke et al. 1990)	-
Ps. aeruginosa (This Thesis)	-0.27	0.64	-0.43	0.89
Ps. aeruginosa (This Thesis with Trulear 1983, Turakhia 1986, and Siebel 1987)	0.55	0.12	-0.18	0.20
Mixed Population (Trulear and Characklis 1982)	-0.64	0.11	0.52	0.13

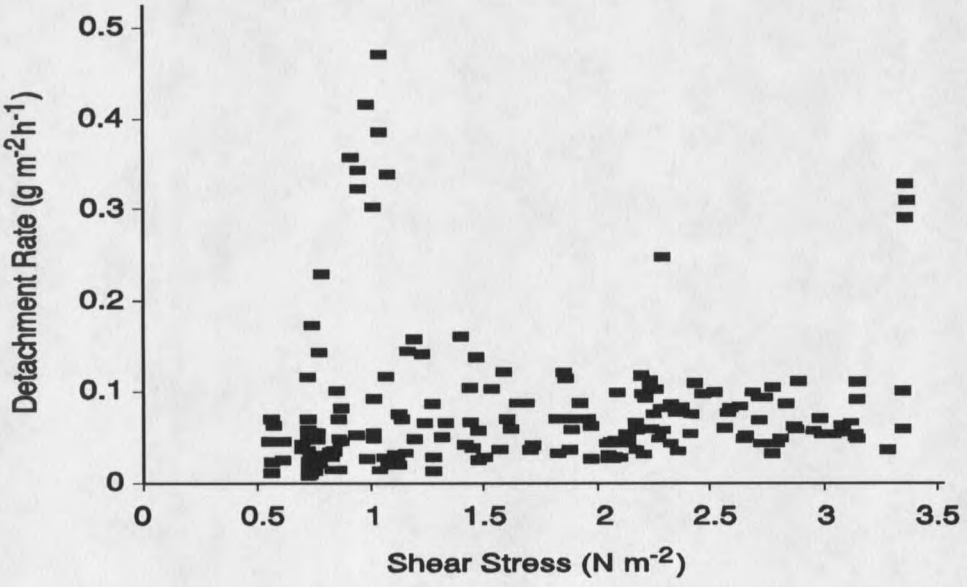

Figure 31. Trulear's (1980) mixed population detachment rates do not correlate with measured shear stress.

The results indicate that over the range of 0.5 to 3.4 N m^{-2} there was no significant influence of shear stress on the cellular detachment rate, for either mono- or mixed populations (Figure 20 and Table 8, and Figure 31). This conclusion is limited to systems under constant or gradually changing shear stress. Bakke (1986) has shown that rapid increases in shear stress can cause transient increases in detachment rates. That research revealed, however, that detachment rate returned to its original level within five reactor residence times, even at the higher shear stress. Rapid decreases in shear stress did not affect the detachment rate. In light of these observations, a detachment rate expression that incorporates the rate of change of the shear stress, rather than the shear stress itself, may be more appropriate:

$$R_d = R_{de} + R_{d\Delta\tau}$$

$$\text{Where } R_{d\Delta\tau} = \begin{bmatrix} k_d \frac{d\tau}{dt} & , \frac{d\tau}{dt} > 0 \\ 0 & , \frac{d\tau}{dt} \leq 0 \end{bmatrix} \qquad (38)$$

Eq. 38 incorporates the continuous detachment rate as a result of erosion and the transient detachment rates which result from increases in the shear stress. Eq. 38 could easily be implemented in computer models and would better reflect the effects of shear stress on biofilm detachment.

Some influence of the bulk liquid velocity on detachment rate may be hypothesized. As the liquid velocity at biofilm-bulk fluid interface increases, the shear forces exerted on the biofilm increase while, at the same time, mass transfer resistance decreases. If detachment rate is independent of shear stress, but is dependent on mass transfer of substrate to the biofilm, then there will be a flow velocity region (at the lower end of the turbulent flow range) where detachment

increases with increasing flow velocity. However, such an increase in detachment rate with increasing fluid velocity is the result of increased mass transfer of substrate to the biofilm and not a direct result of increased shear stress at the biofilm interface. If shear stress does have some effect on the detachment rate, the influence is insignificant when compared to that of the substrate utilization rate.

Substrate Utilization Rate

The accumulation of a biofilm is the net result of processes that produce biomass and processes that remove it. The accumulation continues until the biofilm reaches steady state, at which point the biomass production is balanced primarily by biomass detachment. Thus, material balance considerations alone establish the biomass production rate (Eq. 24), as the upper limit for a sustainable detachment rate. Eq. 25 incorporates this inherent substrate dependence of the biofilm detachment rate into an expression that describes both steady and unsteady state detachment rates for both monopopulation and mixed population biofilms.

Eq. 25 predicts high detachment rates during periods of high growth rates, i.e., high substrate utilization rates. This association has been observed previously (Chang and Rittman, 1988; Speitel and DiGiano, 1987). Eq. 18 was proposed by Speitel and DiGiano (1987) to reflect high detachment rates observed during periods of high growth rate. It is interesting to note that Speitel and DiGiano report some dependence of the growth-associated detachment rate coefficient, k''_d (M L^{-3}), on the type of substrate used. Eq. 25 is also dependent on the type of substrate, since the yield coefficient will be influenced by substrate properties (eg. free energy of oxidation). A substrate which is more difficult to metabolize or provides less energy for producing biomass will result in lower detachment rates for the same substrate conversion rate.

The relationship between the more fundamental variables, μ and X_{fC}, and the substrate utilization rate can be shown by a cell balance on the biofilm (Eq. 39):

$$A\frac{dX_{fC}}{dt} = \bar{\mu}X_{fC}A + R_{aC}A - R_{dC}A \qquad (39)$$

At steady state with a negligible attachment rate, the cell balance reduces to the following:

$$R_{dC_{ss}} = \bar{\mu}X_{fC} \qquad (40)$$

Equating Eqs. 40 and 24 yields the following:

$$\bar{\mu}X_{fC} = \frac{Q}{A}(S_{i(C)} - S_{(C)})Y_{\frac{X}{S}} \qquad (41)$$

Eq. 41 indicates that measurement of the influent and effluent substrate concentrations in the bulk liquid, and an estimate of the observed yield, can be substituted for values of the more difficult to measure μ and X_{fC} in the characterization of steady state detachment rates.

By substituting Eq. 41 into the proposed detachment expression (Eq. 25) it can be shown that Eq. 25 is equivalent to the following:

$$R_{dC} = k_d\,\bar{\mu}\,\rho_{fC}\,L_f^2 \qquad (42)$$

Eq. 42 has been derived as a special case of a proposed mechanistic detachment model (Stewart, 1992).

There is a small discrepancy between two methods of determining the product $\bar{\mu}X_{fC}$. This product can either be calculated directly from measurement of the biofilm

cell number and substrate concentration, or by using Eq. 43 and either the detachment rate or the substrate utilization rate and the yield.

$$\bar{\mu}X_{fC} = \frac{Q}{A}(S_{i(C)}-S_{(C)})Y_{\frac{X}{S}} = \frac{Q}{A}X_{fC} = R_{dC} \qquad (43)$$

There is approximately a factor of 2 difference between the directly measured values of $\bar{\mu}X_{fC}$ and the calculated value of $QA^{-1}(S_{i(C)}-S_{(C)})Y_{X/S}$. This could be the result of either consistently low substrate concentration measurements, or consistently low biofilm cell counts, although it may be a combination of both. For glucose concentrations measured herein, a small underestimation in the glucose concentrations would result in a relatively large underestimation of the specific growth rate (Figure 32). Biofilm areal cell counts are subject to more possible experimental error, with errors tending to occur which might lower the estimated number of cells per unit area. Incomplete removal of cells from the coupon surface and incomplete homogenization of the scraped biofilm material prior to cell counting would each result in a decrease in the observed cell numbers, and could easily compound the error into giving values of X_{fC} which were a factor of 2 low. The less direct, but perhaps more accurate, method to estimate $\bar{\mu}X_{fC}$ at steady state is with either the substrate utilization rate and observed yield, or the detachment rate. While the product $\bar{\mu}X_{fC}$ is sensitive to errors in the measurement of both the areal cell density and the average specific growth rate, calculation of $\bar{\mu}X_{fC}$ by Eq. 43 is not.

A possibly more accurate estimate of $\bar{\mu}X_{fC}$ may be calculated by either of two approaches (Eq. 43). The first method uses the substrate utilization rate and observed yield. The substrate utilization rate is usually measurable for biological systems. The

observed yield can be calculated in a chemostat system (Eq. 44) (Bailey and Ollis, 1986).

$$Y_{\frac{X}{S}} = \frac{Y'_{\frac{X}{S}} D}{D + m Y'_{\frac{X}{S}}} \qquad (44)$$

Eq. 44 has not been applied to biofilm systems. For a steady state chemostat, Eq. 45 is true.

$$\mu = D \qquad (45)$$

Combining Eqs. 44 and 45 gives Eq. 46, which may be applied to biofilm systems.

$$Y_{\frac{X}{S}} = \frac{Y'_{\frac{X}{S}} \mu}{\mu + m Y'_{\frac{X}{S}}} \qquad (46)$$

Using an intrinsic or growth yield of 0.34 g CC [g GC]$^{-1}$ and an observed yield of 0.286 g CC [g GC]$^{-1}$ at D = 0.4 h^{-1} (Robinson et al., 1984), a maintenance coefficient of 0.22 g GC [g CC]$^{-1}$ h^{-1} for *Ps. aeruginosa* was calculated from Eq. 44.

Using m = 0.22, $Y'_{X/S}$ = 0.34, an average specific growth rate over all steady state experiments of 0.104 h^{-1}, and Eq. 46, a value of observed yield was calculated to be 0.198 g CC [g GC]$^{-1}$. The measured value of observed yield was 0.182 ± 0.02. This is very close to the observed yield of 0.20 ± 0.02 measured by Siebel (1987).

The second approach to calculate the product $\bar{\mu}X_{fc}$ is by the detachment rate. This method is easier and more accurate than individual measurement of $\bar{\mu}$ and X_{fc} since there is less experimental error associated with measurement of suspended cells as opposed to sessile cells.

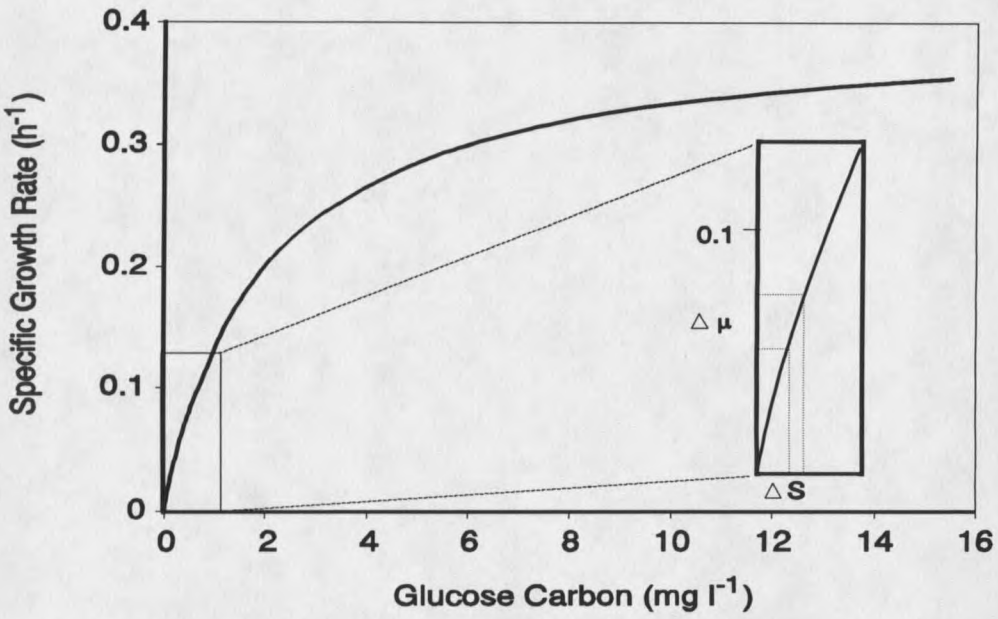

Figure 32. Specific growth rate as calculated by the Monod equation. Inset shows the sensitivity of the specific growth rate to small changes in the substrate concentration.

Particle Size Distribution

The detached particle size distributions show that the average detached particle size was 0.886 ± 0.072, 1.160 ± 0.163, and 0.838 ± 0.152 10^{-12} m^2, for experiments R0, S4, and T4, respectively. This is only slightly larger than the size of an average cell ($0.75 \times 10^{-12} m^2$), indicating that erosion of single cells is the dominant form of detachment occurring from a *Ps. aeruginosa* biofilm in a RotoTorque.

Size distribution information is important for the determination of a mechanistic model of biofilm detachment. Just as detachment of single cells indicates erosion of cells at the biofilm-bulk liquid interface, observation of larger particles is indicative of detachment occurring in the deeper layers of the biofilm. Calculated substrate profiles indicate that there is little difference in the "local" growth rate across a thin *Ps. aeruginosa* biofilm. This indicates that although the detachment rate is dependent on

the average specific growth rate across the growing region, it may not be dependent on "local" specific growth rate. A detachment rate expression which is dependent on the local specific growth rate would predict a nearly uniform distribution of particle sizes from single cells up to particles containing the full biofilm depth. It appears that detachment is an interfacial phenomenon. From material balance considerations the detachment rate is related to the average specific growth rate across the growing region (Eq. 40).

Further research on particle size distributions is necessary for the mechanistic modelling of the detachment phenomena. Although the detachment rates are described well by Eq. 25 for both pure and mixed cultures, detachment mechanisms may be different for motile as compared to non-motile cells, or for filamentous organisms as opposed to non-filamentous organisms. Because particle size distribution data is so labor-intensive (up to one hour per sample), it is proposed that continuous on-line particle counters be applied and modified, if necessary, to the measurement of the detachment rate and characterization of particle sizes. Data of this type would promote insight into more mechanistic detachment models.

Hypothesized Detachment Mechanism

The mechanism proposed below was developed to account for seemingly contradictory information about 1) substrate profiles, 2) detached particle sizes, 3) inert bead tracer studies, and 4) photomicrographs showing a "rippled" biofilm surface.

Detached Particle Size Distribution

Particle size distribution data indicate that the majority of the particles which detach from a biofilm comprise one or two cells, and that only a small fraction contain

more than two cells. This information indicates that more individual particles are detaching from the biofilm surface than from the deeper regions of the film.

Substrate Profiles

The substrate and specific growth rate profile calculated from BAM (Center's biofilm accumulation model) for a bulk glucose carbon concentration of 0.5 g GC m^{-3} with a biofilm thickness of 18 microns (10^{-6}m) are represented schematically in Figure 33. It can be seen that there is relatively little difference in either the glucose concentration or the specific growth rate with biofilm depth. Since the profiles are flat, growth must be occurring throughout the biofilm at a nearly constant rate. This analysis, applicable to thin films only, indicates that although cells are detaching mostly from the biofilm-liquid interface, *this is not a result of higher growth rates near the bulk liquid interface*.

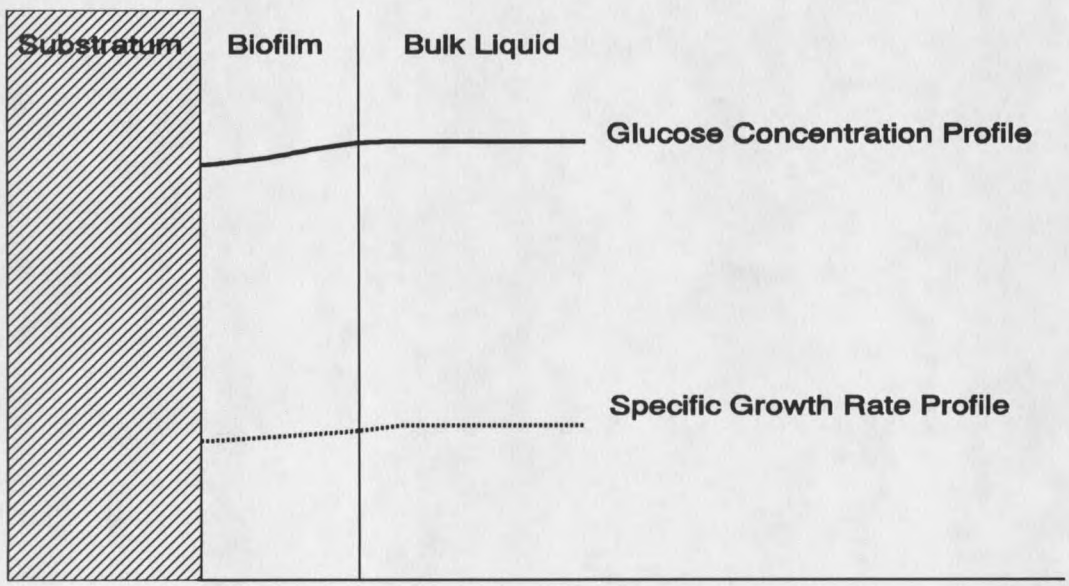

Figure 33. For zero-order kinetics, there is relatively little difference in either the glucose concentration or the specific growth rate with biofilm depth.

Inert Bead Tracer Studies

The research of Drury (1992) indicates that the biofilm does not behave in a plug flow manner with regard to the displacement of inert beads attached to and imbedded in the biofilm. The computer simulations "BIOSIM" and "BAM" both assume a plug flow displacement of biofilm components as a result of growth in the biofilm's deeper layers. This plug flow assumption results in the prediction of bead concentrations up to an order of magnitude lower than measured values. Instead of remaining on the surface, beads are found deep in the biofilm indicating that patchiness or physical mixing, alone or in combination, occurs in the biofilm significantly affecting the residence time of the inert bead in the biofilm.

Photomicrographs

The photomicrographs given in Photos 1 and 2 show a "rippled" biofilm surface. This rippling may have been accentuated, but was not caused by, the harsh treatments required to dry the biofilm samples before SEM analysis. Biofilm ripples similar to those shown in Photos 1 and 2 were observed with phase microscopy. The ripples were, on average, perpendicular to the flow of the bulk liquid, and resembled sand dunes.

Detachment Mechanism

At the microscale, a *Ps. aeruginosa* biofilm in a RotoTorque may resemble sand dunes which develop in the desert under a constant wind. Cells may be lifted off the upstream face of a "dune" and either reattach on the back side in the eddy that results, or be entrained in the bulk liquid and washed from the reactor (Figure 34).

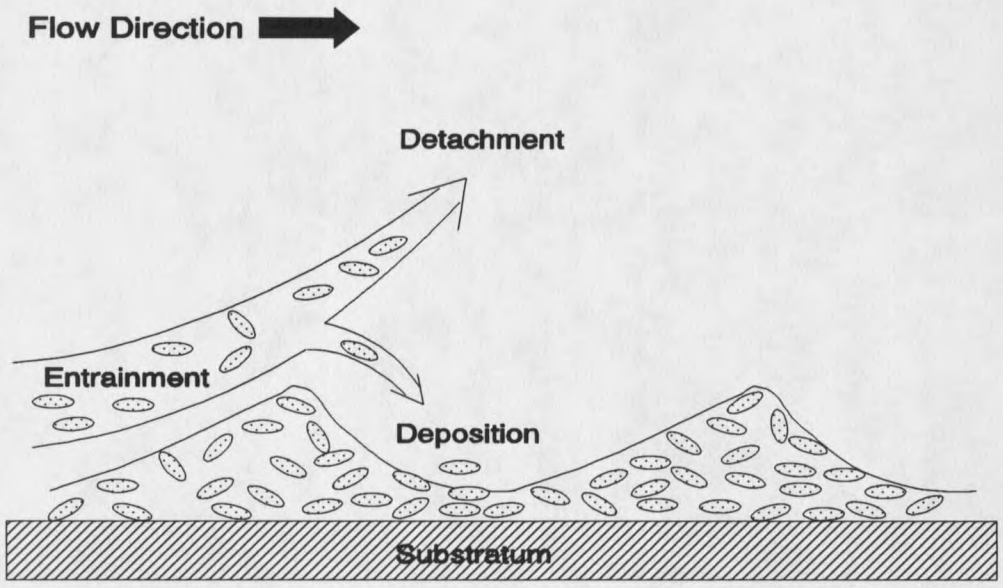

Figure 34. Cells may be lifted off the upstream face of a "dune" and either reattach on the back side or be entrained in the bulk liquid.

Biofilm ripples would, therefore, be dynamic and would travel in much the same way sand dunes move through the desert, burying and uncovering objects in their paths. Inert beads could, therefore, be covered with biofilm even though the bead had attached to the biofilm surface at one time. In the same manner, as the dune passed by, the bead would become exposed on the upstream face and may be lifted off the biofilm surface either to reattach in the eddy behind the dune's crest or to be washed from the reactor. A time series diagram is given in Figure 35.

In summary, particle size distributions given in Appendix I indicate that particles detach primarily from the biofilm-bulk liquid interface, although substrate profiles show very little difference between the specific growth rate at the film surface and at the substratum. Therefore, detachment from the surface, in thin films, is not the result of relatively high growth rates near the bulk liquid interface. Inert bead residence times

are much longer than plug flow displacement theories predict, indicating some type of mixing occurs in the biofilm. This hypothesis states that detachment does occur from the surface of the biofilm as the size distributions indicate, yet still allows for mixing of biofilm components required to match the observed residence time of the inert beads. This hypothesis incorporates seemingly contradictory data and observations into a unified mechanism for biofilm detachment.

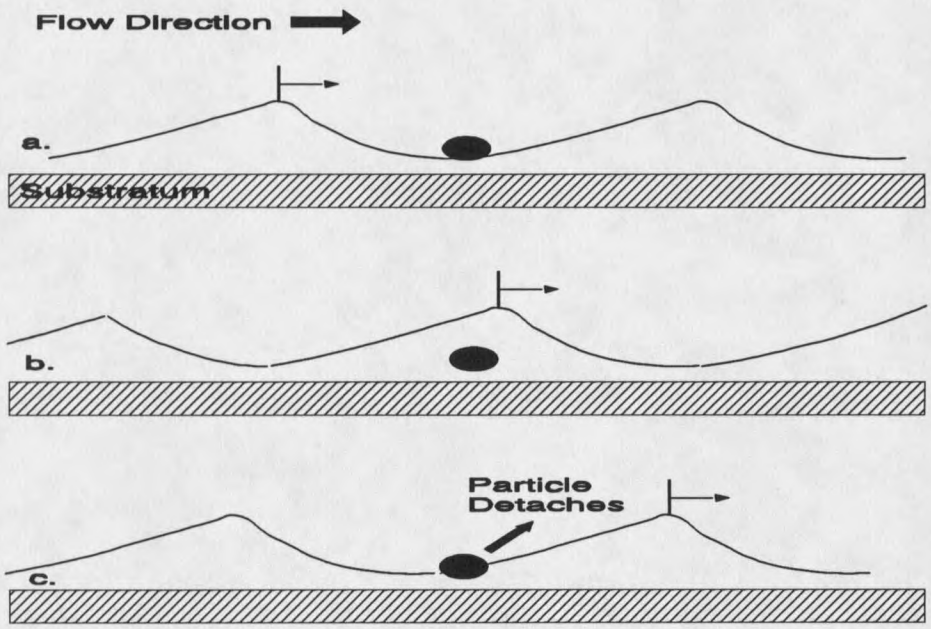

Figure 35. A small arrow marks the crest of a travelling dune (a). An attached inert particle becomes covered with biofilm as the dune passes by (b). The particle is exposed on the upstream slope and detaches.

Industrial Relevance

These results have significance to a wide variety of industries. In drinking water distribution systems it is believed that detachment from biofilms result in the high heterotrophic plate counts (HPC) and high coliform counts even in systems with a significant chlorine residual (van der Wende et al., 1989). It has also been found that

lowering the assimilable organic carbon (AOC) will give lower coliform and HPC counts (LeChevallier et al., 1991). These observations are consistent with the data presented here. A lower AOC concentration is equivalent to a lower substrate loading rate, and subsequently a lower substrate utilization rate. This would result in lower detachment of coliforms and HPC from the biofilm found in the distribution systems. The practice is common in the semi-conductor industry where synthetic scavengers are used to lower the organic carbon levels, thus reducing the substrate available for attached microbial growth and subsequent detachment (Collentro, 1986).

In oilfield injection systems, the biomass which detaches from the pre-injection pipelines is either removed by filtration, or is injected into the formation. In either case, increased detachment leads to increased operation and maintenance costs. If the AOC or electron acceptor concentration in these systems were significantly lowered by biological or chemical pre-treatment, filter life may be extended, and biocide treatments may be reduced. In the absence of pre-injection filters less biomass would be injected downhole, which would result in less acid cleaning of injection wells.

CONCLUSIONS

The results from this investigation, within the range of variables tested, have led to the following conclusions:

1) The cellular detachment rate is dependent on the cellular production rate.

2) An expression which incorporates substrate utilization rate, observed yield coefficient, and biofilm thickness gives better correlation than any previously proposed models for detachment rate.

3) Shear stress had no significant influence on the detachment rate.

4) Steady state biofilm thickness is dependent on the substrate loading rate and is not significantly affected by shear stress.

5) The observed yield can be calculated from the specific growth rate, the intrinsic yield, and the maintenance coefficient.

RECOMMENDATIONS FOR FURTHER RESEARCH

The results of this investigation could be strengthened and expanded by further experimental research on the kinetics of biofilm detachment. Recommendations toward future research are outlined in the following paragraphs.

1) The data indicate that detachment is the result of removal of a wide range of particle sizes. Image analysis measurements of size distributions are very time consuming. Therefore, an on-line particle counter would be of obvious benefit, since both sizes and numbers of detached particles could be enumerated on semi-continuous basis. A proposal written by Dr. Phil Stewart and myself has been funded to purchase and test commercially available equipment for detachment monitoring. If continuous size and number data were available, detachment theory could be rapidly advanced.

2) In this research, shear stress was not found to have a significant effect on detachment rate. Therefore, the range of shear stress studied should be extended. It may be necessary to perform these experiments in a pipeline system or improve the RotoTorque to handle higher rotational speeds. In any case, further research should clearly delineate the effects of shear stress and the effects of transport limitations.

3) Substrate loading rate is the product of influent glucose concentration and volumetric flow rate divided by reactor area. In this investigation only the influent glucose concentration was changed. Further research could determine the effect of changes in volumetric flow rate on detachment. Such changes would affect residence time in the reactor, which may affect substrate utilization and, thus, detachment.

NOMENCLATURE

A Area (L^2)

A_i Vertical surface area of RotoTorque inner cylinder (L^2)

g_0 Gravitational acceleration constant ($L\ t^{-2}$)

$G_{i(C)}$ Glucose carbon concentration in the influent ($M_{G(C)}\ L^{-3}$)

$G_{f(C)}$ Glucose carbon concentration in the biofilm ($M_{G(C)}\ L^{-3}$)

$G_{l(C)}$ Glucose carbon concentration in the liquid phase ($M_{G(C)}\ L^{-3}$)

$j_{fG(C)}$ Flux of glucose carbon into the biofilm ($M_{G(C)}\ L^{-2}\ t^{-1}$)

$j_{lP(C)}$ Flux of product carbon into the liquid phase ($M_{P(C)}\ L^{-2}\ t^{-1}$)

k_d Detachment coefficient (units expression dependent)

k'_d Non-growth associated detachment coefficient ($M\ L^{-1}\ t^{-1}$)

k''_d Growth associated detachment coefficient ($M\ L^{-1}$)

$k_{\rho 1}$ First order volumetric density coefficient ($M\ L^{-3}$)

$k_{\rho 1/2}$ One-half order volumetric density coefficient ($M\ L^{-5/2}$)

L_f Biofilm thickness (L)

m Maintenance coefficient ($M_{G(C)}\ M_{C(C)}^{-1}\ t^{-1}$)

M_i Torque ($M\ L^2\ t^{-2}$)

n Exponent on shear stress (unitless)

$P_{f(C)}$ Product carbon concentration in the biofilm ($M_{P(C)}\ L_{-2}$)

$P_{i(C)}$ Product carbon concentration in the influent ($M_{P(C)}\ L^{-3}$)

$P_{l(C)}$ Product carbon concentration in the liquid phase ($M_{P(C)}\ L^{-3}$)

Q Volumetric flow rate ($L^3\ t^{-1}$)

r_i Radius of RotoTorque inner cylinder (L)

R_a Attachment rate ($M\ L^{-2}\ t^{-1}$)

R_{aC} Cellular attachment rate ($M_C\ L^{-2}\ t^{-1}$)

$R_{aC(C)}$ Cellular carbon attachment rate ($M_{C(C)}\ L^{-2}\ t^{-1}$)

R_d Detachment rate ($M\ L^{-2}\ t^{-1}$)

R_{dC} Cellular detachment rate ($M_C\ L^{-2}\ t^{-1}$)

$R_{dC(C)}$ Cellular carbon detachment rate ($M_{C(C)}\ L^{-2}\ t^{-1}$)

R_{de} Detachment rate due to erosion ($M\ L^{-2}\ t^{-1}$)

$R_{d\Delta\tau}$ Detachment rate due to change in shear stress ($M\ L^{-2}\ t^{-1}$)

$R_{fC(C)}$ Biomass cell carbon production rate in the biofilm ($M_{C(C)}\ L^{-2}\ t^{-1}$)

$R_{fP(C)}$ Specific product carbon production rate in the biofilm ($M_{P(C)}\ M_{C(C)}^{-1}\ t^{-1}$)

$R_{lP(C)}$ Specific product carbon production rate ($M_{P(C)}\ M_{C(C)}^{-1}\ t^{-1}$)

$R_{L(C)}$ Substrate carbon loading rate ($M_{(C)}\ L^{-2}\ t^{-1}$)

$R_{U(C)}$ Substrate carbon utilization rate ($M_{(C)}\ L^{-2}\ t^{-1}$)

$S_{(C)}$ Substrate carbon concentration ($M_{(C)}\ L^{-3}$)

$S_{i(C)}$ Substrate carbon concentration in the influent ($M_{(C)}\ L^{-3}$)

t Time (t)

V Volume (L^3)

X_f Areal biomass density ($M\ L^{-2}$)

$X_{fC(C)}$ Areal cell carbon density in the biofilm ($M_{C(C)}\ L^{-2}$)

$X_{iC(C)}$ Cell carbon concentration in the influent ($M_{C(C)}\ L^{-3}$)

$X_{lC(C)}$ Cell carbon concentration in the liquid phase ($M_{C(C)}L^{-3}$)

X_{fC} Areal cell density in the biofilm ($\#_C\ L^{-2}$)

X_{iC} Cell number concentration in the influent ($\#_C\ L^{-3}$)

X_{lC} Cell number concentration in the liquid phase ($\#_C\ L^{-3}$)

$Y_{P/S}$ Product yield ($M_{P(C)}\ M_{G(C)}^{-1}$)

$Y_{X/S}$ Observed biomass yield ($M_{C(C)}\ M_{G(C)}^{-1}$)

$Y'_{X/S}$ Intrinsic biomass yield ($M_{C(C)}$ $M_{G(C)}^{-1}$)

z Distance from substratum (L)

μ Specific growth rate (t^{-1})

$\bar{\mu}$ Average specific growth rate (t^{-1})

ν Average fluid velocity ($L\ t^{-1}$)

ρ_f Biofilm volumetric density ($M\ L^{-3}$)

$\bar{\rho}_f$ Average biofilm volumetric density ($M\ L^{-3}$)

ρ_{fC} Biofilm volumetric cell density ($M_C\ L^{-3}$)

ρ_{fm} Estimated volumetric density of a monolayer ($M\ L^{-3}$)

ρ_{fz} Local volumetric density ($M\ L^{-3}$)

τ Shear stress at biofilm surface ($M\ L^{-1}\ t^{-2}$)

$\bar{\tau}$ Average shear stress on RotoTorque inner cylinder ($M\ L^{-1}\ t^{-2}$)

BIBLIOGRAPHY

-a-

Abulez, E.-M., and G. Lyberatos 1987. "Periodic Optimization of Continuous Microbial Growth Processes", Biotechnology and Bioengineering, 29:1059.

Applegate, D.H., and J.D. Bryers 1991. "Effects of Carbon and Oxygen Limitations and Calcium Concentrations on Biofilm Removal Processes", Biotechnology and Bioengineering, 37:17.

Arvin, E., and P. Harremoës 1990. "Concepts and Models for Biofilm Reactor Performance", Wat. Sci. Tech., 22(1/2):171.

Atkinson, B., E.L. Swilley, A.W. Busch, and D.A. Williams 1967. "Kinetics, Mass Transfer, and Organism Growth in a Biological Film Reactor", Trans. Instn. Chem. Engrs., 45:T257.

Atkinson, B., and I.S. Daoud 1968. "The Analogy Between Micro-biological 'Reactions' and Heterogeneous Catalysts", Trans. Instn. Chem. Engrs., 46:T19.

Atkinson, B., I.S. Daoud, and D.A. Williams 1968. "A Theory for the Biological Film Reactor", Trans. Instn. Chem. Engrs., 46:T245.

-b-

Baier, R.E., and L. Weiss 1975. "Demonstrations of the Involvement of Adsorbed Proteins in Cell Adhesion and Cell Growth on Solid Surfaces", in R.E. Baier (ed.), Applied Chemistry at Protein Interfaces, Advances in Chemistry Series, 145, American Chemical Society, Washington D.C., p.300.

Baier, R.E. 1980. "Substrata Influences on Adhesion of Microorganisms and Their Resultant New Surface Properties", in G. Bitton and K.C. Marshall (eds.), Adsorption of Microorganisms to Surfaces, John Wiley & Sons Inc., New York, NY, p.59.

Bailey, J.E., and D.F. Ollis 1986. Biochemical Engineering Fundamentals, McGraw-Hill Book Company, New York, NY.

Baillod, R.C., and W.C. Boyle 1970. J. San. Eng. Div., Proceedings of the ASCE, 96(SA4):525.

Bakke, R. 1983. "Dynamics of Biofilm Processes: Substrate Load Variations", Master's thesis, Montana State University, Bozeman, MT.

Bakke, R., M.G. Trulear, J.A. Robinson, and W.G. Characklis 1984. "Activity of *Pseudomonas aeruginosa* in Biofilms: Steady State", Biotechnology and Bioengineering, 26:1418.

Bakke, R. 1986. "Biofilm Detachment", Ph.D. thesis, Montana State University, Bozeman, MT.

Bakke, R., and P.Q. Olsson 1986. "Biofilm Thickness Measurements by Light Microscopy", Journal of Microbiol. Methods, 5:93.

Bakke, R., W.G. Characklis, M.H. Turakhia, and A.-I. Yeh 1990. "Modeling a Monopopulation Biofilm System: *Pseudomonas aeruginosa*", in W.G. Characklis and K.C. Marshall (eds.), Biofilms, John Wiley & Sons Inc., New York, NY, p.487.

Baldwin, W.W., and P.W. Bankston 1988. "Measurement of Live Bacteria by Nomarski Interference Microscopy and Stereologic Methods as Tested with Macroscopic Rod-Shaped Models", Applied and Environmental Microbiology, 54(1):105.

Baltzis, B.C., and A.G. Fredrickson 1988. "Limitation of Growth Rate by Two Complementary Nutrients: Some Elementary but Neglected Considerations", Biotechnology and Bioengineering, 31:75.

Bauer, S., and E. Ziv 1976. "Dense Growth of Aerobic Bacteria in a Bench-Scale Fermentor", Biotechnology and Bioengineering, 18:81.

Belay, N., R. Johnson, B. Rajagopal, E.C. de Macario, and L. Daniels 1988. "Methanogenic Bacteria from Human Dental Plaque", Applied and Environmental Microbiology, 54(2):600.

Bird, R.B., W.E. Stewart, and E.N. Lightfoot 1960. Transport Phenomena, John Wiley & Sons Inc., New York, NY.

Bjørnsen, P.K. 1986. "Automatic Determination of Bacterioplankton Biomass by Image Analysis", Applied and Environmental Microbiology, 51(6):1199.

Bott, T.R., and P.C. Miller 1983. "Mechanisms of Biofilm Formation on Aluminum Tubes", J. Chem. Tech. Biotechnol., 33B:177.

Brash, J.L., and Q.M. Samak 1978. "Dynamics of Interactions between Human Albumin and Polyethylene Surface", Journal of Colloid and Interface Science, 65(3):495.

Brock, T.D., and M.T. Madigan 1988. Biology of Microorganisms, Prentice Hall Inc., Englewood Cliffs, NJ.

Bryers, J.D. 1980. "Dynamics of Early Biofilm Formation in a Turbulent Flow System", Ph.D. thesis, Rice University, Houston, TX.

Bryers, J.D., and W.G. Characklis 1981. "Early Fouling Biofilm Formation in a Turbulent Flow System: Overall Kinetics", Water Research, 15:483.

Bryers, J.D., and W.G. Characklis 1982. "Processes Governing Primary Biofilm Formation", Biotechnology and Bioengineering, 24:2451.

Bryers, J.D. 1984. "Biofilm Formation and Chemostat Dynamics: Pure and Mixed Culture Considerations", Biotechnology and Bioengineering, 26:948.

Bryers, J.D. 1987. "Biologically Active Surfaces: Processes Governing the Formation and Persistence of Biofilms", Biotechnology Progress, 3(2):57.

Buchanan, R.E., and N.E. Gibbons 1974. Bergey's Manual of Determinative Bacteriology, The Williams and Wilkins Company, Baltimore, MD.

Bungay, H.R., W.J. Whalen, and W.M. Saunders 1969. "Microprobe Techniques for Determining Diffusivities and Respiration Rates in Microbial Slime Systems", Biotechnology and Bioengineering, 11:765.

-c-

Carpenter, S., K. Hall, and K. Saul 1990. "Playing the Numbers Game: Achieving Accurate Bacteria Counts Using Epifluorescence", Microcontamination, January:27.

Chang, H.T., and B.E. Rittman 1987. "Mathematical Modeling of Biofilm on Activated Carbon", Environ. Sci. Technol., 21(3):273.

Chang, H.T., and B.E. Rittman 1988. "Comparative Study of Biofilm Shear Loss on Different Adsorptive Media", Journal WPCF, 60(3):362.

Chang, H.T., B.E. Rittman, D. Amar, R. Heim, O. Ehlinger, and Y. Lesty 1991. "Biofilm Detachment Mechanisms in a Liquid-Fluidized Bed", Biotechnology and Bioengineering, 38:499.

Characklis, W.G. 1973. "Attached Microbial Growths - I. Attachment and Growth", Water Research, 7:1113.

Characklis, W.G. 1973. "Attached Microbial Growths - II. Frictional Resistance Due to Microbial Slimes", Water Research, 7:1249.

Characklis, W.G., N. Zelver, and B.F. Picologlou 1977. "Hydraulic Deterioration Due to Microbial Slime Growths", AWWA Water Quality Technology Conference, December 4-7, 1977, Kansas City, MO.

Characklis, W.G. 1978. "Microbial Reaction Rate Expressions", Journal of the Environmental Engineering Division, Proceedings of the ASCE, 104(EE3):531.

Characklis, W.G. 1979. "Biofilm Development and Destruction in Turbulent Flow", Annual Cooling Tower Institute Meeting, January, 1979, Houston, TX.

Characklis, W.G., M.G. Trulear, N. Stathopoulos, and L.-C. Chang 1979. "Oxidation and Destruction of Microbial Films", in R. L. Jolley, W.A. Brungs, and R.B. Cumming (eds.), Water Chlorination: Environmental Impact and Health Effects, Volume 3, Ann Arbor Science Publishers Inc., Ann Arbor, MI.

Characklis, W.G. 1980. "Biofilm Development and Destruction", Final Report, EPRI CS-1554, Project RP902-1, Electric Power Research Institute, Palo Alto, CA.

Characklis, W.G., J.D. Bryers, M.G. Trulear, and N. Zelver 1980. "Biofouling Film Development and Its Effects on Energy Losses: A Laboratory Study", in J.F. Garey et al. (eds.), Condenser Biofouling Control, Ann Arbor Science Publishers Inc., Ann Arbor, MI, p.49.

Characklis, W.G., and M.G. Trulear 1980. "Dynamics of Microbial Film Processes", First National Symposium on Rotating Biological Contactor Technology, February, 1980, Seven Springs, PA.

Characklis, W.G., M.G. Trulear, N. Stathopoulos, and L.C. Chang 1980. "Fundamental Considerations in Biofouling Control", Annual Cooling Tower Institute Meeting, January 21-23, 1980, Houston, TX.

Characklis, W.G., N. Zelver, M. Turakhia, and F.L. Roe 1981. "Energy Losses in Water Conduits: Monitoring and Diagnosis", 42nd Annual International Water Conference, October 26-28, 1981, Pittsburgh, PA.

Characklis, W.G. 1981. "Fouling Biofilm Development: A Process Analysis", Biotechnology and Bioengineering, 23:1923.

Characklis, W.G., N. Zelver, and M. Turakhia 1981. "Microbial Films and Energy Losses", Symposium on Marine Biodeterioration, Office of Naval Research, April, 1981, Bethesda, MD.

Characklis, W.G. 1983. "Process Analysis in Microbial Systems: Biofilms as a Case Study", Mathematics in Microbiology, Academic Press London, London, England.

Characklis, W.G., M.H. Turakhia, and N. Zelver 1984. "Biofouling of Heat Transfer Surfaces - Part II", Corrosion & Maintenance, July-Sept.:213.

Characklis, W.G., R. Bakke, and M.G. Trulear 1984. "Fundamental Considerations of Fixed Film Systems", in C. Cooney and A.E. Humphrey (eds.), Waste Management and Pollution Control, Comprehensive Biotechnology Series, 54, Pergamon Press, New York, NY, p. 945.

Characklis, W.G., and F.L. Roe 1984. "Monitoring Buildup of Fouling Deposits on Surfaces of Fluid Handling Systems", U.S. Patent 4,485,450, November 27, 1984.

Characklis, W.G., R. Bakke, and A.-I. Yeh 1985. "Microbial Fouling and Its Control: A Phenomenological Approach", in W. Chow and Y.G. Mussalli (eds.), Proceedings: Condenser Biofouling Control -- State-of-the-Art Symposium, Electric Power Research Institute, November, 1985, Palo Alto, CA, p. 2.1.

Characklis, W.G., R. Bakke, and M.H. Turakhia 1988. "Theoretical and Experimental Analysis of a *Pseudomonas aeruginosa* Biofilm", International Conference for Water and Wastewater Microbiology, February 8-11, 1988, Newport Beach, CA.

Characklis, W.G. 1990. "Biofilm Processes", in W.G. Characklis and K.C. Marshall (eds.), Biofilms, John Wiley & Sons Inc., New York, NY, p.195.

Characklis, W.G., M.H. Turakhia, and N. Zelver 1990. "Transport and Interfacial Transfer Phenomena", in W.G. Characklis and K.C. Marshall (eds.), Biofilms, John Wiley & Sons Inc., New York, NY, p. 265.

Cleaver, J.W., and B. Yates 1975. "A Sub Layer Model for the Deposition of Particles from a Turbulent Flow", Chemical Engineering Science, 30:983.

Cleaver, J.W., and B. Yates 1976. "The Effect of Re-Entrainment on Particle Deposition", Chemical Engineering Science, 31:147.

Collentro, W.V. 1986. "Synthetic Organic Scavengers", Ultrapure Water, 3(2):51.

Costerton, J.W., and E.S. Lashen 1984. "Influence of Biofilm on Efficacy of Biocides on Corrosion-Causing Bacteria", Materials Performance, February:13.

Crawford, D.J. 1987. "Hydraulic Effects of Biofilm Accumulation in a Simulated Porous Media Flow System", Master's thesis, Montana State University, Bozeman, MT.

Crawford, P.B. 1966. "Water Technology: Continual Changes Observed in Bacterial Stratification Rectification", Prod. Mon., 26:12.

Crouch, C.F., H.W. Fowler, and R.E. Spier 1985. "The Adhesion of Animal Cells to Surfaces: The Measurement of Critical Surface Shear Stress Permitting Attachment or Causing Detachment", J. Chem. Tech. Biotechnol., 35B:273.

-d-

Daugulis, A.J., and D.E. Swaine 1987. "Examination of Substrate and Product Inhibition Kinetics on the Production of Ethanol by Suspended and Immobilized Cell Reactors", Biotechnology and Bioengineering, 29:639.

Dawson, M.P. 1981. "The Effect of Starvation on the Cell Surface Characteristics of Marine Bacteria", Bachelor's Honor's thesis, University of New South Wales.

Doetsch, R.N., and T.M. Cook 1973. Introduction to Bacteria and Their Ecology, University Park Press, Baltimore, MD.

Doran, P.M., and J.E. Bailey 1986. "Effects of Immobilization on Growth Fermentation Properties, and Macromolecular Composition of *Saccharomyces cerevisiae* Attached to Gelatin", Biotechnology and Bioengineering, 28: 73.

Doran, P.M., and J.E. Bailey 1987. "Effects of Immobilization on the Nature of Glycolytic Oscillations in Yeast", Biotechnology and Bioengineering, 29:892.

Drury, W. 1992. "Interactions of One-Micron Latex Beads with Biofilms", Ph.D. thesis, Montana State University, Bozeman, MT.

Dziewulski, D.M., S.P. Fraleigh, D.H. Pope, S. Thomas, P. Puente, and G. Annexstad 1990. "Microbial Production of Hydrogen Sulfide in Gas Storage and Production Fields: Field Studies, Preliminary Modeling and Control", Corrosion '90, April 23-27, 1990, Las Vegas, NV, paper 35.

-e-

Eager, R.G. Jr., A.B. Thies, M.H. Turakhia, and W.G. Characklis 1986. "Glutaraldehyde: Impact on Corrosion Causing Biofilms", Corrosion '86 Symposium on Microbiologically Influenced Corrosion, March, 1986, Houston, TX.

Eagon, R.G. 1962. "Composition of an Extracellular Slime Produced by *Pseudomonas aeruginosa*", Canadian Journal of Microbiology, 8:585.

Escher, A., and W.G. Characklis 1982. "Algal-Bacterial Interactions within Aggregates", Biotechnology and Bioengineering, 24:2283.

Escher, A. 1986. "Colonization of a Smooth Surface by *Pseudomonas aeruginosa*: Image Analysis Methods", Ph.D. thesis, Montana State University, Bozeman, MT.

Escher, A., and W.G. Characklis 1990. "Modelling Initial Events in Biofilm Accumulation", in W.G. Characklis and K.C. Marshall (eds.), Biofilms, John Wiley & Sons Inc., New York, NY, p.45.

-f-

Fenchel, T. 1986. "The Ecology of Heterotrophic Microflagellates", in K.C. Marshall (ed.), Adv. Microbial Ecol., 9:57.

Fletcher, M., and G.D. Floodgate 1973. "An Electron-microscopic Demonstration of an Acidic Polysaccharide Involved in the Adhesion of a Marine Bacterium to Solid Surfaces", Journal of General Microbiology, 74:325.

Fletcher, M. 1976. "The Effects of Proteins on Bacterial Attachment to Polystyrene", Journal of General Microbiology, 94:400.

Fransolet, G., A. Depelchin, G. Villers, R. Goossens, and W.J. Masschelein 1988. "The Role of Bicarbonate in Bacterial Growth in Oligotrophic Waters", Journal AWWA, November:57.

-g-

Geesey, G.G., M.W. Mittelman, and V.T. Lieu 1987. "Evaluation of Slime- Producing Bacteria in Oil Field Core Flood Experiments", Applied and Environmental Microbiology, 53(2):278.

Gehr, R., and J.G. Henry 1983. "Removal of Extracellular Material: Techniques and Pitfalls", Water Research, 17(12):1743.

Gunawan, C. 1991. "The Rate of Cellular Attachment to an Established Biofilm", Master's thesis, Montana State University, Bozeman, MT.

-h-

Hao, O.J., A.P. Davis, and K.K. Phull 1990. "Biological Fixed-Film Systems", Journal WPCF, 62(4):406.

Harrison, J.S. 1967. Process Biochem., 2:41.

Henze, M., C.P.L. Grady Jr., W. Gujer, G.v.R. Marais, and T. Matsuo 1987. "Activated Sludge Model No. 1", by IAWPRC Task Group on Mathematical Modelling for Design and Operation of Biological Wastewater Treatment, London, England.

Herbert, D. 1976. "Stoichiometric Aspects of Microbial Growth", in A.C.R. Dean et al. (eds.), Continuous Culture 6: Applications and New Fields, Ellis Horwood Ltd., Chichester, England, p. 1.

Hermanowicz, S.W., R.E. Danielson, and R.C. Cooper 1989. "Bacterial Deposition on and Detachment from Surfaces in Turbulent Flow", Biotechnology and Bioengineering, 33:157.

Hernandez, E., and M.J. Johnson 1967. "Anaerobic Growth Yields of *Aerobacter cloacae* and *Escheria coli*", Journal of Bacteriology, 94(4):991.

Heukelekian, H., and E.S. Crosby 1956. "Slime Formation in Polluted Waters", Sewage Industrial Waters, 28:78.

Heukelekian, H., and E.S. Crosby 1956. "Slime Formation in Sewage", Sewage Industrial Waters, 28:206.

Hobbie, J.E., R.J. Daley, and S. Jasper 1977. "Use of Nucleopore Filters for Counting Bacteria by Fluorescence Microscopy", Applied and Environmental Microbiology, 35:858.

Hoehn, R.C., and A.D. Ray 1973. J. Wat. Poll. Contr. Fed., 46:2302.

Holben, W.E., J.K. Jansson, B.K. Chelm, and J.M. Tiedje 1988. "DNA Probe Method for the Detection of Specific Microorganisms in the Soil Bacterial Community", Applied and Environmental Microbiology, 54(3):703.

Holt, H.G. 1977. The Shorter Bergey's Manual of Determinative Bacteriology, Eighth Edition, The Williams and Wilkins Company, Baltimore, MD.

Howell, J.A., and B. Atkinson 1976. "Sloughing of Microbial Film in Trickling Filters", Water Research, 10:307.

Hulburt, H.M., and S. Katz 1964. "Some Problems in Particle Technology", Chemical Engineering Science, 19:555.

Hunter, J.S. 1960. "Some Applications of Statistics to Experimentation", Chem. Eng. Progr. Symposium, 56(31):VII-1.

-i-

-j-

Jacangelo, J.G., E.M. Aieta, and K.E. Carns 1989. "Assessing Hollow-Fiber Ultrafiltration for Particulate Removal", Journal AWWA, Nov.:68.

Jacques, M., and B. Foiry 1987. "Electron Microscopic Visualization of Capsular Material of *Pasteurella multocida* Types A and D Labeled with Polycationic Ferritin", Journal of Bacteriology, 169(8):3470.

Jang, L.K., and T.F. Yen 1985. "A Theoretical Model of Diffusion of Motile and Non-motile Bacteria Toward Solid Surfaces", in J.E. Zajic and E.C. Donaldson (eds.), International Bioresources Journal: Microbes and Oil Recovery, 1:226.

Jansen, J., and G.H. Kristensen 1980. "Fixed Film Kinetics: Denitrification in Fixed Films", Report 80-59, Department of Sanitary Engineering, Technical University of Denmark.

Jørgensen, B.B., and D.J. Des Marais 1986. "A Simple Fiber-optic Microprobe for High Resolution Light Measurements: Application in Marine Sediment", Limnol. Oceanogr., 31(6):1376.

-k-

Kirkpatrick, J.P., L.V. McIntire, and W.G. Characklis 1980. "Mass and Heat Transfer in a Circular Tube with Biofouling", Water Research, 14:117.

Kornegay, B.H., and J.F. Andrews 1967. "Characteristics and Kinetics of Fixed Film Biological Reactors", Final Report, Grant WP-01181, Federal Water Pollution Control Administration, U.S. GPO, Washington, D.C.

Kreikenbohm, R., and W. Stephan 1985. "Application of a Two-compartment Model to the Wall Growth of *Pelobacter acidigallici* under Continuous Culture Conditions", Biotechnology and Bioengineering, 27:296.

-l-

Lappin-Scott, H.M., F. Cusack, and J.W. Costerton 1988. "Nutrient Resuscitation and Growth of Starved Cells in Sandstone Cores: a Novel Approach to Enhanced Oil Recovery", Applied and Environmental Microbiology, 54(6):1373.

LeChevallier, M.W., T.M. Babcock, and R.G. Lee 1987. "Examination and Characterization of Distribution System Biofilms", Applied and Environmental Microbiology, 53(12):2714.

LeChevallier, M.W., C.D. Cawthon, and R.G. Lee 1988. "Inactivation of Biofilm Bacteria", Applied and Environmental Microbiology, 54(10):2492.

LeChevallier, M.W., W. Schulz, and R.G. Lee 1991. "Bacterial Nutrients in Drinking Water", Applied and Environmental Microbiology, 57(3):857.

Lee, S.S., A.P. Jackman, and E.D. Schroeder 1975. "Role of Flocculation in Transient Microbial Growth", Water Research, 9:491.

Lewandowski, Z., G. Walser, R. Larsen, B. Peyton, and W.G. Characklis 1990. "Biofilm Surface Positioning", Environmental Engineering Proceedings 1990, EE Div/ASCE, July 8-11, Arlington, VA, p.17.

Little, B.J., and A. Zsolnay 1985. "Chemical Fingerprinting of Adsorbed Organic Materials on Metal Surfaces", Journal of Colloid and Interface Science, 104(1):79.

Logan, B.E., and S.W. Hermanowicz 1987. "Application of the Penetration Theory to Oxygen Transfer to Biofilms", Biotechnology and Bioengineering, 29:762.

Logan, B.E., and J.R. Hunt 1988. "Bioflocculation as a Microbial Response to Substrate Limitations", Biotechnology and Bioengineering, 31:91.

Luong, J.H.T. 1987. "Generalization of Monod Kinetics for Analysis of Growth Data with Substrate Inhibition", Biotechnology and Bioengineering, 29:242.

Luria, S.E. 1960. "The Bacterial Protoplasm: Composition and Organization", in I.C. Gunsalus and R.Y. Stainer (eds.), The Bacteria, Vol. 1, Academic Press Inc., New York, NY.

-m-

Macaskie, L.E., J.M. Wates, and A.C.R. Dean 1987. "Cadmium Accumulation by a *Citrobacter* sp. Immobilized on Gel and Solid Supports: Applicability to the Treatment of Liquid Wastes Containing Heavy Metal Cations", Biotechnology and Bioengineering, 30:66.

Marqués, A.M., I. Estañol, J.M. Alsina, C. Fusté, D. Simon-Pujol, J. Guinea, and F. Congregado 1986. "Production and Rheological Properties of the Extracellular Polysaccharide Synthesized by *Pseudomonas* sp. Strain EPS-5028", Applied and Environmental Microbiology, 52(5):1221.

Marshall, K.C., R. Stout, and R. Mitchell 1971. "Mechanism of the Initial Events in the Sorption of Marine Bacteria to Surfaces", Journal of General Microbiology, 68:337.

Marshall, K.C., and R.H. Cruickshank 1973. "Cell Surface Hydrophobicity and the Orientation of Certain Bacteria at Interfaces", Arch. Mikrobiol., 91:29.

Marshall, K.C. 1979. "Strategies of Microbial Life in Extreme Environments", in M. Shilo (ed.), Dahlem Konferenzen Life Sciences Research Report 13, Verlag Chemie, Weinheim, p.281.

Marshall, K.C. 1985. "Bacterial Adhesion in Oligotrophic Habitats", Microbiological Sciences, 2(11):321.

Marshall, P.A., G.I. Loeb, M.M. Cowan, and M. Fletcher 1989. "Response of Microbial Adhesives and Biofilm Matrix Polymers to Chemical Treatments as Determined by Interference Reflection Microscopy and Light Section Microscopy", Applied and Environmental Microbiology, 55(11):2827.

Masuda, S., Y. Watanabe, and M. Ishiguro 1991. "Biofilm Properties and Simultaneous Nitrification and Denitrification in Aerobic Rotating Biological Contactors", Wat. Sci. Tech., 23:1355.

Matson, J.V., and W.G. Characklis 1976. "Diffusion into Microbial Aggregates", Water Research, 10:877.

Mayberry, W.R., G.L. Prochazka, and W.J. Payne 1968. "Factors Derived from Studies of Aerobic Growth in Minimal Media", Journal of Bacteriology, 96(4):1424.

Meadows, P.S. 1971. "Attachment of Bacteria to Solid Surfaces", Arch. Mikrobiol., 75:374.

Mian, F.A., T.R. Jarman, and R.C. Righelato 1978. "Biosynthesis of Exopolysaccharide by *Pseudomonas aeruginosa*", Journal of Bacteriology, 134(2):418.

Michels, P.A.M., J.P.J. Michels, J. Boonstra, and W.N. Konings 1979. "Generation of an Electrochemical Proton Gradient in Bacteria by the Excretion of Metabolic End Products", FEMS Microbiology Letters, 5:357.

Moraine, R.A., and P. Rogovin 1971. "Xanthan Biopolymer Production at Increased Concentration by pH Control", Biotechnology and Bioengineering, 13:381.

MSUSTAT Statistical Analysis Package Version 3.20 1986. Developed by Richard E. Lund, Montana State University, Bozeman, MT.

Mueller, R.F. 1990. "Characterization of Initial Events of Bacterial Colonization at Solid-Water Interfaces Using Image Analysis", Master's thesis, Montana State University, Bozeman, MT.

Mulcahy, L.T., and W.K. Shieh 1987. "Fluidization and Reactor Biomass Characteristics of the Denitrification Fluidized Bed Biofilm Reactor", Water Research, 21(4):451.

Murgel, G.A., L.W. Lion, C. Acheson, M.L. Shuler, D. Emerson, and W.C. Ghiorse 1991. "Experimental Apparatus for Selection of Adherent Microorganisms under Stringent Growth Conditions", Applied and Environmental Microbiology, 57(7):1987.

-n-

Nagai, S. 1979. "Mass and Energy Balances for Microbial Growth Kinetics", in T.K. Ghose, A. Fletcher, and N. Blakebrough (eds.), Advances in Biochemical Engineering, Springer-Verlag, New York, NY, p.53.

Namkung, E., and B.E. Rittmann 1987. "Evaluation of Bisubstrate Secondary Utilization Kinetics of Biofilms", Biotechnology and Bioengineering, 29:335.

Namkung, E., and B.E. Rittmann 1987. "Modeling Bisubstrate Removal by Biofilms", Biotechnology and Bioengineering, 29:269.

Nelson, C.H., J.A. Robinson, and W.G. Characklis 1985. "Bacterial Adsorption to Smooth Surfaces: Rate, Extent, and Spatial Pattern", Biotechnology and Bioengineering, 27:1662.

Nielsen, P.H. 1987. "Biofilm Dynamics and Kinetics during High-Rate Sulfate Reduction under Anaerobic Conditions", Applied and Environmental Microbiology, 53(1):27.

-o-

Obayashi, A.W., and A.F. Gaudy, Jr. 1973. "Aerobic Digestion of Extracellular Microbial Polysaccharides", Journal WPCF, 45(7):1584.

Otto, R., A.S.M. Sonnenberg, H. Veldkamp, and W.N. Konings 1980. "Generation of an Electrochemical Proton Gradient in *Streptococcus cremoris* by Lactate Efflux", Proc. Natl. Acad. Sci. USA, 77(9):5502.

Otto, F., and K.C. Tsou 1985. "A Comparative Study of DAPI, DIPI, and Hoechst 33258 and 33342 as Chromosomal DNA Stains", Stain Technology, 60(1):7.

-p-

Petersen, R.G. 1985. Design and Analysis of Experiments, Marcel Dekker Inc., New York, NY, p.112.

Picologlou, B.F., N. Zelver, and W.G. Characklis 1980. "Biofilm Growth and Hydraulic Performance", Journal of the Hydraulics Division, Proceedings of the ASCE, 106(HY5):733.

Pipes, D.M. 1974. "Variations in Glucose Diffusion Coefficients through Biological Floc", Master's thesis, Rice University, Houston, TX.

Powell, M.S., and N.K.H. Slater 1983. "The Deposition of Bacterial Cells from Laminar Flows onto Solid Surfaces", Biotechnology and Bioengineering, 25:891.

-q-

-r-

Ramana, K.V., and N.G. Karanth 1989. "Factors Affecting Biosurfactant Production Using *Pseudomonas aeruginosa* CFTR-6 under Submerged Conditions", J. Chem. Tech. Biotechnol., 45:249.

Rittman, B.E., and P.L. McCarty 1978. "Variable-Order Model of Bacterial-Film Kinetics", Journal of the Environmental Engineering Division, Proceedings of the ASCE, 104(EE5):889.

Rittman, B.E., and P.L. McCarty 1980. "Model of Steady-State Biofilm Kinetics", Biotechnology and Bioengineering, 22:2343.

Rittman, B.E., and P.L. McCarty 1981. "Substrate Flux into Biofilms of any Thickness", Journal of the Environmental Engineering Division, Proceedings of the ASCE, 107(EE4):831.

Rittman, B.E. 1982. "The Effect of Shear Stress on Biofilm Loss Rate", Biotechnology and Bioengineering, 24:501.

Rittmann, B.E., L. Crawford, C.K. Tuck, and E. Namkung 1986. "*In Situ* Determination of Kinetic Parameters for Biofilms: Isolation and Characterization of Oligotrophic Biofilms", Biotechnology and Bioengineering, 28:1753.

Rittman, B.E. 1989. "Detachment from Biofilms", in W.G. Characklis and P.A. Wilderer (eds.), Structure and Function of Biofilms, John Wiley & Sons Ltd., New York, NY, p.49.

Robinson, J.A., M.G. Trulear, and W.G. Characklis 1984. "Cellular Reproduction and Extracellular Polymer Formation by *Pseudomonas aeruginosa* in Continuous Culture", Biotechnology and Bioengineering, 26:1409.

Rosevear, A. 1984. "Immobilized Biocatalysts - a Critical Review", J. Chem. Tech. Biotechnol., 34B:127.

-s-

Servizi, J.A., and R.H. Bogan 1963. J. San. Eng. Div., Proceedings of the ASCE, 89:17.

Sherwood, T.K., R.L. Pigford, and C.R. Wilke 1975. Mass Transfer, McGraw-Hill Book Company, New York, NY.

Siebel, M.A. 1987. "Binary Population Biofilms", Ph.D. Thesis, Montana State University, Bozeman, MT.

Siebel, M.A., and W.G. Characklis 1991. "Observations of Binary Population Biofilms", Biotechnology and Bioengineering, 37:778.

Siegrist, H., and W. Gujer 1985. "Mass Transfer Mechanisms in a Heterotrophic Biofilm", Water Research, 19(11):1369.

Siegrist, H., and W. Gujer 1987. "Demonstration of Mass Transfer and pH Effects in a Nitrifying Biofilm", Water Research, 21(12):1481.

Sieracki, M.E., S.E. Reichenbach, and K.L. Webb 1989. "Evaluation of Automated Threshold Selection Methods for Accurately Sizing Microscopic Fluorescent Cells by Image Analysis", Applied and Environmental Engineering, 55(11):2762.

Skowland, C.T., and D.W. Kirmse 1989. "Simplified Models for Packed-Bed Biofilm Reactors", Biotechnology and Bioengineering, 33:164.

Smith, R.L., B.L. Howes, and S.P. Garabedian 1991. "*In Situ* Measurement of Methane Oxidation in Groundwater by Using Natural-Gradient Tracer Tests", Applied and Environmental Engineering, 55(7):1997.

Speitel, G.E. Jr., and F.A. DiGiano 1987. "Biofilm Shearing under Dynamic Conditions", Journal of Environmental Engineering, 113(3):464.

Speitel, G.E. Jr., and F.A. DiGiano 1988. "Determination of Microbial Kinetic Coefficients through Measurement of Initial Rates by Radiochemical Techniques", Water Research, 22(7):829.

Stewart, P.S., and C.R. Robertson 1989. "Microbial Growth in a Fixed Volume: Studies with Entrapped *Escherichia coli*", Appl. Microbiol. Biotechnol., 30:34.

Stewart, P.S. 1992. "A Model of Biofilm Detachment", submitted to Biotechnology and Bioengineering.

Storer, F.F., and A.F. Gaudy, Jr. 1969. "Computational Analysis of Transient Response to Quantitative Shock Loadings of Heterogeneous Populations in Continuous Culture", Environmental Science and Technology, 3(2):143.

Stouthamer, A.H. 1977. "Theoretical Calculations on the Influence of the Inorganic Nitrogen Source on Parameters for Aerobic Growth of Microorganisms", Antonie van Leeuwenhoek, 43:351.

Suidan, M.T., B.E. Rittmann, and U.K. Traegner 1987. "Criteria Establishing Biofilm-Kinetic Types", Water Research, 21(4):491.

Suschka, J. 1987. "Hydraulic Performance of Percolating Biological Filters and Consideration of Oxygen Transfer", Water Research, 21(8):865.

Sutherland, I.W. 1983. "Microbial Exopolysaccharides - Their Role in Microbial Adhesion in Aqueous Systems", CRC Critical Reviews in Microbiology, 10(2):173.

-t-

Tchnobanoglous, G. 1979. "Advanced Wastewater Treatment", in Y.T. Chow, R. Eliassen, and R.K. Linsley (eds.), Wastewater Engineering: Treatment, Disposal, Reuse, Metcalf & Eddy Inc., New York, NY, pp.727-730.

Ten Brink, B., and W.N. Konings 1980. "Generation of an Electrochemical Proton Gradient by Lactate Efflux in Membrane Vesicles of *Escherichia coli*", Eur. J. Biochem., III:59.

Tomlinson, T.G., and D.M. Snaddon 1966. Int. J. Air Wat. Poll., 10:865.

Torbati, H.M., R.A. Raiders, E.C. Donaldson, M.J. McInerney, G.E. Jenneman, and R.M. Knapp 1986. "Effect of Microbial Growth on Pore Entrance Size Distribution in Sandstone Cores", Journal of Industrial Microbiology, 1:227.

Trulear, M.G. 1980. "Dynamics of Biofilm Processes in an Annular Reactor", Master's thesis, Rice University, Houston, TX.

Trulear, M.G., and W.G. Characklis 1982. "Dynamics of Biofilm Processes", Journal WPCF, 54(9):1288.

Trulear, M.G. 1983. "Cellular Reproduction and Extracellular Polymer Formation in the Development of Biofilms", Ph.D. thesis, Montana State University, Bozeman, MT.

Turakhia, M.H., K.E. Cooksey, and W.G. Characklis 1983. "Influence of a Calcium-Specific Chelant on Biofilm Removal", Applied and Environmental Microbiology, 46(5):1236.

Turakhia, M., and W.G. Characklis 1983. "An Observation of Microbial Cell Accumulation in a Finned Tube", The Canadian Journal of Chemical Engineering, 61:873.

Turakhia, M.H. 1986. "The Influence of Calcium on Biofilm Processes", Ph.D. thesis, Montana State University, Bozeman, MT.

Turakhia, M.H. and W.G. Characklis 1989. "Activity of *Pseudomonas aeruginosa* in Biofilms: Effect of Calcium", Biotechnology and Bioengineering, 33:406.

-u-

-v-

van der Wende, E., W.G. Characklis, and D.B. Smith 1989. "Biofilms and Bacterial Drinking Water Quality", Water Research, 23(10):1313.

Van Haecke, E., J.-P. Remon, M. Moors, F. Raes, D. De Rudder, and A. Van Peteghem 1990. "Kinetics of *Pseudomonas aeruginosa* Adhesion to 304 and 316-L Stainless Steel: Role of Cell Surface Hydrophobicity", Applied and Environmental Microbiology, 56(3):788.

van Loosdrecht, M.C.M., J. Lyklema, W. Norde, and A.J.B. Zehnder 1990. "Influence of Interfaces on Microbial Activity", Microbiological Reviews, 54(1):75.

Venosa, A.D., and R. Isaac 1987. "Disinfection", Journal WPCF, 59(6):421.

-w-

Walker, J.D. 1987. "Effects of Chemicals on Microorganisms", Journal WPCF, 59(6):614.

Wanner, O., and W. Gujer 1986. "A Multispecies Biofilm Model", Biotechnology and Bioengineering, 28:314.

Weiss, R.M., and D.F. Ollis 1980. "Extracellular Microbial Polysaccharides. I. Substrate, Biomass, and Product Kinetic Equations for Batch Xanthan Gum Fermentation", Biotechnology and Bioengineering, 22:859.

White, D.C., and M.W. Mittelman 1990. "Biological Fouling of High Purity Waters: Mechanisms and Consequences of Bacterial Growth and Replication", Semiconductor Pure Water Conference, January 1990, Santa Clara, CA.

Williams, A.G., and J.W.T. Wimpenny 1977. "Exopolysaccharide production by *Pseudomonas NCIB11264* Grown in Batch Culture", Journal of General Microbiology, 102:13.

Williamson, K., and P.L. McCarty 1976. "Verification Studies of the Biofilm Model for Bacterial Substrate Utilization", J. Wat. Poll. Contr. Fed., 48:281.

Wuhrmann, K. 1971. "Stream Purification", in R. Mitchell (ed.), Water Pollution Microbiology, John Wiley and Sons Inc., New York, NY, p.119.

-x-

-y-

York, W.S., A.G. Darvill, M. McNeil, T.T. Stevenson, and P. Albersheim 1985. "Isolation and Characterization of Plant Cell Walls and Cell Wall Components", Methods in Enzymology, 118:3.

-z-

Zahid, W.M., and J.J. Ganczarczyk 1990. "Suspended Solids in Biological Filter Effluents", Water Research, 24(2):215.

Zobell, C.E. 1943. "The Effect of Solid Surfaces upon Bacterial Activity", Journal of Bacteriology, 46:39.

APPENDICES

APPENDIX A

RotoTorque Characteristics

Inner cylinder

- height	0.177 m
- diameter	0.102 m
- wetted surface area (total)	0.073 m^2

Outer cylinder

- height	0.220 m
- diameter	0.113 m
- wetted surface area (total)	0.023 m^2

Slides

- number	12
- length	0.220 m
- width	0.017 m
- wetted surface area (one slide)	$3.74 \times 10^{-3} m^2$

Reactor

- wetted surface area	0.186 m^2
- slide surface area	0.045 m^2
- liquid volume (at 200 rpm)	$0.596 \times 10^{-3} m^3$
- width of annular gap	$5.5 \times 10^{-3} m$

For a more detailed list of RotoTorque characteristics see Siebel (1987).

APPENDIX B

Procedures and Methods

A. Phosphate Buffered Formalin (4%) for cell count preservation.

1. Dissolve 34g KH_2PO_4 in 500 ml distilled water.
2. Adjust pH to 7.5 +/- 0.5
3. Add 108 ml of 37% formaldehyde.
4. Fill to 1 liter.
5. Filter sterilize in cell free glassware.

B. TEM/SEM Sample Preservation Method*

1. To make phosphate buffered (0.1M) glutaraldehyde (5%)
   a. Dissolve 13.6g KH_2PO_4 in 500 ml distilled water.
   b. Add 102 ml of 49% active glutaraldehyde.
   c. Fill to 950 ml.
   d. Adjust to pH 7.2 +/- 0.1
   e. Fill to 1 liter.
2. Remove polycarbonate filter from RotoTorque slide and place in Petri dish.
3. Slowly pipette glutaraldehyde solution and allow to fix for 2 hours.
4. Place fixed film into scintillation vial filled with 0.1 M KH_2PO_4.
5. Refrigerate until permanent fixation.

* - Adapted from J. Bacteriology, August 1987, vol 169,#8, p.3470-3472

APPENDIX C

Raw Data 200 rpm

Experiment code: **R-0** Influent Glucose Concentration: **7.2 g GC m^{-3}**

Table 12. Bulk liquid measurements.

Time (hours)	ID #	TOC (g C m^{-3})	SOC (g C m^{-3})	Glucose (g GC m^{-3})	Suspended cells (10^{12} m^{-3})
50.0	1	-	-	0.33	9.78
72.0	2	-	-	0.65	12.5
96.0	3	-	-	0.68	9.75
120.0	4	-	-	0.68	12.6
170.0	5	-	-	0.55	19.7
241.0	6	-	-	-	-

Table 13. Biofilm measurements.

Time (hours)	ID #	Thickness (10^{-6}m)	Roughness* (10^{-6}m)	Areal density (dry g m^{-2})	Biofilm cells (10^{12} m^{-2})	TOC (g C m^{-2})
50.0	1	14.50	4.91	-	-	-
72.0	2	22.17	7.64	0.7899	-	-
96.0	3	30.67	6.53	0.4252	-	-
120.0	4	31.00	6.94	0.6209	-	-
170.0	5	34.17	8.00	0.7294	-	-
241.0	6	31.83	7.00	-	-	-

* - Roughness is defined as the standard deviation of the biofilm thickness as measured optically at 8 locations.

Experiment code: **R-1** Influent Glucose Concentration: **4 g GC m^{-3}**

Table 14. Bulk liquid measurements.

Time (hours)	ID #	TOC (g C m^{-3})	SOC (g C m^{-3})	Glucose (g GC m^{-3})	Suspended cells (10^{12} m^{-3})
24.0	1	-	4.38	1.35	-
48.0	2	1.91	2.17	0.48	8.21
90.0	3	1.62	0.91	0.54	9.77
113.0	4	1.68	2.58	0.52	9.41
143.0	5	2.39	1.62	0.61	7.56
166.0	6	4.49	2.30	0.68	9.51
284.5	7	1.63	1.78	0.58	6.81
311.0	8	4.29	2.29	0.61	21.8
311.1	8d	1.85	1.33	0.57	-
*****		Begin step change to pH 5.8 buffer at time = 313 hours			*****
314.5	9	1.38	1.40	0.68	9.33
317.0	10	4.55	1.53	0.79	15.2
322.0	11	3.13	2.11	1.01	4.61
333.3	12	2.19	-	1.03	4.94

Experiment code: **R-1** Influent Glucose Concentration: **4 g GC m^{-3}**

Table 15. Biofilm measurements.

Time (hours)	ID #	Thickness (10^{-6}m)	Roughness* (10^{-6}m)	Areal density (dry g m^{-2})	Biofilm cells (10^{12} m^{-2})	TOC (g C m^{-2})
24.0	1	-	-	-	-	-
48.0	2	-	-	-	-	-
90.0	3	8.33	2.92	0.8459	0.7317	0.314
113.0	4	12.00	1.89	0.5941	-	-
143.0	5	13.67	3.55	0.8353	-	0.182
166.0	6	13.33	2.67	0.1412	0.4977	0.222
284.5	7	15.00	6.52	1.118	0.3386	-
311.0	8	22.00	6.98	0.9647	0.6323	0.332
311.1	8d	18.83	6.96	1.018	0.0578	0.428
*****		Begin step change to pH 5.8 buffer at time = 313 hours				*****
314.5	9	24.83	5.70	0.2941	0.6347	0.493
317.0	10	20.67	4.89	0.2118	0.5587	0.335
322.0	11	24.83	4.33	0.2882	0.1399	0.391
333.0	12	17.83	7.71	0.4294	0.3821	0.202

* - Roughness is defined as the standard deviation of the biofilm thickness as measured optically at 8 locations.

Experiment code: **R-2** Influent Glucose Concentration: **0.8 g GC m^{-3}**

Table 16. Bulk liquid measurements.

Time (hours)	ID #	TOC (g C m^{-3})	SOC (g C m^{-3})	Glucose (g GC m^{-3})	Suspended cells (10^{12} m^{-3})	
72.0	1	1.12	3.30	0.46	0.829	
120.0	2	4.30	0.78	0.51	1.04	
120.2	2d	-	-	-	-	
236.5	3	2.81	1.06	0.49	1.68	
290.0	4	1.14	0.74	0.43	2.05	
*****		Noticeable contamination on coupon at time = 290 hours				*****
*****		About 15% of coupon is thick and cloudy				*****

Table 17. Biofilm measurements.

Time (hours)	ID #	Thickness (10^{-6}m)	Roughness* (10^{-6}m)	Areal density (dry g m^{-2})	Biofilm cells (10^{12} m^{-2})	TOC (g C m^{-2})
72.0	1	3.17	1.88	0.0471	0.0406	0.270
120.0	2	4.83	1.58	0.2412	0.3443	0.087
120.2	2d	5.17	1.32	-	-	-
236.5	3	5.17	1.81	0.4235	0.1909	-
290.0	4	9.67	3.00	0.5118	0.1864	0.098
*****		Noticeable contamination on coupon at time = 290 hours				*****
*****		About 15% of coupon is thick and cloudy				*****

* - Roughness is defined as the standard deviation of the biofilm thickness as measured optically at 8 locations.

Table 18. Optical thickness data 200 rpm.

Exp't Code #	Time (hours)	Optical Thickness Measurements (10^{-6}m)	Average Optical Thickness (10^{-6}m)	Standard Deviation (10^{-6}m)
R-0	50.00	14, 15, 10, 5, 11, 7, 15, 10	10.88	3.68
	72.00	17, 21, 24, 13, 10, 23, 16, 9	16.63	5.73
	96.00	16, 24, 25, 18, 19, 24, 29, 29	23.00	4.90
	120.0	30, 23, 24, 23, 26, 14, 28, 18	23.25	5.20
	170.0	19, 22, 21, 34, 29, 30, 31, 19	25.63	6.00
	241.0	26, 28, 22, 18, 23, 34, 20, 20	23.88	5.25
R-1	24.00	-	-	-
	48.00	-	-	-
	90.00	7, 4, 4, 10, 8, 7, 4, 6	6.25	2.19
	113.0	6, 9, 10, 9, 10, 10, 8, 10	9.00	1.41
	143.0	11, 9, 9, 9, 16, 11, 10, 7	10.25	2.66
	166.0	11, 10, 10, 10, 9, 6, 13, 11	10.00	2.00
	284.5	16, 9, 6, 17, 9, 18, 8, 7	11.25	4.89
	311.0	21, 11, 18, 15, 23, 8, 15, 21	16.50	5.24
	311.1	9, 9, 14, 18, 22, 20, 11, 10	14.13	5.22
	314.5	13, 25, 22, 20, 13, 20, 16, 20	18.63	4.27
	317.0	15, 18, 10, 21, 17, 12, 13, 18	15.50	3.66
	322.0	19, 24, 18, 13, 16, 19, 21, 19	18.63	3.25
	333.0	12, 6, 10, 15, 26, 12, 14, 12	13.38	5.78
R-2	72.00	3, 1, 4, 0, 2, 3, 2, 4	2.38	1.41
	120.0	5, 4, 3, 5, 2, 4, 4, 2	3.63	1.19
	120.2	3, 5, 3, 4, 5, 3, 3, 5	3.88	0.99
	236.5	7, 3, 4, 3, 3, 4, 4, 3	3.88	1.36
	290.0	10, 5, 5, 10, 5, 8, 9, 6	7.25	2.25

Table 19. Percent water data 200 rpm.

Exp't Code #	Time (hours)	Percent Water (%)
R-0	50.00	-
	72.00	88.55
	96.00	96.03
	120.0	96.67
	170.0	94.21
	241.0	-
R-1	24.00	-
	48.00	-
	90.00	92.44
	113.0	-
	143.0	95.20
	166.0	99.19
	284.5	94.71
	311.0	94.27
	311.1	95.61
	314.5	97.56
	317.0	98.69
	322.0	98.65
	333.0	96.17

APPENDIX D

Raw Data 300 rpm

Experiment code: **R-3** Influent Glucose Concentration: **7.2 g GC m^{-3}**

Table 20. Bulk liquid measurements.

Time (hours)	ID #	TOC (g C m^{-3})	SOC (g C m^{-3})	Glucose (g GC m^{-3})	Suspended cells (10^{12} m^{-3})
24.15	1	-	2.76	0.80	5.81
91.25	2	7.05	5.16	4.69	15.2
115.8	3	2.74	5.71	5.20	19.9
145.8	4	-	-	0.43	18.9

Table 21. Biofilm measurements.

Time (hours)	ID #	Thickness (10^{-6}m)	Roughness* (10^{-6}m)	Areal density (dry g m^{-2})	Biofilm cells (10^{12} m^{-2})	TOC (g C m^{-2})
24.15	1	2.33	1.98	0.1176	0.2534	0.533
91.25	2	15.00	5.32	-0.0588	1.042	0.108
115.8	3	21.67	4.38	0.5294	0.9179	0.188
145.8	4	31.00	8.69	1.882	0.9953	-

* - Roughness is defined as the standard deviation of the biofilm thickness as measured optically at 8 locations.

Experiment code: **R-4** Influent Glucose Concentration: **4 g GC m^{-3}**

Table 22. Bulk liquid measurements.

Time (hours)	ID #	TOC (g C m^{-3})	SOC (g C m^{-3})	Glucose (g GC m^{-3})	Suspended cells (10^{12} m^{-3})
47.00	1	0.96	3.65	0.23	3.12
113.7	2	2.70	1.34	0.56	7.37
140.7	3	3.82	1.46	0.51	9.63
161.7	4	2.35	0.96	0.15	9.23
185.7	5	1.55	1.27	0.32	7.84

Table 23. Biofilm measurements.

Time (hours)	ID #	Thickness (10^{-6}m)	Roughness* (10^{-6}m)	Areal density (dry g m^{-2})	Biofilm cells (10^{12} m^{-2})	TOC (g C m^{-2})
47.00	1	5.00	2.54	0.1235	-	0.038
113.7	2	14.83	5.54	1.206	0.5530	0.166
140.7	3	19.67	8.72	0.7941	0.7171	0.224
161.7	4	16.50	5.09	-	0.7929	0.223
185.7	5	22.33	7.67	-	0.4076	0.100

* - Roughness is defined as the standard deviation of the biofilm thickness as measured optically at 8 locations.

Experiment code: **S-4** Influent Glucose Concentration: **4 g GC m^{-3}**

Table 24. Bulk liquid measurements.

Time (hours)	ID #	TOC (g C m^{-3})	SOC (g C m^{-3})	Glucose (g GC m^{-3})	Suspended cells (10^{12} m^{-3})
48.00	1	1.54	1.14	0.83	2.01
122.0	2	1.97	1.35	0.61	5.22
146.0	3	1.80	-	0.56	7.52
146.1	3d	-	-	-	8.61
170.0	4	1.81	1.30	0.51	5.35
236.5	5	1.59	2.24	0.56	8.37

Table 25. Biofilm measurements.

Time (hours)	ID #	Thickness (10^{-6}m)	Roughness* (10^{-6}m)	Areal density (dry g m^{-2})	Biofilm cells (10^{12} m^{-2})	TOC (g C m^{-2})
48.00	1	7.00	2.74	0.2059	0.2097	0.108
122.0	2	17.83	4.99	0.5588	0.3490	0.231
146.0	3	23.50	3.83	1.000	0.7340	0.241
146.1	3d	-	-	-	-	-
170.0	4	17.00	4.66	0.7529	1.336	0.312
236.5	5	16.00	4.83	1.053	0.6911	0.288

* - Roughness is defined as the standard deviation of the biofilm thickness as measured optically at 8 locations.

Experiment code: **T-4** Influent Glucose Concentration: **4 g GC m^{-3}**

Table 26. Bulk liquid measurements.

Time (hours)	ID #	TOC (g C m^{-3})	SOC (g C m^{-3})	Glucose (g GC m^{-3})	Suspended cells (10^{12} m^{-3})	
48.00	1	1.71	1.38	0.54	6.06	
122.0	2	1.61	1.53	0.57	2.87	
146.0	3	2.21	1.33	0.52	4.13	
*****		Major sloughing occurred before time = 170 hours				*****
170.0	4	2.07	1.51	0.59	7.21	
236.5	5	1.43	-	0.50	6.16	

Table 27. Biofilm measurements.

Time (hours)	ID #	Thickness (10^{-6}m)	Roughness* (10^{-6}m)	Areal density (dry g m^{-2})	Biofilm cells (10^{12} m^{-2})	TOC (g C m^{-2})
48.00	1	5.50	3.66	0.3353	0.7639	0.156
122.0	2	17.33	5.83	0.5824	0.4506	0.215
146.0	3	17.67	6.64	0.7647	0.8373	0.155
*****		Major sloughing occurred before time = 170 hours				*****
170.0	4	13.67	9.56	0.5706	1.490	0.240
236.5	5	20.33	3.32	0.6471	1.529	0.199

* - Roughness is defined as the standard deviation of the biofilm thickness as measured optically at 8 locations.

Experiment code: **R-5** Influent Glucose Concentration: **0.8 g GC m^{-3}**

Table 28. Bulk liquid measurements.

Time (hours)	ID #	TOC (g C m^{-3})	SOC (g C m^{-3})	Glucose (g GC m^{-3})	Suspended cells (10^{12} m^{-3})
47.25	1	2.12	1.60	0.82	0.806
113.7	2	0.72	0.80	0.15	0.670
140.7	3	1.18	1.11	0.38	0.711
161.7	4	1.77	1.20	0.45	0.674
186.7	5	0.75	0.81	0.14	0.921
186.8	6	-	-	-	-
186.9	7	-	-	-	-

Table 29. Biofilm measurements.

Time (hours)	ID #	Thickness (10^{-6}m)	Roughness* (10^{-6}m)	Areal density (dry g m^{-2})	Biofilm cells (10^{12} m^{-2})	TOC (g C m^{-2})
47.25	1	1.17	1.11	0.1118	-	-
113.7	2	4.17	3.45	0.1235	0.0643	0.091
140.7	3	4.83	4.62	0.8176	0.0993	0.254
161.7	4	7.17	5.38	0.4294	0.0985	0.096
186.7	5	7.50	4.78	0.5235	0.2025	0.114
186.8	6	7.33	6.25	1.235	0.0979	0.131
186.9	7	7.67	5.69	0.6706	0.1730	0.396

* - Roughness is defined as the standard deviation of the biofilm thickness as measured optically at 8 locations.

Table 30. Optical thickness data 300 rpm.

Exp't Code #	Time (hours)	Optical Thickness Measurements (10^{-6}m)	Average Optical Thickness (10^{-6}m)	Standard Deviation (10^{-6}m)
R-3	24.15	4, 3, 0, 2, 3, 1, 0, 1	1.75	1.49
	91.25	10, 10, 20, 8, 10, 14, 8, 10	11.25	3.99
	115.8	15, 17, 20, 15, 20, 15, 10, 18	16.25	3.28
	145.8	33, 25, 29, 16, 19, 21, 15, 28	23.25	8.69
R-4	47.00	5, 2, 6, 1, 2, 4, 6, 4	3.75	1.91
	113.7	18, 10, 17, 10, 8, 7, 11, 8	11.13	4.16
	140.7	30, 13, 15, 8, 12, 13, 15, 12	14.75	6.54
	161.7	13, 12, 20, 15, 9, 8, 10, 12	12.38	3.81
	185.7	22, 9, 27, 16, 14, 15, 12, 19	16.75	5.75
S-4	48.00	9, 5, 2, 6, 4, 4, 6, 6	5.25	2.05
	122.0	12, 12, 11, 14, 9, 19, 19, 11	13.38	3.74
	146.0	17, 19, 20, 12, 20, 18, 20, 15	17.63	2.88
	146.1	-	-	-
	170.0	12, 11, 14, 10, 15, 10, 20, 10	12.75	3.49
	236.5	8, 12, 11, 17, 8, 15, 16, 9	12.00	3.63
T-4	48.00	7, 0, 7, 2, 5, 2, 7, 3	4.13	2.75
	122.0	6, 10, 16, 12, 9, 17, 18, 16	13.00	4.38
	146.0	20, 17, 9, 8, 8, 10, 16, 18	13.25	4.98
	170.0	8, 17, 10, 0, 1, 15, 20, 11	10.25	7.17
	236.5	17, 13, 14, 13, 14, 14, 17, 20	15.25	2.49
R-5	47.25	0, 1, 0, 2, 1, 2, 0, 1	0.88	0.83
	113.7	7, 0, 5, 3, 1, 0, 5, 4	3.13	2.59
	140.7	6, 0, 0, 8, 2, 7, 6, 0	3.63	3.46
	161.7	8, 7, 0, 1, 9, 10, 1, 7	5.38	4.03
	186.7	10, 4, 7, 0, 5, 7, 10, 2	5.63	3.58
	186.8	3, 10, 7, 1, 8, 0, 13, 2	5.50	4.69
	186.9	2, 12, 7, 10, 2, 3, 9, 1	5.75	4.27

APPENDIX E

Raw Data 400 rpm

Experiment code: **R-6** Influent Glucose Concentration: **7.2 g GC m^{-3}**

Table 31. Bulk liquid measurements.

Time (hours)	ID #	TOC (g C m^{-3})	SOC (g C m^{-3})	Glucose (g GC m^{-3})	Suspended cells (10^{12} m^{-3})	
48.0	1	6.61	6.88	5.66	5.63	
121.8	2	3.63	3.14	2.03	16.2	
144.5	3	4.78	4.78	1.63	18.3	
168.5	4	5.75	3.54	1.36	19.5	
188.5	5	3.82	3.20	1.41	16.2	
188.6	5d	-	-	-	15.7	
*****		Glucose stopped at time = 190 hours				*****
190.5	6	5.68	-	0.14	23.2	
191.0	7	7.80	-	0.07	29.3	
192.0	8	4.71	-	1.97	17.6	
193.0	9	5.36	-	-	6.00	
193.1	9d	-	-	-	10.0	

Experiment code: **R-6** Influent Glucose Concentration: **7.2 g GC m^{-3}**

Table 32. Biofilm measurements.

Time (hours)	ID #	Thickness (10^{-6}m)	Roughness* (10^{-6}m)	Areal density (dry g m^{-2})	Biofilm cells (10^{12} m^{-2})	TOC (g C m^{-2})
48.0	1	12.33	3.32	1.647	0.4042	1.953
121.8	2	31.83	12.66	-	1.260	0.350
144.5	3	22.67	9.77	1.941	0.6944	0.407
168.5	4	33.83	11.99	1.177	0.7484	0.596
188.5	5	38.17	13.12	1.647	0.9217	0.844
188.6	5d	-	-	-	-	-
*****		Glucose stopped at time = 190 hours				*****
190.5	6	23.67	9.39	-	-	-
191.0	7	15.50	9.82	-	-	-
192.0	8	9.50	7.18	-	-	-
193.0	9	10.33	6.60	-	-	-
193.1	9d	-	-	-	-	-

* - Roughness is defined as the standard deviation of the biofilm thickness as measured optically at 8 locations.

Experiment code: **R-7** Influent Glucose Concentration: **4 g GC m^{-3}**

Table 33. Bulk liquid measurements.

Time (hours)	ID #	TOC (g C m^{-3})	SOC (g C m^{-3})	Glucose (g GC m^{-3})	Suspended cells (10^{12} m^{-3})
49.00	1	3.08	3.23	0.76	9.81
49.01	1d	-	1.56	-	10.6
138.0	2	2.21	-	3.96	3.58
171.0	3	2.61	4.23	0.78	6.04
189.0	4	2.22	3.15	0.67	1.67

Table 34. Biofilm measurements.

Time (hours)	ID #	Thickness (10^{-6}m)	Roughness* (10^{-6}m)	Areal density (dry g m^{-2})	Biofilm cells (10^{12} m^{-2})	TOC (g C m^{-2})
49.00	1	8.67	5.29	1.059	0.0715	0.168
49.01	1d	-	-	-	-	-
138.0	2	19.17	10.69	0.9412	0.5644	0.201
171.0	3	22.17	8.37	1.000	0.8059	-
189.0	4	20.33	7.67	1.178	0.6716	1.700

* - Roughness is defined as the standard deviation of the biofilm thickness as measured optically at 8 locations.

Experiment code: **S-7** Influent Glucose Concentration: **4 g GC m^{-3}**

Table 35. Bulk liquid measurements.

Time (hours)	ID #	TOC (g C m^{-3})	SOC (g C m^{-3})	Glucose (g GC m^{-3})	Suspended cells (10^{12} m^{-3})
114.0	1	2.18	1.24	0.58	10.4
143.0	2	2.32	1.44	0.57	7.95
210.0	3	1.61	1.28	0.47	6.62

Table 36. Biofilm measurements.

Time (hours)	ID #	Thickness (10^{-6}m)	Roughness* (10^{-6}m)	Areal density (dry g m^{-2})	Biofilm cells (10^{12} m^{-2})	TOC (g C m^{-2})
114.0	1	12.50	3.96	0.5824	0.3964	0.204
143.0	2	14.50	5.98	0.5471	0.6242	1.124
210.0	3	19.17	5.28	0.9176	0.8441	1.328

* - Roughness is defined as the standard deviation of the biofilm thickness as measured optically at 8 locations.

Experiment code: **R-8** Influent Glucose Concentration: **0.8 g GC m^{-3}**

Table 37. Bulk liquid measurements.

Time (hours)	ID #	TOC (g C m^{-3})	SOC (g C m^{-3})	Glucose (g GC m^{-3})	Suspended cells (10^{12} m^{-3})
114.0	1	1.04	0.42	0.02	2.77
161.0	2	1.00	1.29	0.39	1.61
186.0	3	1.22	0.86	0.26	2.33
258.0	4	1.06	0.91	0.17	2.31
354.0	5	2.01	0.66	0.18	2.96

Table 38. Biofilm measurements.

Time (hours)	ID #	Thickness (10^{-6}m)	Roughness* (10^{-6}m)	Areal density (dry g m^{-2})	Biofilm cells (10^{12} m^{-2})	TOC (g C m^{-2})
114.0	1	3.33	2.76	0.3588	0.0239	-
161.0	2	4.17	3.06	0.1118	0.0711	0.077
186.0	3	3.50	3.49	0.1588	0.0927	0.277
258.0	4	5.67	2.74	0.2000	0.1744	0.245
354.0	5	3.83	2.89	0.1588	0.0849	0.073

* - Roughness is defined as the standard deviation of the biofilm thickness as measured optically at 8 locations.

Table 39. Optical thickness data 400 rpm.

Exp't Code #	Time (hours)	Optical Thickness Measurements (10^{-6}m)	Average Optical Thickness (10^{-6}m)	Standard Deviation (10^{-6}m)
R-6	48.00	14, 9, 9, 7, 12, 8, 7, 8	9.00	2.49
	121.8	30, 22, 10, 40, 28, 23, 13, 25	23.88	9.49
	144.5	13, 13, 25, 10, 20, 10, 15, 30	17.00	7.33
	168.5	15, 35, 20, 25, 38, 30, 27, 13	25.38	8.99
	188.5	22, 15, 25, 35, 32, 35, 45, 20	28.63	9.84
	188.6	-	-	-
	190.5	15, 8, 10, 17, 29, 25, 18, 20	17.75	7.05
	191.0	8, 10, 17, 5, 22, 21, 7, 3	11.63	7.37
	192.0	5, 10, 2, 1, 13, 9, 2, 15	7.13	5.38
	193.0	4, 11, 4, 2, 15, 7, 5, 14	7.75	4.95
	193.1	-	-	-
R-7	49.00	5, 14, 0, 5, 8, 5, 7, 8	6.50	3.96
	49.01	-	-	-
	138.0	10, 10, 20, 17, 15, 30, 5, 8	14.38	8.02
	171.0	20, 13, 22, 10, 15, 10, 28, 15	16.63	6.28
	189.0	15, 21, 15, 11, 18, 4, 16, 22	15.25	5.75
S-7	114.0	10, 5, 7, 9, 15, 11, 10, 8	9.38	2.97
	143.0	13, 11, 8, 5, 17, 15, 5, 13	10.88	4.49
	210.0	8, 17, 15, 10, 18, 19, 12, 16	14.38	3.96
R-8	114.0	0, 3, 1, 0, 2, 4, 5, 5	2.50	2.07
	161.0	0, 2, 3, 6, 6, 5, 2, 1	3.13	2.30
	186.0	5, 6, 0, 4, 5, 0, 1, 0	2.63	2.62
	258.0	3, 4, 6, 5, 0, 4, 6, 6	4.25	2.05
	354.0	6, 6, 1, 3, 0, 2, 2, 3	2.88	2.17

APPENDIX F

Torque Data and Shear Stress Calculation

Shear stress on the inner cylinder of the RotoTorque was calculated from direct measurements of the gap opening time of the torque monitor. The torque monitor consists of two aluminum disks which would be free to rotate except for a calibrated spring connection. The spring was calibrated by hanging known weights at known distances and measuring the angular change in the gap opening between the two disks. A linear regression of the calibration data gave a spring constant of 8.093×10^{-5} kg m degree^{-1}. A correction for the friction of the RotoTorque bearings is found by subtracting the torque required to rotate the inner cylinder at given rpm when the rototorque is empty, from the torque required to rotate the inner cylinder at the same rpm when the rototorque is full of water. This gives the additional torque required to overcome the friction of the water. The difference of the gap opening times for both a full and empty rototorque as a function of rotational speed is given in Figure 36. From these regression curves, the change in the gap opening angle can be calculated by subtraction. Using the change in the gap opening angle and knowing the spring constant, the torque can be calculated directly from the spring constant. Assuming negligible friction in the draft tubes and the upper and lower inner cylinder surfaces the torque can be used to calculate the shear stress using Eq. 47.

$$\bar{\tau} = \frac{M_i \, g_0}{r_i \, A_i} \tag{43}$$

The shear stress is given in Figure 37.

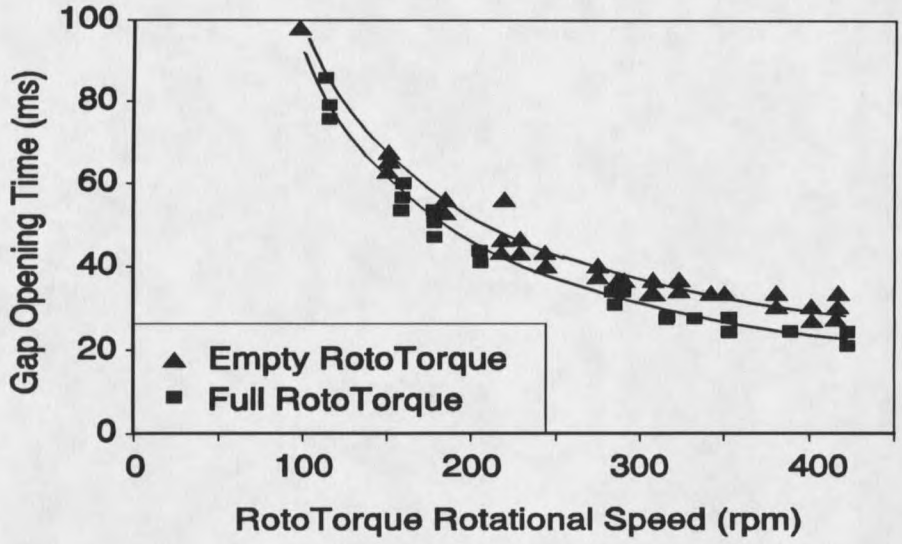

Figure 36. Measured amount of time for the gap opening to pass through the optical sensor's path. For a given rotational speed, torque can be calculated from the difference of the empty opening time and the full opening time.

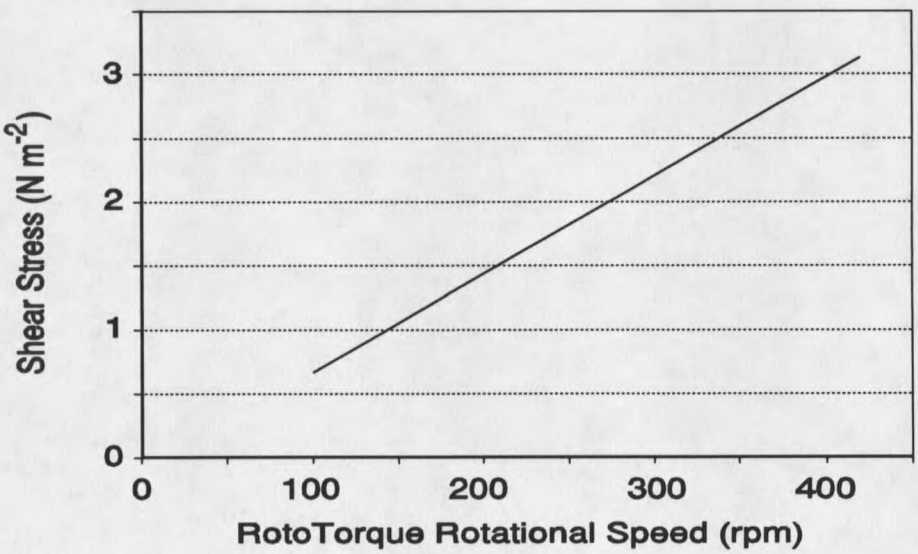

Figure 37. Calculated shear stress was linear with rotational speed of the inner cylinder.

APPENDIX G

ANOVA Results for Steady State Data Only

Table 40. Effluent glucose concentration (g m^{-3}).

OVERALL:

FOR VARIABLE: GLUC
MEAN (N=33) = 0.564

FOR TREATMENT COMBINATIONS:

TREATMENT/CLASS		N	MEANS GLUC
200	7.2	1	0.548
300	7.2	1	0.428
400	7.2	3	1.465
200	4.0	5	0.610
300	4.0	9	0.470
400	4.0	5	0.614
200	0.8	2	0.462
300	0.8	3	0.325
400	0.8	4	0.250

CLASSIFYING FACTOR = RPM:

TREATMENT/CLASS	N	CLASS MEANS GLUC	UNWEIGHTED MEANS GLUC
200	8	0.565	0.540
300	13	0.434	0.408
400	12	0.705	0.776

CLASSIFYING FACTOR = SLR:

TREATMENT/CLASS	N	CLASS MEANS GLUC	UNWEIGHTED MEANS GLUC
7.2	5	1.074	0.814
4.0	19	0.545	0.564
0.8	9	0.322	0.346

ANALYSIS OF VARIANCE:

SOURCE	DF	S.S.	M.S.	F-VALUE	P-VALUE
RPM	2	2.9945	1.4972	16.40	0.0000
SLR	2	4.7117	2.3558	25.80	0.0000
RPM*SLR	4	6.7499	1.6875 1	8.48	0.0000
RESIDUAL	24	2.1914	0.91306E-01		

Table 41. Glucose utilization rate (10^{-3}g GC m^{-2} h^{-1}).

OVERALL:

FOR VARIABLE: GUR
MEAN (N=33) = 0.2711E-01

FOR TREATMENT COMBINATIONS:

TREATMENT/CLASS		N	MEANS GUR
200	7.2	1	0.5920E-01
300	7.2	1	0.6020E-01
400	7.2	3	0.5100E-01
200	4.0	5	0.3014E-01
300	4.0	9	0.3140E-01
400	4.0	5	0.3012E-01
200	0.8	2	0.3000E-02
300	0.8	3	0.4233E-02
400	0.8	4	0.4875E-02

CLASSIFYING FACTOR = RPM:

TREATMENT/CLASS	N	CLASS MEANS GUR	UNWEIGHTED MEANS GUR
200	8	0.2699E-01	0.3078E-01
300	13	0.2735E-01	0.3194E-01
400	12	0.2692E-01	0.2866E-01

CLASSIFYING FACTOR = SLR:

TREATMENT/CLASS	N	CLASS MEANS GUR	UNWEIGHTED MEANS GUR
7.2	5	0.5448E-01	0.5680E-01
4.0	19	0.3073E-01	0.3055E-01
0.8	9	0.4244E-02	0.4036E-02

ANALYSIS OF VARIANCE:

SOURCE	DF	S.S.	M.S.	F-VALUE	P-VALUE
RPM	2	0.38000E-04	0.19000E-04	16.36	0.0000
SLR	2	0.95689E-02	0.47845E-02	4119.72	0.0000
RPM*SLR	4	0.85394E-04	0.21349E-04	18.38	0.0000
RESIDUAL	24	0.27873E-04	0.11614E-05		

Table 42. Suspended cell concentration (cells ml^{-1}).

OVERALL:

FOR VARIABLE: SUSPC
MEAN (N=32) = 0.7812E+07

FOR TREATMENT COMBINATIONS:

TREATMENT/CLASS		N	MEANS SUSPC
200	7.2	1	0.1970E+08
300	7.2	1	0.1885E+08
400	7.2	4	0.1743E+08
200	4.0	3	0.7960E+07
300	4.0	9	0.7769E+07
400	4.0	5	0.6536E+07
200	0.8	2	0.1865E+07
300	0.8	3	0.7687E+06
400	0.8	4	0.2303E+07

CLASSIFYING FACTOR = RPM:

TREATMENT/CLASS	N	CLASS MEANS SUSPC	UNWEIGHTED MEANS SUSPC
200	6	0.7885E+07	0.9842E+07
300	13	0.7006E+07	0.9129E+07
400	13	0.8584E+07	0.8755E+07

CLASSIFYING FACTOR = SLR:

TREATMENT/CLASS	N	CLASS MEANS SUSPC	UNWEIGHTED MEANS SUSPC
7.2	6	0.1804E+08	0.1866E+08
4.0	17	0.7440E+07	0.7422E+07
0.8	9	0.1694E+07	0.1645E+07

ANALYSIS OF VARIANCE:

SOURCE	DF	S.S.	M.S.	F-VALUE	P-VALUE
RPM	2	0.41404E+13	0.20702E+13	0.67	0.5202
SLR	2	0.10160E+16	0.50802E+15	165.04	0.0000
RPM*SLR	4	0.73678E+13	0.18420E+13	0.60	0.6675
RESIDUAL	23	0.70796E+14	0.30781E+13		

Table 43. Cellular detachment rate (cells m^{-2} s^{-1}).

OVERALL:

FOR VARIABLE: RD
MEAN (N=32) = 0.2779E+08

FOR TREATMENT COMBINATIONS:

TREATMENT/CLASS		N	MEANS RD
200	7.2	1	0.7008E+08
300	7.2	1	0.6706E+08
400	7.2	4	0.6199E+08
200	4.0	3	0.2832E+08
300	4.0	9	0.2764E+08
400	4.0	5	0.2325E+08
200	0.8	2	0.6635E+07
300	0.8	3	0.2734E+07
400	0.8	4	0.8191E+07

CLASSIFYING FACTOR = RPM:

TREATMENT/CLASS	N	CLASS MEANS RD	UNWEIGHTED MEANS RD
200	6	0.2805E+08	0.3501E+08
300	13	0.2492E+08	0.3248E+08
400	13	0.3054E+08	0.3114E+08

CLASSIFYING FACTOR = SLR:

TREATMENT/CLASS	N	CLASS MEANS RD	UNWEIGHTED MEANS RD
7.2	6	0.6418E+08	0.6638E+08
4.0	17	0.2647E+08	0.2640E+08
0.8	9	0.6026E+07	0.5853E+07

ANALYSIS OF VARIANCE:

SOURCE	DF	S.S.	M.S.	F-VALUE	P-VALUE
RPM	2	0.52377E+14	0.26188E+14	0.67	0.5203
SLR	2	0.12859E+17	0.64293E+16	165.03	0.0000
RPM*SLR	4	0.93242E+14	0.59768E+14	0.60	0.6675
RESIDUAL	23	0.89606E+15	0.38959E+14		

Table 44. Average biofilm thickness (10^{-6} m).

OVERALL:

FOR VARIABLE: LF
MEAN (N=36) = 16.57

FOR TREATMENT COMBINATIONS:

TREATMENT/CLASS		N	MEANS LF
200	7.2	2	33.00
300	7.2	1	31.00
400	7.2	3	31.56
200	4.0	5	16.57
300	4.0	9	18.52
400	4.0	5	17.73
200	0.8	2	7.420
300	0.8	5	6.900
400	0.8	4	4.293

CLASSIFYING FACTOR = RPM:

TREATMENT/CLASS	N	CLASS MEANS LF	UNWEIGHTED MEANS LF
200	9	18.19	19.00
300	15	15.48	18.81
400	12	16.71	17.86

CLASSIFYING FACTOR = SLR:

TREATMENT/CLASS	N	CLASS MEANS LF	UNWEIGHTED MEANS LF
7.2	6	31.94	31.85
4.0	19	17.80	17.61
0.8	11	6.046	6.204

ANALYSIS OF VARIANCE:

SOURCE	DF	S.S.	M.S.	F-VALUE	P-VALUE
RPM	2	6.0533	3.0266	0.23	0.7945
SLR	2	2706.7	1353.3	103.75	0.0000
RPM*SLR	4	20.389	5.0973	0.39	0.8134
RESIDUAL	27	352.19	13.044		

Table 45. Biofilm roughness (10^{-6} m).

OVERALL:

FOR VARIABLE: ROUGH
MEAN (N=36) = 5.959

FOR TREATMENT COMBINATIONS:

TREATMENT/CLASS		N	MEANS ROUGH
200	18	2	7.500
300	18	1	8.690
400	18	3	11.63
200	10	5	5.336
300	10	9	6.036
400	10	5	6.252
200	2	2	2.405
300	2	5	5.344
400	2	4	3.045

CLASSIFYING FACTOR = RPM:

TREATMENT/CLASS	N	CLASS MEANS ROUGH	UNWEIGHTED MEANS ROUGH
200	9	5.166	5.080
300	15	5.982	6.690
400	12	6.527	6.975

CLASSIFYING FACTOR = SLR:

TREATMENT/CLASS	N	CLASS MEANS ROUGH	UNWEIGHTED MEANS ROUGH
18	6	9.762	9.272
10	19	5.908	5.875
2	11	3.974	3.598

ANALYSIS OF VARIANCE:

SOURCE	DF	S.S.	M.S.	F-VALUE	P-VALUE
RPM	2	17.101	8.5503	2.96	0.0690
SLR	2	133.65	66.827	23.11	0.0000
RPM*SLR	4	21.854	5.4634	1.89	0.1412
RESIDUAL	27	78.068	2.8914		

Table 46. Areal mass density (dry kg m^{-2}).

OVERALL:

FOR VARIABLE: AMD
MEAN (N=33) = 0.8031E-03

FOR TREATMENT COMBINATIONS:

TREATMENT/CLASS		N	MEANS AMD
200	7.2	1	0.7290E-03
300	7.2	1	0.1882E-02
400	7.2	3	0.1588E-02
200	4.0	5	0.8154E-03
300	4.0	7	0.7976E-03
400	4.0	5	0.8448E-03
200	0.8	2	0.4680E-03
300	0.8	5	0.7354E-03
400	0.8	4	0.1575E-03

CLASSIFYING FACTOR = RPM:

TREATMENT/CLASS	N	CLASS MEANS AMD	UNWEIGHTED MEANS AMD
200	8	0.7178E-03	0.6708E-03
300	13	0.8571E-03	0.1138E-02
400	12	0.8016E-03	0.8635E-03

CLASSIFYING FACTOR = SLR:

TREATMENT/CLASS	N	CLASS MEANS AMD	UNWEIGHTED MEANS AMD
7.2	5	0.1475E-02	0.1400E-02
4.0	17	0.8167E-03	0.8193E-03
0.8	11	0.4766E-03	0.4536E-03

ANALYSIS OF VARIANCE:

SOURCE	DF	S.S.	M.S.	F-VALUE	P-VALUE
RPM	2	0.77913E-06	0.38956E-06	5.21	0.0132
SLR	2	0.32128E-05	0.16064E-05	21.48	0.0000
RPM*SLR	4	0.13060E-05	0.32651E-06	4.37	0.0086
RESIDUAL	24	0.17949E-05	0.74789E-07		

Table 47. Volumetric mass density (dry kg [wet m]$^{-3}$).

OVERALL:

FOR VARIABLE: VMD
MEAN (N=33) = 56.77

FOR TREATMENT COMBINATIONS:

TREATMENT/CLASS		N	MEANS VMD
200	7.2	1	21.35
300	7.2	1	60.72
400	7.2	3	54.52
200	4.0	5	48.82
300	4.0	7	44.27
400	4.0	5	47.03
200	0.8	2	67.46
300	0.8	5	111.0
400	0.8	4	37.23

CLASSIFYING FACTOR = RPM:

TREATMENT/CLASS	N	CLASS MEANS VMD	UNWEIGHTED MEANS VMD
200	8	50.05	45.88
300	13	71.19	71.98
400	12	45.64	46.26

CLASSIFYING FACTOR = SLR:

TREATMENT/CLASS	N	CLASS MEANS VMD	UNWEIGHTED MEANS VMD
7.2	5	49.13	45.53
4.0	17	46.42	46.71
0.8	11	76.24	71.88

ANALYSIS OF VARIANCE:

SOURCE	DF	S.S.	M.S.	F-VALUE	P-VALUE
RPM	2	3160.2	1580.1	2.25	0.1268
SLR	2	3127.5	1563.7	2.23	0.1293
RPM*SLR	4	5435.6	1358.9	1.94	0.1366
RESIDUAL	24	16827	701.14		

Table 48. Areal cell density (cells m^{-2}).

OVERALL:

FOR VARIABLE: ACD
MEAN (N=33) = 0.5526E+12

FOR TREATMENT COMBINATIONS:

TREATMENT/CLASS		N	MEANS ACD
200	7.2	0	0.0000
300	7.2	1	0.9953E+12
400	7.2	3	0.7882E+12
200	4.0	4	0.3816E+12
300	4.0	9	0.9483E+12
400	4.0	5	0.6684E+12
200	0.8	2	0.1886E+12
300	0.8	5	0.1342E+12
400	0.8	4	0.1058E+12

CLASSIFYING FACTOR = RPM:

TREATMENT/CLASS	N	MEANS ACD
200	6	0.3173E+12
300	15	0.6801E+12
400	12	0.5108E+12

ANALYSIS OF VARIANCE:

SOURCE	DF	S.S.	M.S.	F-VALUE	P-VALUE
TREATMENTS	2	0.59701E+24	0.29851E+24	1.82	0.1798
RESIDUAL	30	0.49264E+25	0.16421E+24		

CLASSIFYING FACTOR = SLR:

TREATMENT/CLASS	N	MEANS ACD
7.2	4	0.8400E+12
4.0	18	0.7446E+12
0.8	11	0.1338E+12

ANALYSIS OF VARIANCE:

SOURCE	DF	S.S.	M.S.	F-VALUE	P-VALUE
TREATMENTS	2	0.29237E+25	0.14618E+25	16.87	0.0000
RESIDUAL	30	0.25997E+25	0.86658E+23		

Table 49. Volumetric cell density (cells m^{-3}).

OVERALL:

FOR VARIABLE: VCD
MEAN (N=33) = 34.12

FOR TREATMENT COMBINATIONS:

TREATMENT/CLASS		N	MEANS VCD
200	7.2	0	0.0000
300	7.2	1	32.11
400	7.2	3	25.63
200	4.0	4	22.93
300	4.0	9	54.15
400	4.0	5	37.63
200	0.8	2	28.10
300	0.8	5	19.44
400	0.8	4	24.11

CLASSIFYING FACTOR = RPM:

TREATMENT/CLASS	N	MEANS VCD
200	6	24.65
300	15	41.11
400	12	30.13

ANALYSIS OF VARIANCE:

SOURCE	DF	S.S.	M.S.	F-VALUE	P-VALUE
TREATMENTS	2	1461.6	730.80	1.82	0.1797
RESIDUAL	30	12057	401.92		

CLASSIFYING FACTOR = SLR:

TREATMENT/CLASS	N	MEANS VCD
7.2	4	27.25
4.0	18	42.62
0.8	11	22.71

ANALYSIS OF VARIANCE:

SOURCE	DF	S.S.	M.S.	F-VALUE	P-VALUE
TREATMENTS	2	2920.9	1460.5	4.13	0.0260
RESIDUAL	30	10598	353.27		

Table 50. Biofilm TOC (g C m^{-2}).

OVERALL:

FOR VARIABLE: BTOC
MEAN (N=30) = 0.3697

FOR TREATMENT COMBINATIONS:

TREATMENT/CLASS		N	MEANS BTOC
200	7.2	0	0.0000
300	7.2	1	0.1880
400	7.2	3	0.6157
200	4.0	4	0.2910
300	4.0	9	0.2202
400	4.0	3	1.383
200	0.8	1	0.0980
300	0.8	5	0.1982
400	0.8	4	0.1680

CLASSIFYING FACTOR = RPM:

TREATMENT/CLASS	N	MEANS BTOC
200	5	0.2524
300	15	0.2107
400	10	0.6669

ANALYSIS OF VARIANCE:

SOURCE	DF	S.S.	M.S.	F-VALUE	P-VALUE
TREATMENTS	2	1.3311	0.66557	5.96	0.0072
RESIDUAL	27	3.0133	0.11160		

CLASSIFYING FACTOR = IGC:

TREATMENT/CLASS	N	MEANS BTOC
10	16	0.4560
2	10	0.1761
18	4	0.5087

ANALYSIS OF VARIANCE:

SOURCE	DF	S.S.	M.S.	F-VALUE	P-VALUE
TREATMENTS	2	0.57131	0.28566	2.04	0.1491
RESIDUAL	27	3.7731	0.13974		

APPENDIX H

Mixed Population Results 200 rpm

Experiment code: **M1** Influent Glucose Concentration: **7.2 g GC m^{-3}**

Table 51. Bulk liquid measurements.

Time (hours)	ID #	Glucose (g GC m^{-3})	Total Suspended Solids (g m^{-3})	TOC (g C m^{-3})	SOC (g C m^{-3})
24	1	3.90	0.05	-	-
48	2	-	0.28	-	-
72	3	1.19	0.33	-	-
96	4	0.35	0.30	-	-
120	5	0.01	0.85	-	-
144	6	0.03	1.00	-	-
168	7	0.07	2.13	-	-
192	8	0.06	5.24	-	-
216	9	0.44	2.40	-	-
240	10	0.00	3.40	-	-
264	11	0.01	1.77	-	-
288	12	0.02	1.57	4.49	1.40
312	13	0.00	1.08	2.24	1.25
*****	Glucose turned off after time = 312 hours				*****
312.7	14	0.00	4.50	6.82	-
314.5	15	0.00	0.70	1.70	-
316.5	16	0.00	0.28	0.71	-
318.3	17	0.00	0.11	-	-
319.7	18	0.00	0.01	0.68	-
329.5	19	0.00	0.43	9.05	0.83

Experiment code: M1 Influent Glucose Concentration: **7.2 g GC m^{-3}**

Table 52. Biofilm measurements.

Time (hours)	ID #	Thickness (10^{-6}m)	Roughness (10^{-6}m)	Areal Density (dry g m^{-2})	
24	1	-	-	-	
48	2	37.0	-	2.15	
72	3	39.5	-	3.84	
96	4	97.5	-	5.65	
120	5	173.5	-	8.48	
144	6	224.0	-	5.47	
168	7	-	-	-	
192	8	265.0	-	1.63	
216	9	256.2	-	6.33	
240	10	150.4	-	5.40	
264	11	218.3	-	8.40	
288	12	186.4	-	9.55	
312	13	-	-	-	
*****	Glucose turned off after time = 312 hours				*****
312.7	14	-	-	-	
314.5	15	-	-	-	
316.5	16	-	-	-	
318.3	17	-	-	-	
319.7	18	-	-	-	
329.5	19	106.8	-	2.66	

Experiment code: **M1** Influent Glucose Concentration: **7.2 g GC m^{-3}**

Table 53. Biofilm thickness* distribution on RotoTorque coupons+ removed at time = 288 hours.

Upstream Third	Middle Third	Downstream Third
213	300	37
333	237	5
293	160	24
247	69	16
427	208	17
360	240	33
340	200	40
360	168	17
327	113	33
407	99	24
307	75	32
413	240	23
407	209	43
347	293	20
293	333	43
333	168	24

* Thickness (10^{-6}m)

\+ Bulk Liquid flow is from left to right. Coupon dimensions are 0.017 m wide X 0.22 m long, so each reported thickness represents the average of an area 0.0057 m wide X 0.0138 m long.

Experiment code: **M2** Influent Glucose Concentration: **0.8 g GC m^{-3}**

Table 54. Bulk liquid measurements.

Time (hours)	ID #	Glucose (g GC m^{-3})	Total Suspended Solids (g m^{-3})	TOC (g C m^{-3})	SOC (g C m^{-3})
24	1	0.57	0.05	-	-
48	2	-	0.72	-	-
72	3	0.33	0.00	-	-
96	4	0.30	0.00	-	-
120	5	0.15	0.02	-	-
144	6	0.01	0.05	-	-
168	7	0.00	0.28	-	-
192	8	0.00	0.03	-	-
216	9	0.00	0.10	-	-
240	10	0.00	0.20	-	-
264	11	0.00	0.27	-	-
288	12	0.00	0.55	0.51	1.34
312	13	0.00	0.38	1.11	1.15
*****	Glucose turned off after time = 312 hours				*****
312.7	14	0.00	0.33	0.38	-
314.5	15	0.00	0.23	0.31	-
316.5	16	0.00	0.50	1.03	-
318.3	17	0.00	0.18	-	-
319.7	18	0.00	0.07	0.31	-
329.5	19	0.00	0.08	0.33	1.01

Experiment code: **M2** Influent Glucose Concentration: **0.8 g GC m^{-3}**

Table 55. Biofilm measurements.

Time (hours)	ID #	Thickness (10^{-6}m)	Roughness (10^{-6}m)	Areal Density (dry g m^{-2})	
24	1	-	-	-	
48	2	-	-	-	
72	3	-	-	-	
96	4	-	-	-	
120	5	-	-	0.28	
144	6	24.3	8.80	0.73	
168	7	-	-	-	
192	8	34.0	15.9	-	
216	9	45.5	32.3	1.83	
240	10	68.5	20.9	2.91	
264	11	113.9	56.8	3.29	
288	12	80.7	-	1.63	
312	13	66.7	55.8	1.07	
*****	Glucose turned off after time = 312 hours				*****
312.7	14	-	-	-	
314.5	15	-	-	-	
316.5	16	-	-	-	
318.3	17	-	-	-	
319.7	18	-	-	-	
329.5	19	13.7	-	1.07	

Experiment code: **M2** Influent Glucose Concentration: **0.8 g GC m^{-3}**

Table 56. Biofilm thickness* distribution on RotoTorque coupons+ removed at time = 288 hours.

Upstream Third	Middle Third	Downstream Third
170	88	90
136	127	43
64	90	20
101	29	20
88	110	31
80	53	33
51	23	40
53	36	21
17	67	11
176	60	19
160	131	28
104	31	57
65	139	84
136	67	93
78	64	20
187	101	16

* Thickness (10^{-6}m)

\+ Bulk Liquid flow is from left to right. Coupon dimensions are 0.017 m wide X 0.22 m long, so each reported thickness represents the average of an area 0.0057 m wide X 0.0138 m long.

APPENDIX I

Particle Size Distribution Data

Table 57. Experiment code **R0.**

PARTICLE SIZE ($10^{-12}m^2$)	PARTICLE CONCENTRATION ($10^{12}m^{-3}$)				
	50 Hrs	72 Hrs	96 Hrs	120 Hrs	170 Hrs
0.122	0.054	0.389	0.232	0.071	0.036
0.161	0.018	0.456	0.161	0.107	0.036
0.212	0.116	0.295	0.500	0.232	0.107
0.280	0.161	0.616	0.733	0.286	0.250
0.368	0.313	1.139	1.376	0.482	0.536
0.486	0.858	1.755	1.483	1.751	0.822
0.640	1.644	1.635	1.805	2.144	1.930
0.844	2.341	2.090	1.179	2.305	3.877
1.113	1.581	0.884	0.983	2.037	3.645
1.467	0.867	0.817	0.411	1.001	2.376
1.934	0.456	0.523	0.179	0.607	1.394
2.549	0.170	0.335	0.054	0.161	0.715
3.360	0.071	0.201	0.036	0.054	0.286
4.430	0.036	0.107	0.018	0.036	0.232
5.839	0.009	0.054	0.018	0.000	0.232
7.698	0.000	0.094	0.000	0.000	0.089
10.148	0.000	0.040	0.000	0.000	0.036
13.377	0.000	0.000	0.000	0.000	0.000
17.634	0.000	0.000	0.000	0.000	0.000
23.247	0.000	0.013	0.000	0.000	0.036
30.645	0.000	0.000	0.000	0.000	0.000
40.398	0.000	0.000	0.000	0.000	0.018
AVG. SIZE:	0.970	0.995	0.679	0.901	1.394

Table 58. Experiment code **S4.**

PARTICLE SIZE ($10^{-12}m^2$)	PARTICLE CONCENTRATIONS ($10^{12}m^{-3}$)				
	48 Hrs	122 Hrs	146 Hrs	170 Hrs	236½ Hrs
0.122	0.157	0.000	0.000	0.000	0.000
0.161	0.269	0.041	0.085	0.202	0.247
0.212	0.179	0.041	0.009	0.034	0.112
0.280	0.325	0.041	0.304	0.067	0.213
0.368	0.504	0.082	0.351	0.157	0.269
0.486	0.729	0.329	0.484	0.258	0.392
0.640	0.695	0.329	1.043	0.493	1.121
0.844	0.796	0.247	0.939	0.617	1.412
1.113	0.594	0.123	0.892	1.233	1.132
1.467	0.482	0.000	0.588	1.031	0.863
1.934	0.325	0.041	0.294	0.717	0.740
2.549	0.303	0.000	0.114	0.381	0.269
3.360	0.146	0.000	0.085	0.247	0.247
4.430	0.034	0.000	0.047	0.090	0.078
5.839	0.045	0.000	0.019	0.067	0.078
7.698	0.022	0.000	0.000	0.011	0.045
10.14	0.022	0.000	0.009	0.090	0.056
13.37	0.011	0.000	0.000	0.000	0.022
17.63	0.000	0.000	0.000	0.000	0.022
23.24	0.000	0.000	0.000	0.000	0.011
30.64	0.000	0.000	0.000	0.000	0.011
40.39	0.000	0.000	0.000	0.000	0.000
AVG. SIZE:	1.076	0.669	1.015	1.569	1.473

Table 59. Experiment code **T4.**

PARTICLE SIZE ($10^{-12}m^2$)	PARTICLE CONCENTRATION ($10^{12}m^{-3}$)		
	48 Hrs	122 Hrs	146 Hrs
0.122	0.070	0.000	0.000
0.161	0.070	0.159	0.117
0.212	0.000	0.159	0.023
0.280	0.280	0.255	0.187
0.368	0.070	0.478	0.350
0.486	0.210	0.382	0.654
0.640	1.051	0.605	0.864
0.844	1.051	0.350	0.490
1.113	0.490	0.223	0.514
1.467	0.525	0.096	0.210
1.934	0.350	0.032	0.117
2.549	0.140	0.000	0.070
3.360	0.070	0.000	0.000
4.430	0.105	0.000	0.000
5.839	0.035	0.000	0.023
7.698	0.000	0.000	0.000
10.148	0.000	0.000	0.000
13.377	0.000	0.000	0.000
17.634	0.000	0.000	0.000
23.247	0.000	0.000	0.000
30.645	0.000	0.000	0.000
40.398	0.000	0.000	0.000
AVG. SIZE:	1.116	0.593	0.804